2023-08

Fabrication of liposome-chitosa N-ZnO nanohybrid integrated with Carissa Spinarum extract for antibacterial application

Rubaka, Clarence

NM-AIST

https://doi.org/10.58694/20.500.12479/2189

Provided with love from The Nelson Mandela African Institution of Science and Technology

FABRICATION OF LIPOSOME-CHITOSAN-ZnO NANOHYBRID INTEGRATED WITH *CARISSA SPINARUM* EXTRACT FOR ANTIBACTERIAL APPLICATION

Clarence Rubaka

A Thesis Submitted in Fulfilment of the Requirements for the Degree of Doctor of Philosophy in Life Sciences of the Nelson Mandela African Institution of Science and Technology

Arusha, Tanzania

August, 2023

ABSTRACT

Innovative biomaterials provide a stimulating and adaptable platform for the implementation of new and more effective methods to prevent bacterial infection. Built on biomimetic-inorganic hybrid material, Dual Nanohybrid Delivery System (DN-DS) has advantageous properties for biomedical applications, such as the delivery of herbal formulations for the treatment of bacterial infections.

Using microwave assisted extraction (MAE), the polyphenols of *Carissa spinarum* were extracted. The Dual Nanohybrid Delivery System (LipCsP-ZnONPs)-CT was formed by combining LipCsP-Chitosan and ZnO-Chitosan, which were both generated using different methods of co-precipitation and ion gelation, respectively. A Zetasizer was used to characterize the nanosystems' size, zeta potential, and polydispersity index (PDI). A UV-visible spectrophotometer was utilized for the optical study, and a scanning electron microscope was employed to investigate at the surface morphology. The interaction of coated chitosan with liposomes and ZnONPs was evaluated using Fourier Transformation Infrared (FTIR) spectroscopy. Different kinetic models were fitted to the results of the encapsulation and release profiles of polyphenols in the liposome nanosystems to determine the mechanism of release. Antibacterial activity of the nanoformulations was assessed by an agar diffusion assay and the micro plate blue assay (MABA).

The Zeta potential of LipCsP changed from -45.3 ± 0.78 to +34.43 ±1.36 due to chitosan coatings. Polyphenol-encapsulation efficiency was higher in LipCsP-Chitosan (81 ± 2.5%) than in LipCsP (66.11 ± 1.11%). Conversely, the size of LipCsP (176.17 ± 1.05 nm) increased to 365.2 ± 0.70 nm. FTIR analysis revealed the interaction of the liposome with chitosan due to the disappearance of N-H primary amine. Interaction between chitosan and zinc oxide was revealed by the formation of new absorption peaks at 670 cm^{-1} and 465 cm^{-1} as observed in the FTIR analysis. (LipCsP-ZnONPs)-CT presented high bioaccessibility of polyphenols in the simulated gastric phase (82.14 ± 0.80%) than in simulated intestinal phase (71.60 ± 0.86%), a stable system for sustained release of polyphenols, and prominent antibacterial activity. (LipCsP-ZnONPs)-CT exhibited a relative inhibition zone diameter (RIZD) of 89.60 ± 1.32, significant high viability reduction ($P<0.05$) against *Klebsiella pneumoniae* as compared to LipCsP-Chitosan and ZnO-chitosan. The nanohybrid systems (LipCsP-Chitosan and ZnO-chitosan) exhibited synergistic effect against *Klebsiella pneumoniae*. This study successfully demonstrated the utility of the nanohybrid as a potential antibacterial agent against *K*.

pneumoniae, therefore, the fabricated dual nano delivery system is an efficacy material for treatment of pneumococcal infections.

DECLARATION

I, Clarence Rubaka, do hereby declare to the Senate of the Nelson Mandela African Institution of Science and Technology that this dissertation is my work and that it has neither been submitted nor being concurrently submitted for degree award in any other institution.

Clarence Rubaka   21/08/2023

Name of the Candidate   **Signature**   **Date**

The above declaration is confirmed

Prof. Askwar Hilonga   21/08/2023

Supervisor 1   **Signature**   **Date**

Prof. Hulda Swai   21/08/2023

Supervisor 2   **Signature**   **Date**

Prof. Hamis Malebo   21/08/2023

Supervisor 3   **Signature**   **Date**

COPYRIGHT

CERTIFICATION

The undersigned certify that they have read and hereby recommend for acceptance for the dissertation entitled ". Fabrication of Liposome-Chitosan-ZnO nanohybrid integrated with *Carissa spinarum* extract for antibacterial application. In fulfillment of the Award of Doctorate of Philosophy in Life Sciences at the Nelson Mandela African Institution of Science and Technology.

Prof. Askwar Hilonga   21/08/2023
Supervisor 1   **Signature**   **Date**

Prof. Hulda Swai   21/08/2023
Supervisor 2   **Signature**   **Date**

Prof. Hamis Malebo   21/08/2023
Supervisor 3   **Signature**   **Date**

motivated me to finish my studies. It is hard to name everyone; I owe them a great debt of gratitude for their assistance both within and outside of the study. To those I missed, I say thank you and wish you all the best in life.

DEDICATION

To the loving memory of my parents, the late Mr. and Mrs. Charles Rubaka. May God rest their souls in peace.

TABLE OF CONTENTS

LIST OF TABLES

LIST OF FIGURES

LIST OF ABREVIATION

(LipCsP/ZnO)-CT	(Liposome loaded Carissa Spinarum Polyphenols/Zinc oxide)-Chitosan
ABTS	2,2′-azino-bis (3-ethylbenzothiazoline-6-Sulfonic Acid
add	Addition
ANOVA	Analysis of Variance
ASGPR	Asialoglycoprotein Receptor
ATCC	American Type Culture Collection
ATCR	African Technical Research Center
ATP	Adenosine Triphosphate
CA	Caffeic Acid
CBPs	Choline Binding Proteins
$C_{digesta}$	Concentration of the CsP in the Mixed Micelle Phase
ChiDENPs	Chitosan- Diethylamino Ethyl Nanoparticles
Ci	Initial concentration of CsP
Cipro	Ciprofloxacin
CMC	Critical Micelle Concentration
C_o	Initial Amount of Polyphenols Before Released by Nanoformulations
CS	Chitosan
CsP	Carissa Spinarum Polyphenols
CsP	Carissa Spinarum Polyphenol
C_t	Cumulative Amount of Polyphenol Released by Nanoformulation After Elapsed Time(t)
Cur	Curcumin
DLS	Dynamic Light Scattering
DMG	Dimethylglycoxime
DMPC	Dimyristoyl Phosphatidyl Choline
DNA	Deoxyribonucleic Acid
DNA	Deoxyribonucleic Acid
DN-DS	Dual Nanohybrid Delivery System
DOPC	Diocyl Phosphatidly Choline
DOTAP	Dioteoyl-3-Trimethylammonium Propane

DOX	Doxorubicin
DPPE	Dipalmitoyl Phosphatidyl Ethanolamine
DPPG	Dipalmitoyl Phosphatidyl Glycerol
DPPH	1,1-diphenyl-2-picrylhydrazyl
DSPC	Distearoyl Phosphatidly Choline
EE	Encapsulation Efficiency
EGCG	Epigallocatechin Gallate
F-C	Folin- Ciocalteu
FDA	Food and Drug Administration
FIC	Fractional Inhibitory Concentration
FTIR	Fourier Transform Infrared
FTIR	Fourier Transform Infrared
GAE	Gallic Acid Equivalence
GI	Gastro Intestine
GI	Gastro Intestinal
GO	Graphene Oxide
Hb	Hemoglobin
HCC cells	Hepatocellular Carcinoma
HLB	High Lipid Bilayer
IgG	Immunoglobulin G
IZD	Inhibition Zone Diameter
k	Rate Constant
K_H	Higuchi Constant
L.S. D	Fisher Least's Significance Difference
LCHNPs	Lipid-coated Hybrid Nanoparticles
LipCsP	Carissa Spinarum Polyphenol Loaded Liposome
LipCsP	Liposome-Carissa Spinarum Polyphenol
LipCsP-chitosan	chitosan (CS) Coated Liposome (LipCsP-Chitosan) Nanocarrier fabricated for delivery of *Carissa spinarum* (CsP) polyphenols
LipoLLA	Liposome Loaded Linolenic Acid
L-MSN	Lipid Coated Mesoporous Silica
MABA	Micro Dilution Alamar Blue Assay
MAE	Microwave Assisted Extraction

MAE	Microwave Assistance Extraction
MIC	Minimum Inhibition Concentration
MLV	Multilamellar Vesicles
MPA	Mercaptopropionic Acid
MRSA	*Methicillin-resistant Staphylococcus aureus*
n	Exponential Factor Which Predicts Korsmeyer-Peppas Model
NAR	Flavonoid Naringenin
NM-AIST	Nelson Mandela African Institution of Science and Technology
NPs	Nanoparticles
OPP	O-Palmitoyl PULLUTAN
PBA	Phenyl Boronic Acid
PBS	Phosphate Buffer Saline
PBS	Phosphate Buffer Saline
PDI	Polydipersity Index
PEG	Polyethylene glycol
PLGA	Poly (Lactic-co-glycolic acid)
RES	Reticuloendothelia System
RIZD	Relative Inhibition Zone Diameter
RIZD	Relative Inhibition Zone Diameter
RNA	Ribonucleic Acid
ROS	Reactive Oxygen Species
RT-PCR	Real Time- Polymerase Chain Reaction
SARs	Severe Acute Respiratory Syndrome
SD	Standard Deviation
SEM	Scanning Electron Microscope
SGF	Simulated Gastric Fluid
SIF	Simulate Intestinal Fluid
SMF	Simulated Mouth Fluid
SUV	Small Unilamellar Vesicles
syn	Synergy
t	Time
TB	Tuberculosis
TEM	Transmission Electron Microscope

Tm or Tc	Lipid Phase Transition Temperature
TPC	Total Phenolic Content
UTI	Urinary Tract Infections
UV	Ultra Violet
Van-LCHNPs	Vancomycin- Chitosan- Diethylamino Ethyl Nanoparticles
Van-PLGA	Vancomycin-poly (Lactic-co-glycolic acid)
VEGF	Vascular endothelial growing factor
XRDs	*X-ray diffractions*
Zp	Zeta Potential

CHAPTER ONE

INTRODUCTION

1.1   Background of the problem

For safety, cultural acceptance, and less side effects, herbal medicine provides a versatile source for medicine for couple of years. Because of the medicinal and pharmacologically significant active substances in plants, there is interest in studying them (Kumar *et al*., 2017). However, the utility of herbal medicine is challenged by poor bioavailability (Mukherjee, 2015). Polyphenol is one of the classes of phyto-based antibacterials that have shown the potential to eradicate a number of bacterial infections, but their limited bioavailability due to oxidation degradation in gastrointenstinal environment reduce their potential as antibacterial agents (Cory *et al.,* 2018; Ydjedd *et al*., 2017; He *et al.,* 2019; Wang *et al*., 2019; Dai *et al.,* 2020).

Investigation of the bioaccessibility of several classes of polyphenols reveals degradation highly demonstrated in some compounds, such as flavonoids apigenin (Wang *et al.*, 2019) This compound demonstrated bioaccessibility of $20.26 \pm 3.06\%$, with a loss of $79.74 \pm 3.06\%$ in the gastric phase. Epigallocatechin gallate (EGCG) was reported to be mostly affected in gastrointenstinal environment (Dai *et al.,* 2020), degraded by half of its amount (50%) after staying for half an hour and disappeared completely after two (2) hours (Di Salle, 2016).

Oral administration is a viable route for drugs, with three major phases: mouth, gastric, and intestinal. These environments have acidic and alkaline conditions and have enzymes which extensively degrade some compounds such as polyphenols (Nguyen *et al.,* 2016). Over the last decade, polymeric nanostructures, inorganic nanoparticles, dendrimers, and liposomes, among others provided an extensively nanodelivery system for herbal based antibacterial such as polyphenols (Abeylath & Turos, 2008; Prakash *et al*., 2017; Vankataraju *et al*., 2014)

Liposomes, which are now FDA-approved, have been applied in the field of nanomedicine to deliver drugs and nutraceuticals (Hatamie *et al*., 2015). Liposomes have small vesicle size range of 20 to 100 nm (Sanwal & Chaudhary, 2011; Mutlu *et al*., 2022)), cellular biocompatible and have the ability to mimic biological structures such as cell membranes, and biodegradability (Farouk *et al*., 2012). They also have the capacity to carry high payloads of drugs (Farouk *et al.,* 2012). Further more, they lack immune system activation (Song *et al.,*

2015), and are low-toxic and easily metabolized (Farouk *et al*., 2012). Despite the fact that liposomes are credited as good nanodrug carriers in the field of nanomedicine, their stability in colloidal systems remains a concern (Yadav *et al.,* 2017).

Surface functionalization of liposomes with other nanoparticles provides their stability and improves their delivery function (Cao *et al.,* 2022). To improve the delivery performance of liposomes, surface functionalization has been applied. Hosny *et al*. (2013) conducted a study to improve the delivery function of liposomes by coating a liposome surface with Eudragit L100 to increase the bioavailability of loaded sodium dendronate. Interestingly, the bioavailability of dendronate was improved by 12-fold by using rats' models as compared with commercial tablets. Other studies reported on the withstand of arabinoside loaded liposomes not being damaged by bile salt in small intestinal fluid when coated with O-palmitoyl pullutan (OPP) (Sehgal & Rogers, 1995).

Engineering the surface of a liposome by coating it with a capping agent such as biopolymer material is considered a plausible strategy for a nanocarrier to resist the harsh gastro-intestinal environment. Coating liposomes with polymer materials improves their stability (Sriwidodo *et al*., 2022; Lee, 2020). The enhancement of the surface charge of the liposome will fundamentally stabilize the liposome, reduce degradation, and facilitate the binding and destruction of bacterial cells (Nag *et al.,* 2021). Ag Seleci (2016) states that a biopolymer coating such as chitosan on the liposome surface increases the efficacy of the loaded drug since it enables cellular uptake of the liposomes (Adibkia *et al*., 2016) facilitates drug target specificity, and ensures the drug is sustained. Indeed, the ideal binding of the chitosan layer, which is attributed to mucoadhesive attributes, increases residence time during absorption of the drug through the intestinal wall and has a high ability to destruct the bacterial cell wall (Sriwidodo *et al*., 2022).

Metal oxides such as zinc oxide are credited as potential antibacterial oxides (Kadiyala *et al*., 2018; Sirelkhatim *et al*., 2015). The United States Food and Drug Administration (FDA) has approved zinc oxide (ZnO) as safe for food and medicinal application (Jiang & Cai, 2018). When ZnONPs enter the cell membrane, they destroy the lipid bilayer and allows molecules such as adenosine triphosphate (ATP) and lipolysaccharides to discharge out of the cell, impede the transportation of potassium ions (Wang & Shao, 2017; Wang & Shao, 2017) hence causing cell death. Even though ZnONPs are better at killing bacteria than other inorganic nano oxides, they tend to aggregate in different environments. This situation reduces its effectiveness against

bacteria. Surface functionalization of ZnO improves the antibacterial activity (Sirelkhatim *et al.,* 2015). One of strategy which improves antibacterial activity of ZnO is capping with polymeric biomaterial such as chitosan.

Carissa spinarum a medicinal plant used as both food and as medicine (Berhane *et al.,* 2020) is a shrub found in the family Apocyneceae, survive at drought area and widely distributed in tropical regions (Fatima *et al*., 2013), used to treat several diseases, including gonorrhoea, diarrhea, sphillis, cough remedies (Ansari & Patit, 2018), viral diseases (Fatima *et al*., 2013), chest pains (Mworia *et al*., 2015), anti-inflammatory (Ansari & Patit, 2018). More over the parts of this plant exhibit antioxidant properies (Mundaragi & Thangadurai, 2018), a purgative, and be used to treat worms (Harwansh *et al.,* 2010). The plant contains medicinal compounds, such as polyphenols, for the treatment of many diseases (Rubaka *et al*., 2014). Nevertheless, the antimicrobial activity is limited by low efficacy (Rubaka *et al.,* 2014).

The need underscored for the utilization of *Carissa spinarum* for treatments of several diseases is due to its safety for human use (Fatima *et al.*, 2013). The government of Tanzania approved *Carissa spinarum* as safe for human use (Malebo & Mwambo, 2012). *Carissa spinarum* kept much attention in the community as a magic tree (Slathia *et al.*, 2017), attracting the users with its potential for treating several ailments. *Carissa spinarum* leaves are highly distributed with polyphenols (Sharma *et al.*, 2023) and have traditionally been used for the treatment of diseases such as pneumonia (Ibrahim *et al.*, 2010; Maobe *et al.*, 2012). For instance, the analysis of phytochemicals in *Carissa spinarum* leaf extract was reported by Tiruneh *et al.* (2022) to be trihydroxyl pentanoic acid, a polyphenol reported to contribute antibacterial activity against tested respiratory infectious pathogens (*S. aureus, S. pneumoniae, and K. pneumoniae*).

The utilization of *Carissa spinarum* leaves has an advantage as compared to roots, bark, and fruits. Harvesting roots and bark can be challenged by environmental deterioration, while fruits are seasonal (Siyum & Meresa, 2021). The leaves are abundant and can be harvested with minimal plant damage. Propagation of the *Carissa spinarum* species in botanical gardens and industrial synthetics of the similar or analogue antibacterial compound as found in the leaves of *Carissa spinarum* will sustain the availability of the potential antibacterial compounds. In silico and biomolecule computation approaches would help to screen the most potent analogues against bacterial infectious disease before synthesizing and testing their activity (Breijyeh & Karaman, 2023; Rahman *et al.*, 2022).

Limited findings have been reported on the integration of two nanohybrid systems to form the Dual Nanohybrid Delivery System (DN-DS) for the advancement delivery of a phyto-active antibacterial substance. In this study, a Dual Nanohybrid Delivery System (DN-DS) was generated by the fabrication of liposome-chitosan-ZnO and integrated with *Carissa spinarum* polyphenols (LipCsP/ZnO)-CT for improvement of the efficacy of *Carissa spinarum* against *Klebsiella pneumoniae* and *Staphylococcus aureus*. Interestingly, DN-DS delivered herbal antibacterial (polyphenol) and inorganic antibacterial (zinc oxide) agents simultaneously against *Klebsiella pneumoniae and S. aureus*. The two antibacterial substances delivered by DN-DS, polyphenol and zinc oxide, are essentially combined to improve antibacterial activity against *Klebsiella pneumoniae* and *S. aureus* by the mechanism depicted in Fig. 1. The system was shown to be more stable, improve the bioavailability of polyphenols, and be more effective against bacteria than LipCsP, LipCsP-chitosan, and ZnO-chitosan on their own.

Streptococcus pneumoniae and *S. aureus* are pathogens that contribute to some bacterial infections, such as respiratory and urinary tract infections (Caneiras *et al.*, 2019). These are among the pathogens causing respiratory infections (Control & Prevention, 2010). Bacterial infections were reportedly the second-leading cause of death in 2019 after ischemic heart disorders, affecting all age groups and contributing to 7.7 million fatalities globally (Kravanja *et al.*, 2019). Five bacteria *Staphylococcus aureus*, *Streptococcus pneumoniae*, *Klebsiella pneumoniae*, *Pseudomonas auregnosa*, and *E. coli* were responsible for 55% of the 7.7 million deaths, with *S. aureus* being mostly responsible for up to 1.1 million of those deaths (Gatica *et al.*, 2023; Ravanja *et al.*, 2019).

According to this data, respiratory pathogens (such as *S. aureus*, *Streptococcus pneumoniae*, and *Klebsiella pneumoniae*) accounted for the majority of the recorded deaths. According to Nguyen *et al.* (2017), *K. pneumoniae* causes more newborn fatalities than *Streptococcus pneumoniae* does for deaths in children and the elderly. Finding effective medications to prevent the aforementioned pathogens that cause respiratory infections is necessary because restricted breathing is one of the most dangerous symptoms of an acute respiratory infection, making respiratory illness a particularly dangerous condition (Nguyen *et al.*, 2017). Furthermore, due to the fact that their immune systems continue to develop, babies and children who are 2 years old or less are more vulnerable (Zhang *et al.*, 2022). For older adults, age 65 or older, their immune system generally weakens as they age (Simon *et al.*, 2015).

According to Vila-Corcoles *et al.* (2009), older persons are also more likely to have other chronic (long-term) health issues that increase the risk of pneumonia. Apart from the risky respiratory infections that lower immune individuals are more susceptible to, the rapid increase in antibiotic resistance increases the need for the development of alternative antibacterials for treating pneumonia (Arato *et al.*, 2021; O'Neill, 2016). According to Thai *et al.* (2023), the fluoroquinolone antibiotic ciprofloxacin is used to treat bacterial illnesses such as pneumonia and urinary tract infections. According to Hangas *et al.* (2018), bacterial DNA topoisomerase and DNA gyrase are both inhibited by the antibiotic ciprofloxacin, which prevents DNA replication. Fluoroquinolones are the best at treating bacterial infections, although they are constrained by antibiotic resistance (Shariati *et al.*, 2022)

Three bacterial targets, cell wall synthesis, translational machinery, and DNA replication machinery, are among the targets of the main classes of antibiotics currently in use. Each of these routes of action, however, is susceptible to bacterial resistance developing (Uddin *et al.*, 2021). The development of enzymes like -lactamase and aminoglycosides, which alter or break down antibiotics, is an important aspect of the emergence of resistance (Munita & Arias, 2016) Vancomycin resistance is caused by modifications to cell components such the cell wall while tetracycline resistance is caused by modifications to the ribosome and expression of the efflux pump (De Gaetano *et al.*, 2023). In comparison to conventional antibiotics, nanoparticles can circumvent existing resistance mechanisms and may be less susceptible to selection for resistance.

Drug delivery methods such liposomes, polymeric delivery systems, and mettalic nanoparticles have been shown to interact with bacterial cell walls, trigger innate and adaptive host immunological responses, and produce reactive oxygen species (Hosseini *et al.*, 2022). Nanoparticles can affect the innate immune system response against bacteria in a variety of ways, such as coating the surface of the bacteria (Imran *et al.*, 2022; Makabenta *et al.*, 2021), which inhibits cellular uptake. Some bacterial strains, for example, *Staphylococcus aureus*, have developed an immune system bypass mechanism by releasing biofilms that lead to a significant reduction in the detection of any immune response.

Frequent administration of conventional formulations of several antibiotics with short half-lives is required to sustain antibacterial action. Otherwise, during anti-infective treatment, concentrations below the MIC commonly occur, which promotes antibiotic resistance (Gao *et al.*, 2011). Extended-release dosage forms optimize the therapeutic efficacy of antibiotics while

reducing antibiotic resistance by sustaining a steady plasma drug concentration over the MIC for an extended period of time. Drug delivery systems that enable the delivery of antibiotics at the proper concentrations, for the proper lengths of time, and also at the proper location in the case of drug targeting might be of great assistance (Abeylath & Turos, 2008).

In addition to enhancing bioavailability, liposomal encapsulation of herbal antibiotics like *Carissa spinarum* polyphenols delivers the proper concentration at the right target while maintaining its constant concentration over the MIC for sustained release, helping to reduce antibacterial resistance. Contrarily, due to limited transport, current antibiotics typically do not reach high intracellular concentrations, and the situation only gets worse when resistance mechanisms, such as decreased uptake and greater efflux, are present. The high surface area-to-volume ratio is responsible for NPs' high reactivity: as the surface area-to-volume ratio increases, so does the percentage of atoms at the surface, and surface forces become more dominant (Vassallo *et al.*, 2020). Therefore, the Dual Nano Delivery System is considered an advanced solution tool for an ideal herbal antibacterial delivery.

Some of the structures that build the cell wall of these bacteria are complex surface proteins, lipid structure, polysaccharides, and teichoic acid, which are attributed to the presence of charged moieties (Adibkia *et al.,* 2016). Engineering of nano-antibiotic which attracted by their counter charges in those charged biomolecules enabling interaction and disruption of bacterial cell wall. The surface modification of nanobiomaterials by the incorporation of prominent binding moieties to complex surface proteins triggers the disintegration of the bacterial cell wall. The ability of the polycationic surface of DN-DS to adhere to the bacterial cell wall significantly improves the antibacterial activity. The nanohybrid system could interact with microorganisms by fusing with their cell wall or membrane and releasing active substances, or by binding to the cell wall and acting as an antibiotic depot to release molecules.

1.2   Statement of the problem

For safety, cultural acceptance, and fewer side effects, people have used herbal medicine for decades. However, the utility of herbal medicine is challenged by poor bioavailability (Mukherjee, 2015). Polyphenol is one of the classes of phyto based antibacterials that have shown the potential to eradicate a number of bacterial infections, but their limited bioavailability and efficacy may reduce their potential as antibacterial agents (Cory *et al.,* 2018). Polyphenol is one of the classes of phyto-based antibacterials that have shown the

potential to eradicate a number of bacterial infections, but their limited bioavailability due to oxidation degradation in gastrointenstinal environment reduce their potential as antibacterial agents (Cory *et al.,* 2018; Ydjedd *et al*., 2017; He *et al.,* 2019; Wang *et al*., 2019; Dai *et al.,* 2020). For instance, Flavonoid apigenin upon subjection to Gatrointenstinal environment reported to degrade by almost three-quarter of its composition, while bioassessibility was 20.26 ± 3.06% (Wang *et al., 2019*).

Epigallocatechin gallate (EGCG), which contains a large number of active phenolic hydroxyl groups, was reported to be unstable in simulated gastrointestinal fluid (Dai *et al.,* 2020). Another study conducted by Di Salle (2016) on the investigation of the degradation effect on polyphenols in the presence of a simulated gastrointenstinal environment, reported that EGCG degraded by half of its amount (50%) after staying for half an hour and disappeared completely after two (2) hours. Oral administration is a viable route for drugs, with three major phases: mouth, gastric, and intestinal. These environments have acidic and alkaline conditions. For example, in the gastric phase, the pH ranges from 1 to 3, rises to 7.7 in the ileum, and becomes 7 in the colon. Another harsh environment the drugs face in the digestive gut is the presence of pancreatic enzymes and bile salts, which contribute to the degradation of drug carriers.

Variation of pH and the presence of pancreatic enzymes such as lipase play roles in the degradation of delivery systems such as liposomes (Nguyen *et al.,* 2016). Herbal -based antibacterial have lesser effect of inhibiting bacterial growth as compared to conventional medicine. According to Rubaka *et al*. (2014), methanol extract of Carissa spinarum displayed 66.97% percentage relative inhibition zone diameter (RIZD) against E. coli, which was lower than the percentage RIZD exhibited by ciprofloxacin, which virtually completely eradicated those bacteria (Rubaka *et al*., 2014). To improve bioavailability and efficacy, liposome has been used to deliver herbal medicine. However, its application is limited by the high susceptibility to degradation particularly when subjected to gastrointestinal environment. Modified liposome-based coating of cationic capping agent embedded in inorganic nanoparticles to form Dual Nanohybrid Delivery System (DN-DS) is plausible approach to overcome the poor stability of liposome delivery system and improve the bioavailability of herbal based antibacterial.

1.3 Rationale of the study

Several delivery systems for improving the bioavailability of herbal-based antibacterials have been reported in the literature. However, none have been studied using a Dual Nanohybrid Delivery System (DN-DS) based on biomimetic-inorganic hybrid material that is smartly fabricated to deliver both herbal antibacterial (polyphenol) and inorganic antibacterial (ZnO) simultaneously against *Klebsiella pneumoniae* and *S. aureus*. The enhancement of the surface charges of DN-DS creates high affinity for binding with bacterial cellular surface (Fig.1), which leads to destruction of the bacterial cell. The DN-DS system is stabilized by cationic capping agent (chitosan), which improves the DN-DS positive charge.

Klebsiella pneumoniae and *S. aureus* are pathogens that contribute to bacterial infections, such as respiratory and urinary tract (Caneiras *et al.*, 2019). Some of the structures that build the cell wall of these bacteria include complex surface proteins, lipid structures, polysaccharides, and teichoic acid, which are attributed to the presence of charged moieties (Adibkia *et al.,* 2016). The special receptor molecules, such as the complex surface proteins of the bacterial cell wall, have structures that enable the engineering of the antibacterial nanomaterial with prominent binding affinity to the bacterial wall. Some of the features of the complex surface protein are the charged species that can bind electrostatically with engineered antibacterial nanomaterial.

The surface modification of nanobiomaterial by incorporating binding moieties to complex surface proteins triggers disintegration of the bacterial cellular wall. The ability of the polycationic surface of DN-DS to adhere to the bacterial cellular wall significantly improves the antibacterial activity. In order to adhere to the bacterial cellular wall, the synthesized nanohybrid system may fuse with the cell wall or membrane and release active ingredients, or it may adsorb to the cell wall and provide an antibiotic depot there that will release molecules.
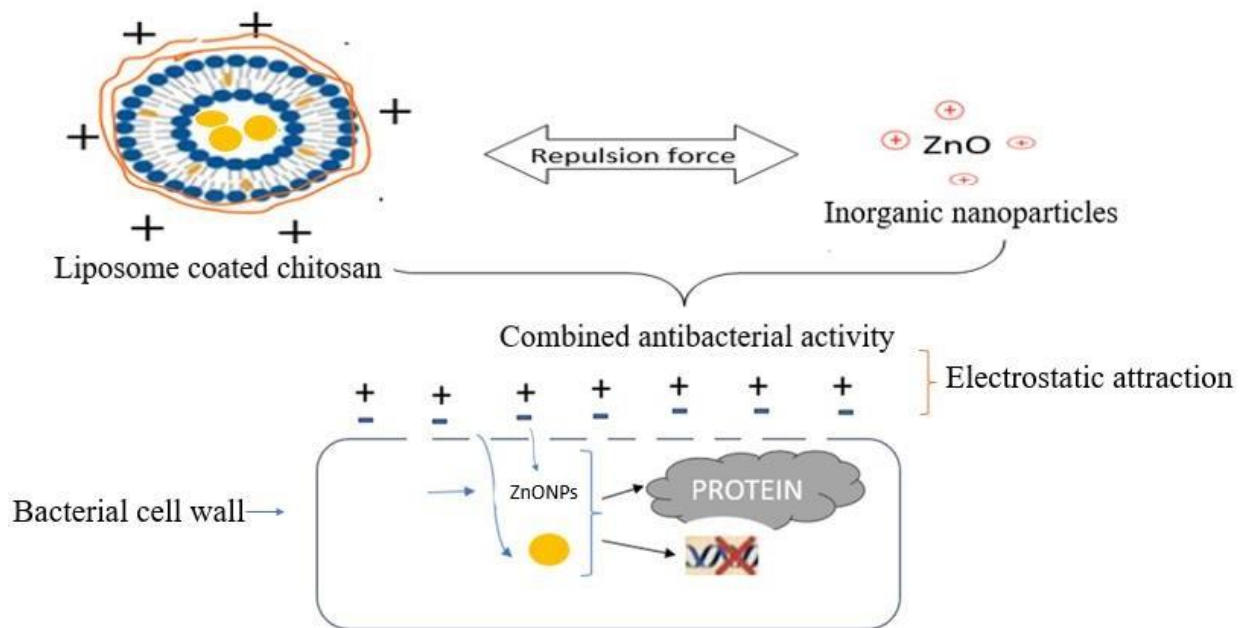
Figure 1: Antibacterial interaction between lipid nanoparticles and inorganic nanoparticles to generate Zinc oxide nanoparticles (ZnO) and polyphenol against bacteria

1.4   Study objective

1.4.1   General objective

To develop a dual nanohybrid system based on polymer and inorganic materials combined with herbal antibiotic like *Carissa spinarum* polyphenols in order to establish a viable drug delivery method against bacterial infections.

1.4.2   Specific objectives

(i)   Characterization and development of the nanoformulations: LipCsP, LipCsP-chitosan, ZnONPs, ZnO-Chitosan, and (LiPCsP/ZnO)-CT in terms of their size, shape, functional group interaction, and capacity to encapsulate and release polyphenols

(ii)   Evaluate the bioavailability of *Carissa spinarum* polyphenol (CsP) encapsulated by LipCsP, LipCsP, LipCsP-chitosan and (LiPCsP/ZnO)-CT in simulated gastro-intestinal fluid.

(iii)   Combine LipCsP and ZnO nanoparticles, both of which are coated with chitosan, in order to ascertain how they interact in a Dual Nano Delivery System (LipCsP/ZnO)-CT to increase antibacterial activity against *Klebsiella pneumoniae* and *Staphylococcus aureus.*

9

(iv)   Evaluate the in vitro-inhibitory effect of antimicrobial nanoformulations (CsP, LiPCsP, LipCsP -Chitosan, ZnONPs, ZnO -Chitosan, LipCsP-ZnO)-CT against *Klebsiella pneumoniae* and *Staphylococcus aureus*.

1.5   Research hypothesis

(i)   There is a significance difference in antibacterial activity among CsP, LiPCsP, LipCsP-Chitosan, ZnONPs, ZnO-Chitosan formulations against *K. pneumoniae* and *S. aureus.*

(ii)   There is a significance difference in polyphenols bioavailability between CsP, LiPCsP, LipCsP-Chitosan, ZnONPs, ZnO-Chitosan and (LipCsP-ZnO)-CT formulations.

(iii)   There is a significance interaction of LipCsP-Chitosan and ZnO-chitosan nanohybrid systems against K. pneumoniae and *S. aureus*.

1.6   Significance of the study

The development of the Dual Nanohybrid Delivery System (LipCsP-ZnO)-CT, which combines *Carissa spinarum* extract with chitosan, ZnO, and liposomes, has shown significant potential to effectively eradicate bacterial pathogens such as *K. pneumoniae* and *S. aureus*. The materials used to fabricate this system, including chitosan, ZnO, and liposomes, are safe for human use and have been approved by the FDA for consumption. Therefore, the Dual Nanohybrid Delivery System (LipCsP-ZnO)-CT has the potential to be advanced into a viable antibacterial agent, improving the management and prevention of *Staphylococcus aureus* and *Klebsiella pneumoniae* infections, including those that cause pneumonia.

1.7   Delineation of the study

The bacterial cell wall is a preferred target choice because it possesses a crucial structural component that permits the binding of (LipCsP-ZnONPs)-CT. The surface of bacterial cells is negatively charged structurally. The kind of charges present in nano antibacterial material restricts the design of nano antibacterial that relies on the binding mechanism with bacterial cellular wall. It is crucial that the (LipCsP-ZnONPs)-CT be stabilized with a cationic surface in order to generate a strong binding affinity with the bacterial cell surface and cause the bacterial cell wall to be destroyed.

CHAPTER TWO

LITERATURE REVIEW

2.1   **Medicinal and Antimicrobial Properties of *Carissa spinarum***

Carissa spinarum L., a medicinal plant that may grow up to 3 meters tall and has green leaves, belongs to the Apocynaceae family and is a widely distributed shrub (Rubaka *et al*., 2014). In tropical areas, it is known as "Magic Shrub," capable of treating of diseases (Table 1) affecting human such as bacterial, worm and viral diseases (Ansari & Patit, 2018). *Carissa spinarum* has long been used to treat bacterial diseases such as pneumonia, sphillis, and typhoid fever, according to Dhatwalia *et al*. (2021). Some plant parts, such as fruits, are utilized as nourishment for humans and animals in addition to being used as a cure for ailments (Berhanu *et al*., 2020; Dhatwalia *et al*., 2021; Pap *et al*., 2021). The fruits are consumed because they are high in vitamin C and iron (Tsao, 2010).

The presence of phytochemicals in this plant, such as phenolic compounds tannins, attests to its potential for disease therapy (Berhanu *et al*., 2020; Dossou-Yovo *et al*., 2021). *Carissa spinarum* leaves are high in polyphenols, such as flavonoids (Ansari & Patil, 2018). Polyphenols are distinguished by the presence of a hydroxyl function group (Gorniak & Kroliczewski, 2018), which is one of the primary moieties exhibiting antibacterial action (Kumar & Goel, 2019; Ofosu *et al*., 2020; Pandey & Rizvi, 2009; Swallah *et al*., 2020). This function group involves inhibition of the bacteria through hydrogen bonding and damage to the cellular wall (Gorniak & Kroliczewski, 2018), despite its easy degradation in the gastric and enzymes that lower its bioavailability (Manach *et al*., 2004; Marin *et al*., 2015; Scheepens*et al*., 2010).

Carrissa spinarum leaves contains antibacterial which saves as raw materials in the pharmaceutical industry for the advancement of potential antibacterial drugs for the prevention of bacterial infectious diseases. Propagation of the *Carissa spinarum* species in botanical gardens and industrial synthetics of the similar or analogue antibacterial compound as found in the leaves of *Carissa spinarum* will sustain the utility of this potential plant as an antibacterial. Since the plant belongs to a shrub, it glows with the bulkiness of the leaves and the availability of primary raw materials for production.

Table 1: Antibacterial activity of parts of *C. Spinarum* against different bacteria species

Part of plant investigated	Tested bacteria	MIC (mg/mL)	Reference
Leaves	*Pseudomonas aeruginosa* *Proteus mirabilis* *Staphylococcus aureus*	0.5	Berhanu *et al*. (2020)
Leaves, roots, stem, stembark	*Mycoplasma mycoides*	0.02	Kama-Kama *et al*. (2016)
Root, Leaf	*E. coli, Proteus, P. auregnosa*	6.25	Kumar and Singh (2017)
Root, leaf and bark	*Escherichia coli, Staphylococcus aureus*	0.312	(Rubaka *et al*. (2014)
Roots	*Staphylococcus aureus, Streptococcus species*	0.125	Sanwal and Chaudhary (2011)
Fruits	*Staphylococcus aureus, Bacillus subtilis, Salmonella typhii, Escherichia coli*	0.600	Doshi *et al*. (2017)

*Note: Minimum Inhibition Concentration (MIC)

Figure 2: *Carissa spinarum* **(Fatima *et al.*, 2013)**

Table 2: Polyphenols from medicinal plant and their activity

Medicinal plant	Activity	Literature
Aspiria Africana	Antioxidant	Okello *et al.* (2021)
Ayapana triplinervis	Antioxidant	Checkouri *et al.* (2020)
Ceratonia siliqua L.	Anticancer	Gregoriou *et al.* (2021)
Ipomoea purpurea	Anticancer	Beheshti *et al.* (2021)
Moringa oleifera leaves	Anticancer	Mumtaz *et al.* (2021)
Cistus salviifolius	Antibacterial	Alvarez-Martinez *et al.* (2021)
Eggplant peel	Anti-salmonelosis	Rochin-Medina *et al.* (2019)
Mangifera indica	Anti-salmonelosis	Kamble *et al.* (2016)
Uvaria chamae, Lantana camara and Phyllanthus amarus	Anti-salmonella	Legba *et al.* (2020)
Canarium schweinfurthii	Antisalmonella	Sokoudjou *et al.* (2020)
Areca catechu	Anti TB	Raju *et al.* (2021)
Piper sarmentosum Roxb	Anti TB	Hussain *et al.* (2009)
Pomegranate Peel Extract	Anti SARS	Tito *et al.* (2021)
Euphorbia umbellate	Anti –Peptide ULCER	Minozzo *et al.* (2016)
Malus pumila Mill leaf	Anti-peptide ulcer	Song *et al.* (2015)

2.2   Phospholipids

The lipids that contain one or more phosphate groups are known as phospholipids (van Hoogevest & Fahr, 2019). The structure of phospholipid is indicated by Fig. 3. The primary structural element of biological membranes is phospholipids, of which glycerol and sphingosine are the main categories (Kalepu *et al.*, 2013). Phosphatidyl glycerol, phosphatidylcholine, phosphatidylethanolamine, phosphatidyl serine, phosphatidyl inositol, and cardiolipin are among the glycerol phospholipids with names based on variations in R-groups at the hydrophilic head (van Hoogevest & Fahr, 2019; Monteiro *et al.*, 2014). The most prevalent lipids in nature are glycerol phospholipids (Daraee *et al.*, 2016; Monteiro *et al.*, 2014).

Approximately 50% of the weight of biological membranes is made up of glycerol phospholipids (Daraee *et al.*, 2016). The substantial saturation of the glycerol phospholipid as it appears in fatty acid ester contributes to its structural characteristics. Additionally, variations in chain length contribute to modifications in glycerol's structural characteristics. (Renne & de Kroon, 2018). Variations in head structure also affect the characteristics of phospholipids; for instance, the amide bond is more stable than the ester bond and more resistant to deterioration and hydrolysis processes (van Hoogevest & Fahr, 2019; Li *et al.*, 2015). In presence of alkaline environment, the phospholipid exhibit hydrolysis reaction (Narasimhan *et al.*, 1997).
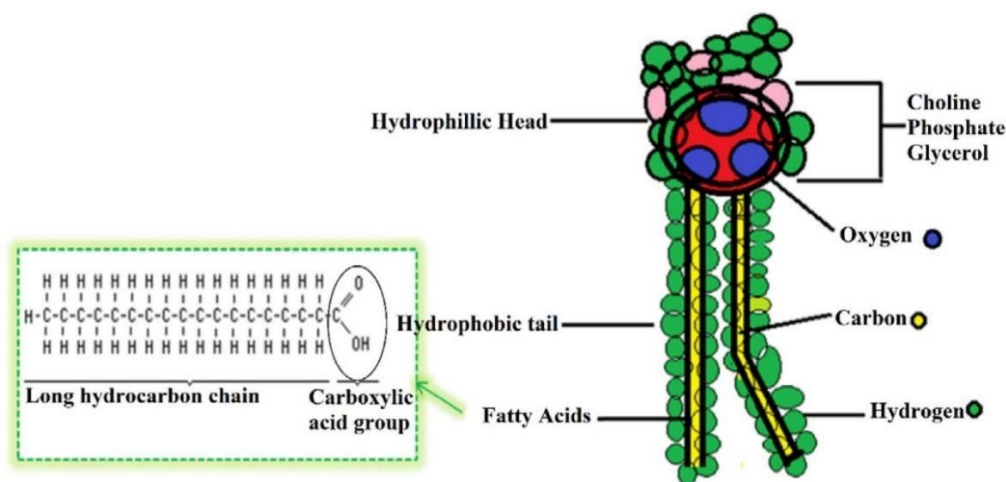
Figure 3: General structure and constituents of phospholipids (Manikandan *et al.*, 2019)

2.3   Vesicle formation

When exposed to an aqueous environment, phospholipids self-rearrange into bilayer vesicles and form a lipid bilayer (non-polar ends) that encloses the core structure (polar ends) (Ag Seleci *et al.*, 2016; Kundu *et al.*, 2018). The entropy of water hydrogen carbon interaction associated with the self assembly of lipids when dissolve to exceed Critical Micellar Concentration. (Huang *et al.*, 2017). In addition to vesicles like liposomes, the fabrication of lipid materials results in the synthesis of hexagonal phases, cubic phases, and micelles (Huang *et al.*, 2017; Jain *et al.*, 2014). During lipid assembly, a generally low energy equilibrium between the hydrophobic and repulsive interactions between the restricted head groups is reached (Kundu *et al.*, 2018).

Temperature, pH fluctuation, CMC, and lipid chemical structure, among other factors, influence the morphology and size of liposomes during their formation (Sych *et al.*, 2018; Ashok *et al.*, 2004). When double bonds are present in the lipid chain in the Cis or Trans

configuration, the melting transition temperature decreases (Monteiro *et al*., 2014). Liposome production is affected by changes in the geometry of the phospholipids' heads (Tapia *et al*., 2013). Depending on the form of the lipid molecules, micelles over bilayers may be preferred if electrostatic repulsion between the head groups is strong (Cooke & Deserno, 2006). When the head of a lipid molecule is larger than the tail, micelle formation occurs (Monteiro *et al*., 2014).

Under the CMC, a vesicle or planar membrane stable liposome forms when the head's size is comparable to the tail's size, turning the lipid molecule into an effective cylinder (Claessens *et al.*, 2007; Monteiro *et al.,* 2014). The temperature at which a lipid molecule enters a phase change is known as Tm (Miaorong Yu *et al.*, 2019). Under the transition point (Tm), lipid is a liquid, and above Tm, it is a solid (Zook & Vreeland, 2010). Temperature also influences membrane elasticity, viscosity, free energy, diffusion coefficient, and growth rate (Zook &Vreeland, 2010). Understanding lipid TM is crucial because it influence formation of liposomes; for instance, thin film hydration is sensitive to TM, which should be above for optimal lipid vesicle formation (Chen *et al*., 2018). Table 3 lists various phospholipids' transition temperatures.

Table 3: Transition temperature of some phospholipids

Name of phospholipids	Molecular weight	Transition temperature (TM)
DMPC	677.94	23
DOPC	786.12	-22
DSPC	790.15	55
DPPE	691.97	67
DPPC	734.05	41
DPPG	744.96	41

Phospholipid transition temperature: dipalmitoyl phosphatidyl ethanolamine (DPPE), dipalmitoyl phosphatidyl glycerol (DPPG), diocyl phosphatidyl choline (DOPC), distearoyl phosphatidyl choline (DSPC), and dimyristoyl phosphatidyl choline (DMPC).

2.4   Liposomes: Preparation and characterization

Liposomes (Fig. 4) are considered to be amphipathic lipid assemblies (Abdul *et al*., 2014; Aisha *et al*., 2014). When phospholipid interacts with the aquatic environment, it forms a vesicle construct (liposome) with hydrophilic part and hydrophobic part (Dua *et al*., 2012; Heneweer & Penate- Medina, 2012; Gao *et al*., 2013). The majority of liposomes are produced utilizing diverse methods (Fig. 5). The loading of the drug depends on its compatibilityin hydrophobic

or hydrophilic parts of liposome, normally loaded before or during preparation of liposome (Nsairat *et al*., 2022), however for lipophilic substance, and ionizable drug they are loaded through remote loading (Dua *et al.*, 2012).

The choices of the method for liposome preparation influencies lamellar structure, morphology and size of liposome (Lombardo & Kiselev, 2022). The major steps for formation of lipid film are dissolution of lipid in organic solvent followed by solvent removal by using rotary evaporation (Chen *et al*., 2019; Dua *et al*., 2012). The liposome formed by dissolution of lipid in organic solvent followed by hydration results into formation of large vesicles (Varona *et al., 2012;* Mansoori *et al*., 2012; Zhang, 2017). Coupling the lipid thin film hydration technique with sonication method enabling reduction of liposome into small Unilamellar (Cho *et al.*, 2013).

The sonic energy supplied by a probe or bath sonicator in sonication procedures effectively forms liposomes with sizes ranging from 15 to 50 nm (Dua *et al*., 2012). Bath sonication is generally preferred over probe sonication since the probe can emit titanium oxide and excessive heat, which can contribute to the breakdown and degradation of liposomes (Hadian *et al*., 2014). French pressure cells are a more rapid, and reproducible method than sonication, which includes the extrusion of huge multilamellar vesicles through a small aperture (Ojha & Sharma, 2018). Reverse-phase evaporation involves the formation of water in oil emulsions by brief sonication of a two-phase system containing phospholipids in an organic solvent and an aqueous buffer (Watwe & Bellare, 1995). Reverse-phase evaporation method entails formation of water in oils emulsions by removing organic solvent under reduced pressure. In this method the formation of liposome occurs when organic solvent is removed. The application of rotary evaporation enabling the removal of organic solvent (Fathalla *et al.*, 2015; Shi & Qi, 2017).

During ethanol injections, a lipid solution dissolved in ethanol is gently injected to the drugs dissolved in buffered aquous media (Bnyan *et al*., 2020). Following the elimination of ethanol by rotary evaporation, liposomes were formed (Gouda *et al*., 2021). Solubilizing lipids has been accomplished with detergents at crucial micelle concentrations (Keller *et al*., 2005). The detergent is removed once the lipids have been solubilized using dialysis, dilution, or column chromatography (Lombardo & Kiselev, 2022). Jiskoot *et al*. (1986), for example, produced liposomes by mixing micellar solutions containing octyl glucoside and egg phosphatidylcholine; dialysis was employed to remove detergent and was more effective than washing octyl glucoside.
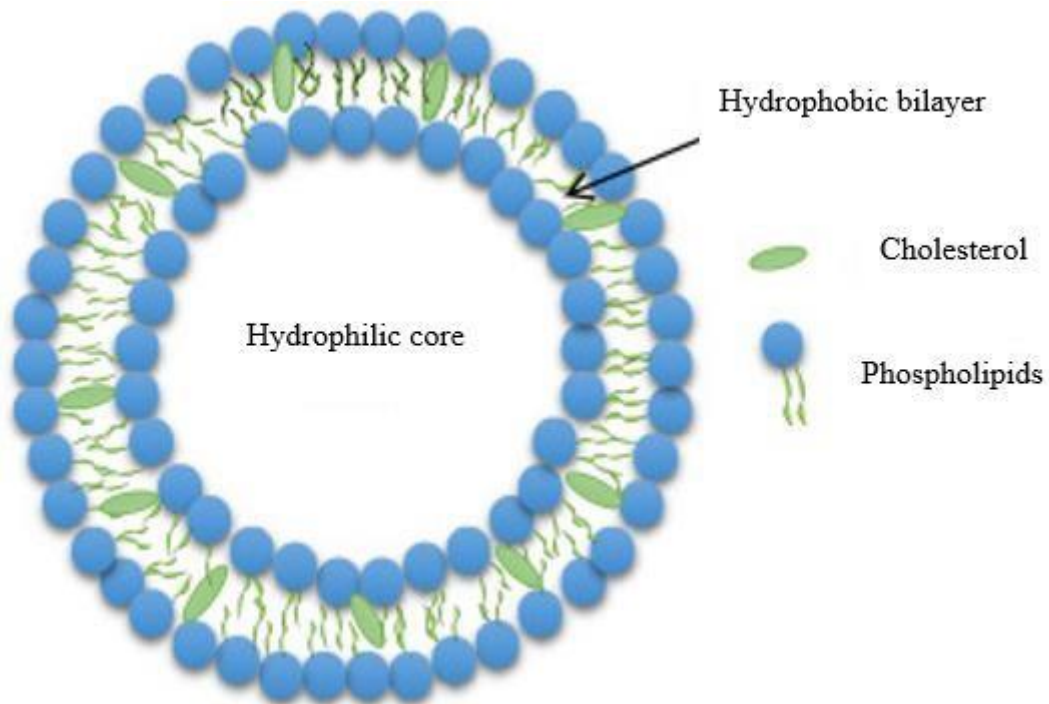
Figure 4: Liposome structure (Nsairat *et al*., 2022)
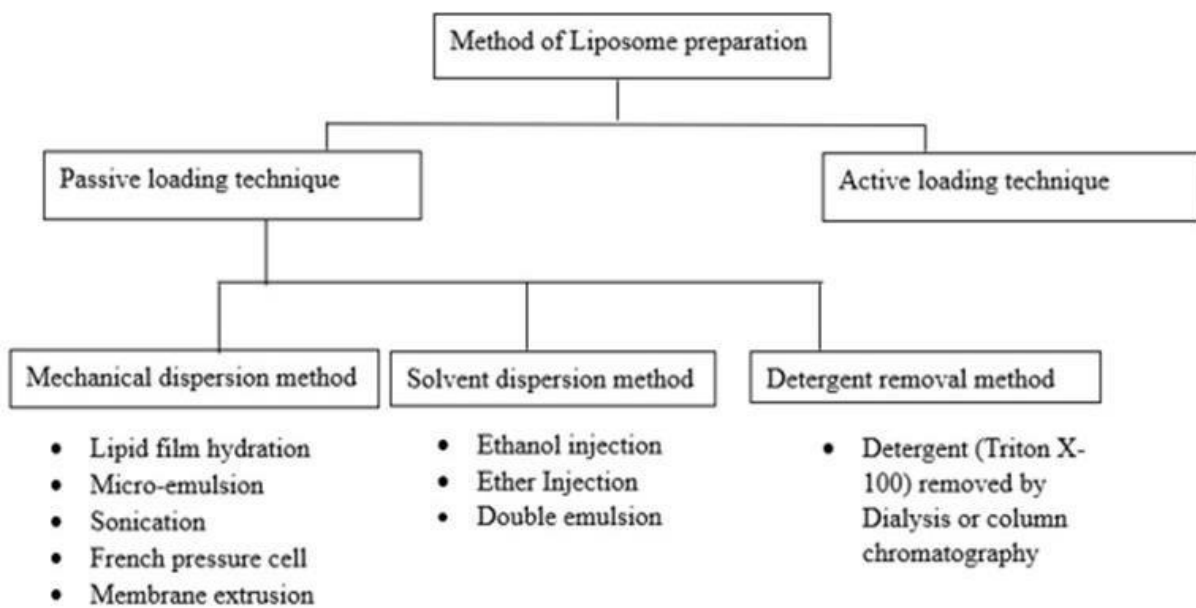
Figure 5: Method of liposome preparation (Dua *et al*., 2012)

Table 4: Different methods for nanoparticle characterization reported by Raliya *et al*. (2016)

Nano particle properties	Microscopy technique	Centrifugation and filtration technique	Spectroscopy and technique
Agglomeration	STEM, TEM, SEM, AFM, STM		
Nanomaterial structure	AFM, CFM		NMR, XPS, Auger AES, AAS, ICP-MS/OES, XRD, EBSD
Particle concentration	AFM, CFM		
Morphology	STEM, TEM, SEM, AFM, STM		
Particle Size/dimension	STEM, TEM, SEM, AFM		
Size distribution	STEM, TEM, SFM, AFM	CFF, UC, CFUF	SPMS, SAXS
Dissolution		Dialysis, CFUF	
Speciation structure	STEM, TEM, SEM, AFM, STM		XAFS, XRD, SANS
Surface area and porosity			
Surface chemistry	AFM, CFM		FTIR, Raman spectroscopy

STEM stands for Scanning Transmission Electron Microscope; TEM stands for Transmission Electron Microscopy; SEM stands for Scanning Electron Microscopy; AFM stands for Atomic Force Microscope.STM stands for Scanning Tunneling Microscope.CFF stands for cross-flow filtration. CFUC stands for cross-flow ultrafiltration. SANS: small-angle neutron scattering; XRD: X-ray diffraction NMR stands for nuclear magnetic resonance. XPS stands for X-ray photoelectron spectroscopy; AES stands for Auger electron spectroscopy; and AAS stands for atomic absorption spectroscopy. ICP-MS/OES stands for inductive coupled plasma mass spectrometry and optical emission spectrometry. EBSD stands for electron backscatter diffraction. SPMS stands for solid phase molecular spectroscopy. SAXS stands for short angle x-ray scattering spectroscopy, and XAFS stands for X-ray absorption fine structure. CPC is for condensation particle counter; DMA stands for differential mobility analyzer; and UCPC stands for ultrafine condensation particle counter. SMPS stands for scanning mobility particle sizer. FTIR: Fourier Transform infrared, BET: Brunauer-Emmet-Teller.

2.5   Challenges of liposomes as drug delivery system

Liposomes may deliver pharmaceuticals and nutrients (Shade, 2016; Wen *et al.*, 2011) and remarkably a potential drug delivery system nevertheless challenges have been identified, including stability problems, short half-lives caused by modifying the permeability of the lipid bilayer membrane, leakage, and drug fusion (Chen *et al.*, 2019; Lee & Thompson, 2017). According to this review, lipid peroxidation, lipid hydrolysis, changing the transition temperature, and nanoparticle aggregation are some of the factors that impair liposome delivery (Ayala *et al.*, 2014). Lipid peroxidation occurs when polyunsaturated acid chains and free radicals interact to produce dienes (Catalá, 2013; Sadak *et al.*, 2020).

In the presence of acidic and basic environments, liposomes hydrolyze into fatty acid and glycerol phospholipid molecules, facilitating degradation and short lifetimes (Ayala & Arguelles, 2014; Ickenstein *et al.*, 2006). Tc is the temperature at which the lipid bilayer membrane loses its ordered packing and becomes much more fluid. The bilayer membrane's permeability rises. The increase in Tc allows the things within to leak out, reducing liposome stability (Yu *et al.*, 2019). Liposome aggregation occurs when liposome vesicles come together and bind (Toh & Chiu, 2013; Rosická & Embera, 2013).

2.6   Liposome as drug delivery and surface modification.

Fundamentally, the presence of phosphate groups at the phospholipid allows for functionalization (Shariare *et al.*, 2020; Weingart *et al.*, 2013; Liu *et al.*, 2022; Toh & Chiu, 2013; Liu *et al.*, 2022). The loading of herbal drugs into liposomes has improved their efficacy against infections, as shown in Table 5. The negatively charged moieties on the liposome's surface allow it to interact with molecules such as inorganic oxide and biopolymers (Shashidhar & Manohar, 2018; Fu & Kao, 2010). Liposome-based polymeric surface functionalization, for example, provides a stable liposomal system and improves stimuli-responsiveness (Cao *et al.*, 2022; Sriwidodo *et al.*, 2022). Liposomes typically contain polymers by grafting or coating (Fig. 6).
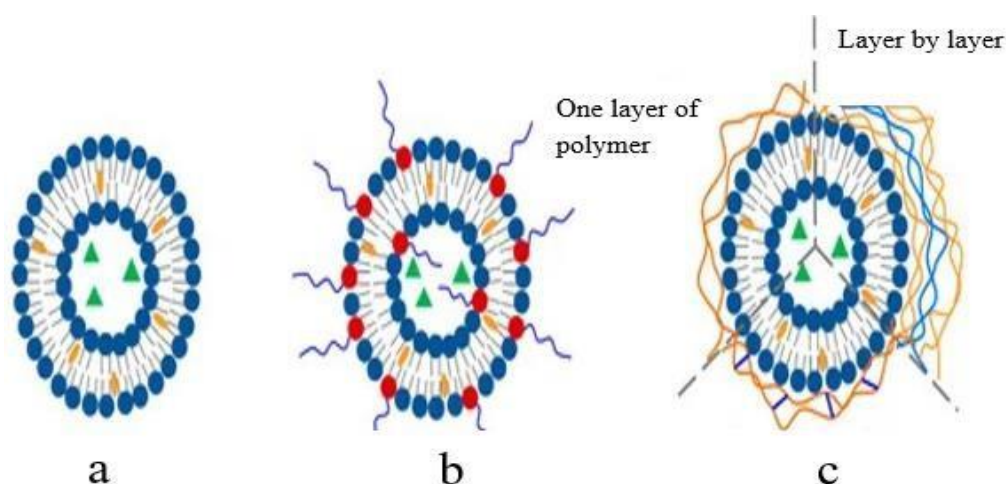
Figure 6: Liposome -polymer functionalization: conventional liposome (a), polymer-grafted liposome (b), polymer-coated liposome (c), (Yifeng Cao *et al.*, 2022)

Table 5: Phytoconstituents loaded in liposome delivery system and activity

Plant extract/Phytoconstituents	Activity	Reference
Atractylodes Macrocephala extract /Sesquiterpenes	Antiviral	Wen *et al*. (2011)
Panaxquinguefolus extract /Saponin	Antioxidant	Hao *et al*. (2016)
Polygonum aviculare extract /Quercetin	Antiviral	Chen *et al*. (2019)
Orthosiphon stamineuse extract /Rosmarinic acid	Antioxidant	Aisha *et al*. (2014)
Silybum marianum L/Silymarin	Anti-carcinogenic and anti-inflammatory effects.	Piazzini *et al*. (2018)
Bergamol essential oil	Anticancer	Celia *et al*. (2013)
Roselle extract	Antioxidant	Gyamera and Kim, (2019)
Thymus species extract	Antibacterial and antioxidant	Gorzi *et al*. (2006)
Liposome loaded linolenic acid (LipoLLA)	bactericidal activity	Obonyo *et al*. (2012)

The primary source of phospholipid used in the manufacturing of conventional liposomes is vesicles, which are used to encapsulate pharmaceuticals such as herbal medicine. Several liposome preparation methods have been discussed. For example, lipid thin hydration can be combined with sonication to modify the size from giant multilamellar vesicles to small

unilamellar vesicles. Conventional liposomes serve as the foundation for modifying feasible drug delivery via surface functionalization. The modifications result in a more stable and high-performance distribution system.

2.7   Chitosan

Chitosan is a versatile biopolymer used for drug administration. The potential sources of chitosan are fungi, insects, and crabshells, which are embedded in their exoskeleton (Cheung *et al.*, 2015; Aranaz *et al.*, 2021). Chitosan is extensively used for drug delivery because of its properties, including mucoadhesion, bioactivity, compatibility with cellular tissues, and biodegradability (Ahmed *et al.*, 2019; Elieh-Ali-Komi & Hamblin, 2016; Zhao *et al.*, 2018). Chitosan has the ability to chelate several mettalic ions (Jimenez-Gomez & Cecilia, 2020; Szymanska & Winnicka, 2015).

Chitosan's primary functional groups are the hydroxyl and amine groups (Mourya & Inamdar, 2008). Through hydrogen bonding and electrostatic attraction, these groups facilitate chitosan's mucoadhesive characteristics (Szymanska & Winnicka, 2015). Normally, enzymes such as lysozymes and chitonase (Andrea *et al.*, 2017) convert chitosan into small molecular fragments known as monosaccharides and oligosaccharides (Horn *et al.*, 2012; Qiu *et al.*, 2022). Chitosan's use is impeded by its weak solubility as well as its limited antibacterial action (Zhao *et al.*, 2018). To increase solubility and antibacterial activity (Herdiana *et al.*, 2022; TM *et al.*, 2018), chitosan derivatives are generated by altering the ammonium and hydroxyl groups of chitosan (Jess *et al.*, 2018).

A wide range of compounds have been incorporated with chitosan for delivery (Kravanja *et al.*, 2019). Among these materials involve phytomedicine (Riccucci *et al.*, 2021), lipid nanoparticles such as liposomes (Henriksen *et al.*, 1994), and inorganic nanoparticles (Farouk *et al.*, 2012). Integration of chitosan with the aforementioned material improves some properties, including protection from gastrointestinal fluid digestion (Pathomthongtaweechai & Muanprasat, 2021), improved drug-pathogen binding affinity (Mikuová & Miku, 2021), improved solubility and shelf life, controlled drug release, reduced toxicity, and enhanced stability (Amin & Boateng, 2022).
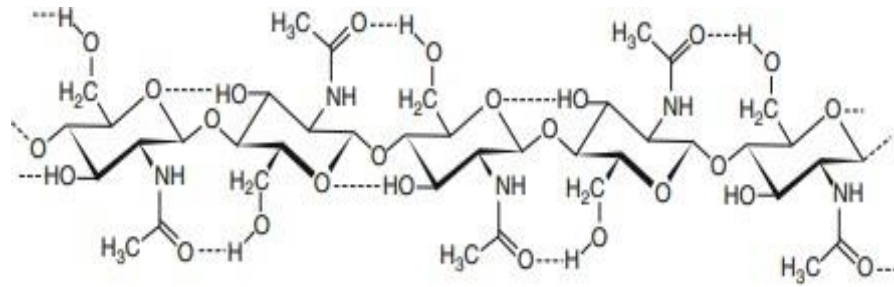
Figure 7: Chitin's chemical structure with intramolecular hydrogen bonding (dotted lines) (Zikakis, 2012)

NaOH, KOH, Na$_2$SO$_3$,25-100 ^{0}C, 0 - 2.5M for 72h

Acetone, Ethyl/alcohol, diethylether, KMnO$_4$, NaClO, H$_2$O$_2$,20-60^{0}C, 0.25 − 12 h

Crustacean waste → Protein removal → Mineral removal → Pigment removal → Chitin → Chitosan

Washing and grinding

HCl, HNO$_3$, CH$_3$COOH, HCOOH, 25-100 ^{0}C,0.5-48h,0.1-0.2M

Deacetylation: NaOH/KOH (30-50% w/v),80-150 ^{0}C,1-8h
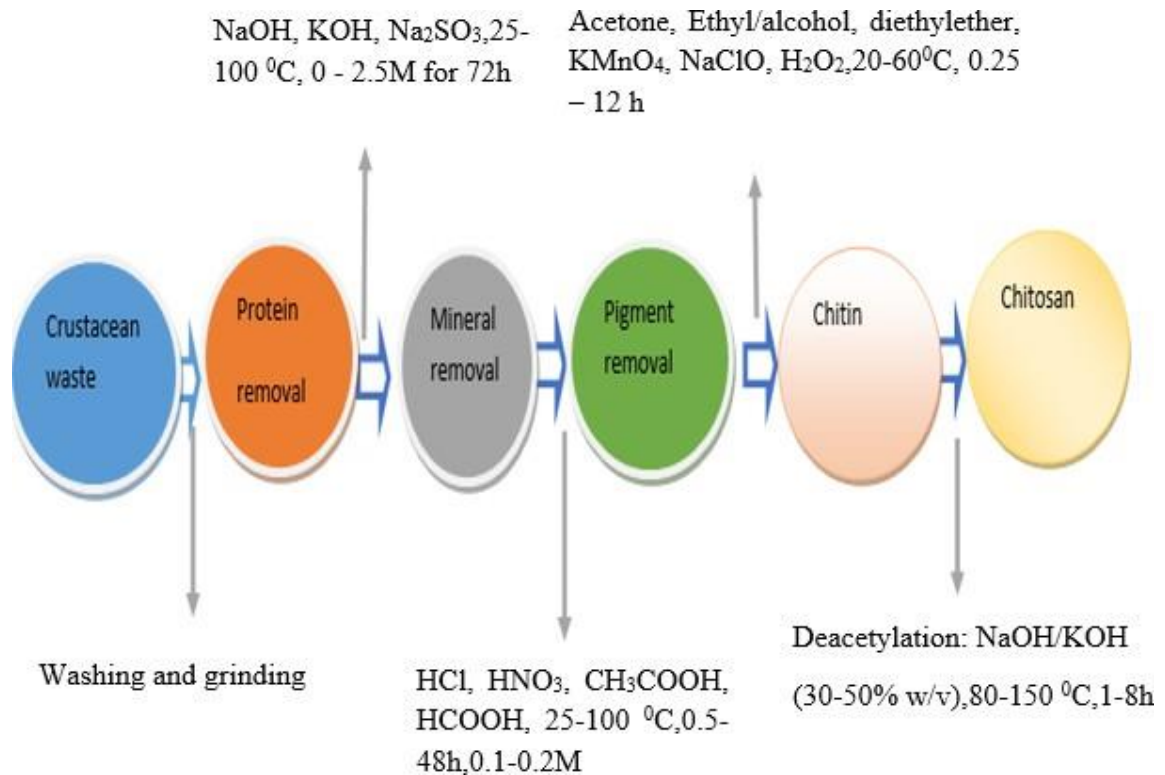
Figure 8: Schematic synthesis of chitosan from crustacean waste (Kannan *et al.*, 2021)
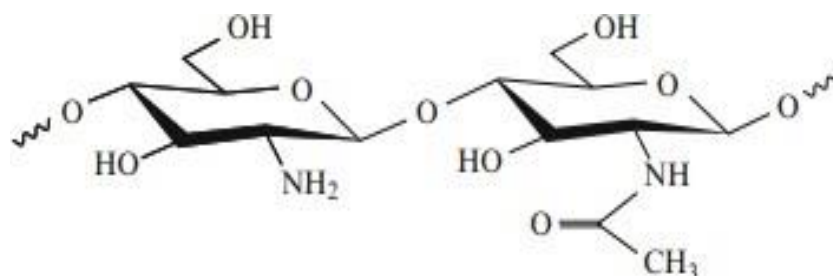
Figure 9: Chemical structure of chitosan (Zikakis, 2012)

The polycationic surface of chitosan interacts electrostatically with the bacterial cell wall, causing the membrane to rupture (Fernandes *et al.*, 2014; Mourya & Inamdar, 2008). The electrostatic interaction between negatively charged bacteria and cationic surfaces causes more significant cell membrane rupture in Gram-negative bacteria (Auer & Weibel, 2017). Gram-negative bacteria have higher chitosan polycation binding strength than Gram-positive bacteria, which lack lipopolysaccharide molecules (Fig. 10), (Ke *et al.*, 2021). Lipopolysaccharide molecules are very negatively charged (Ke *et al.*, 2021). These negativelycharged molecules have a higher affinity for the positive ions that are largely produced with the nanoparticles, resulting in a buildup and increased uptake of ions that eventually cause intracellular damage (Slavin *et al.*, 2017).
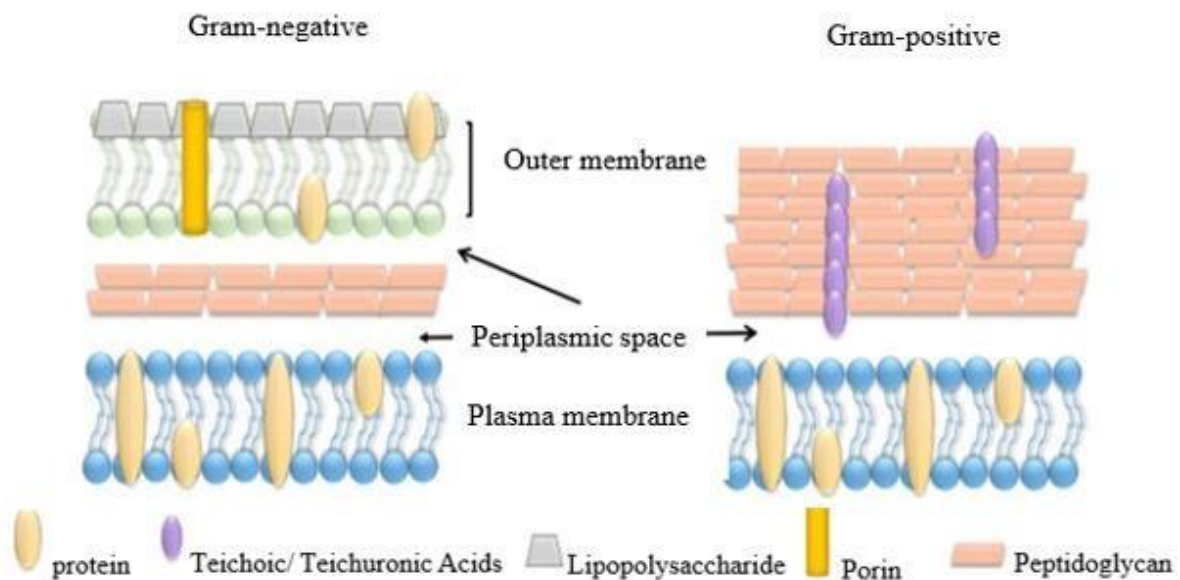
Figure 10: Structure of bacterial cell wall (Slavin *et al.*, 2017)

The structure of the bacteria affecting antimicrobial susceptibility (Khameneh *et al.*, 2019; Makhlouf *et al.*, 2023) The Gram-negative bacteria contain a lipopolysaccharide layer enriched with anionic charges (Khare *et al.*, 2021; Wintola & Afolayan, 2015). This feature provides a prominent binding with positive charges in fabricated polymeric antibacterials. The polycationic nature of chitosan due to protonated NH_3^+ provides a versatile binding to the anionic site of the bacteria. Since the Gram-positive bacteria lack lipopolysaccharide (Auer & Weibel, 2017), the binding force exhibited at its cellular surface with polycationic ions is lower as compared to the binding exhibited between the Gram-positive bacteria and the fabricated positively charged surface of the chitosan (Kravanja *et al.*, 2019; Piekarska *et al.*, 2023; Gupta *et al.*, 2020; Jackson *et al.*, 2018; Kravanja *et al.*, 2019; Wang *et al.*, 2006)

2.7.1   Chitosan-metal complex

Chitosan metal complexes are generally formed by the Lewis-base reaction (Ardean *et al.*, 2021; Rashid *et al*., 2018; Yan *et al*., 2021). The complex formed modified the binding affinity of the bacterial cellular wall. The mettalic ion referred to as super acid provides extensively higher antibacterial activity than that exhibited by the polycationic surface of chitosan (Kong *et al*., 2022).
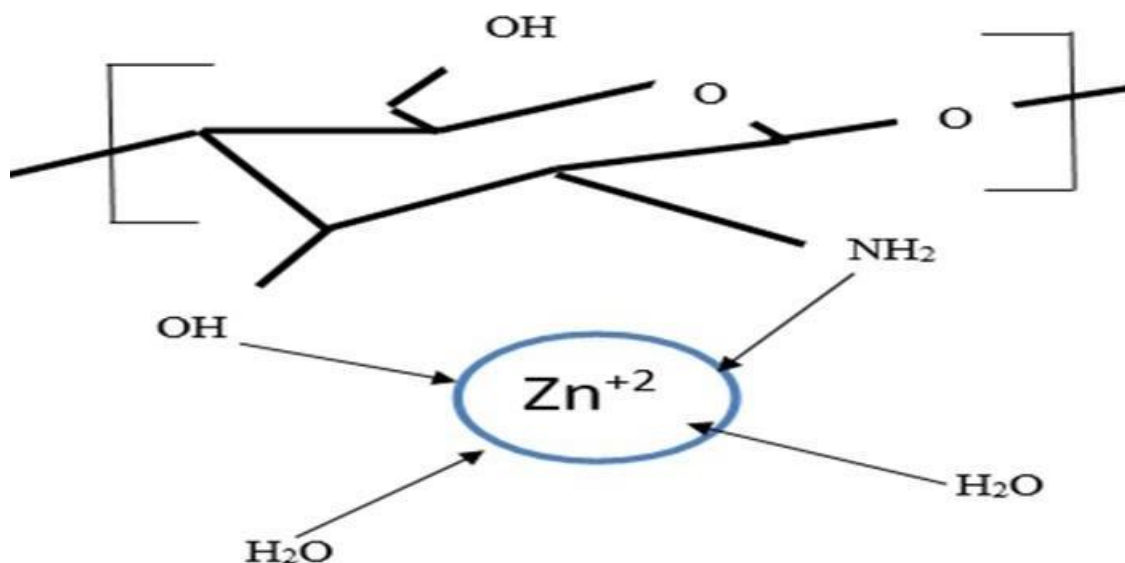
Figure 11: Chitosan-Zinc (II) complex (Yazdani *et al.*, 2018)

2.7.2   Chitosan coated Liposome

The effect of fusion of the liposome in a colloidal system allows the discharge of its internal components (Nkanga *et al*., 2020; Zhou *et al*., 2021). This phenomenon led to the decline of its stability (Nsairat *et al.,* 2022). The adhesion of the polycationic layer of chitosan to the surface of the liposome confers stability. The advantage of integrating chitosan on the surface of the liposome layer is accredited to the control release mechanism for modulating drug release. Release (Herdiana *et al*., 2022).

This is congruent with the findings of Mohammadi *et al*. (2016), who coated DPPC liposomes and investigated the rate of doxorubicin release from the chitosan-liposomal system (Mohammadi *et al*., 2016). According to the published results, the uncoated liposome releases doxorubicin more quickly than the coated system. A plane liposome's rapid disintegration makes it unstable (Pandur *et al*., 2020), resulting in a larger release rate (Fig. 13) than a coated

system, which slows down the release (Hawthorne *et al*., 2022). To maintain effective concentrations and avoid toxicity, drug releases in biomedical applications should adhere to a control pattern (Sung & Kim, 2020). Chitosan is a popular biomaterial that is included into liposomes to prevent the negative effects of instability in uncoated systems (Mengoni *et al*., 2017).
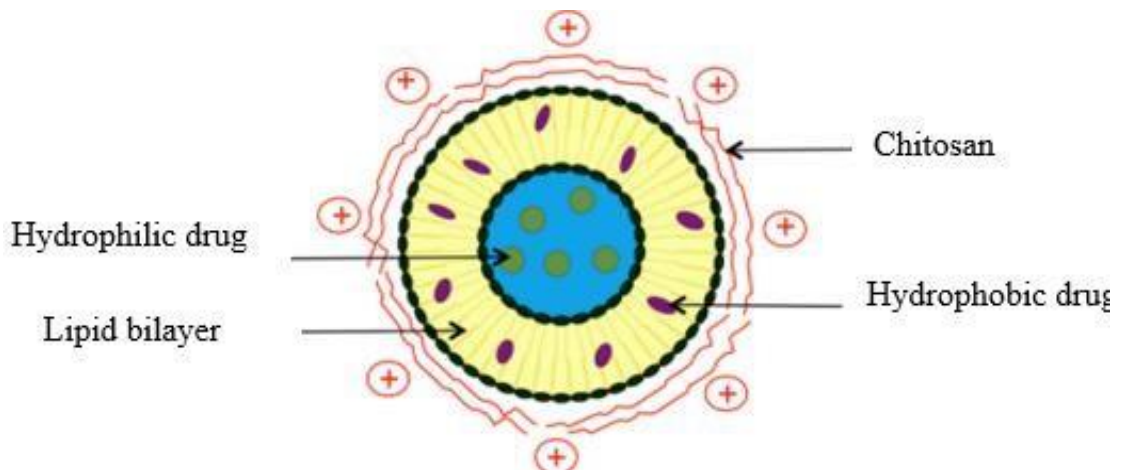
Figure 12: **Chitosan coated liposome loaded hydrophilic and hydrophobic drug as reported by Mady and Darwish (2010)**
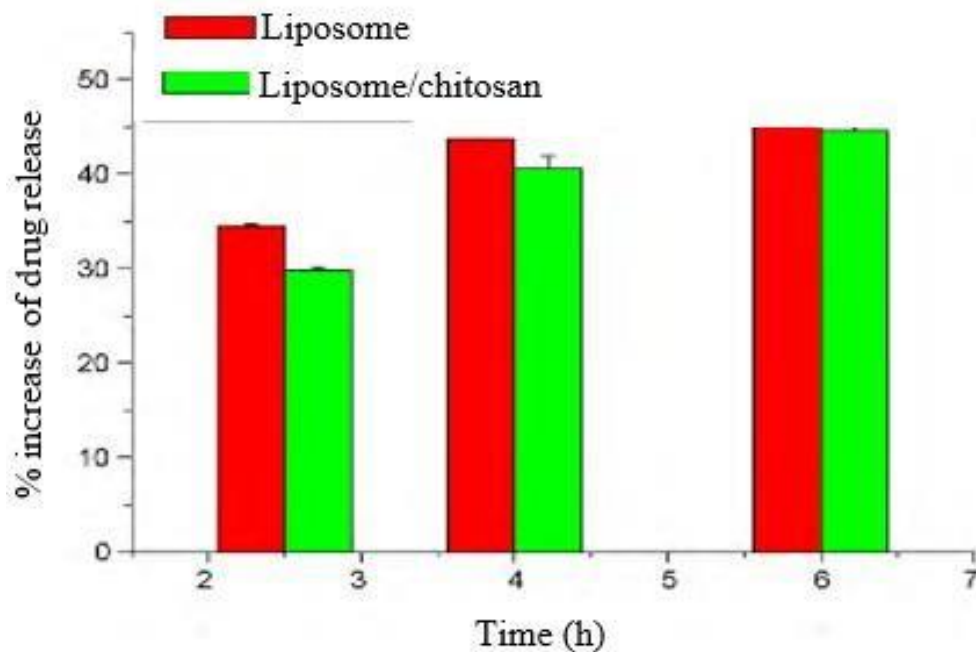
Figure 13: Percentage increase of drug release from liposomes and chitosan- coated liposome as reported by Mady and Darwish (2010)

2.7.3   Future trends for antimicrobial applications of chitosan-based materials

In the future, chitosan derivatives (Wang *et al*., 2020) may be able to display "release on command" systems, in which an antimicrobial agent is released concurrently with microbial growth, in addition to increasing antibacterial properties and offering a stable system. In the future, these technologies will be used on antimicrobial materials associated with modern technology. The principle behind this technology is that when microbial action presents itself in the medium, such as a change in pH (Alrbyawi *et al*., 2022), temperature (Ta & Porter, 2013), or UV radiation (Barhoumi *et al*., 2015; Spratt *et al*., 2003), the antimicrobial system responds promptly and properly. As a result, such a mechanism would only operate in response to very specific circumstances. This technology is based on bioactive substances, the release of which is activated at the precise moment and location where it is required. The common assumption is that if one or more types of bacterial growth occur, antibiotic substances will be generated, blocking the growth of new bacteria. Of course, this would allow for a reduction in the amount of active agent required to produce an effect.

2.8   Inorganic nanoparticles

Inorganic nanoparticles are gaining importance as prospective delivery strategies in recent years (Patra *et al*., 2018). Targeting the delivery property and efficacy of natural therapeutic agents against pathogens, the functionalization of phytoconstituents into inorganic nanoparticles has been extensively explored (Patra *et al*., 2018; Rudramurthy *et al*., 2016). For instance, it has been demonstrated that zinc oxide-curcumin (ZnO-Cum) core shell nanoparticles exhibit better antibacterial activity than the widely used antibiotic amoxicillin against a variety of microorganisms.

Inorganic nanoparticles are potential material for the delivery of drugs and pharmaceuticals due to to their distinctive physical properties, such as electronic, catalytic, magnetic, and optical (Agarwal *et al*., 2018; Chen *et al*., 2016; Ojea-Jimenez, 2013). Inorganic nanoparticle stability in colloid environments has been achieved through surface functionalization by a variety of ligands (Chen *et al*., 2016). Functionalization enhances pharmacokinetics and lessens the toxicity effect by preventing aggregation, protecting their surface from oxidation, and providing a surface to conjugate drug and target ligand (Amina & Guo, 2020; Ghaffari *et al*., 2017; Lee *et al*., 2017). For instance, Rajan *et al*. (2019) asserted that the production of

magnetite with zinc oxide and graphine oxide (Fe3O4@ZnOrGO) improved antibacterial activity

Additionally, inorganic nanoparticles exhibit distinct biological behavior and an extensive range of physiochemical multifunctionality (Pandey & Dahiya, 2016). Some inorganic nanoparticles, such as silver, AgNPs (Buszewski *et al*., 2016), superparamagnetic iron oxide nanoparticles, SPION (Beyth *et al*.,2015), titanium oxide, TiO$_2$NPs (Santa *et al*., 2020), copper oxide, CuNPs, (Khalid *et al*., 2021), and zinc oxide (ZnONPs), exhibit antibacterial activity by generating reactive oxygen species (Abdal Dayem *et al*., 2017). According to Hatamie *et al*. (2015) and Marassi *et al*. (2018), zinc oxide and silver oxide have been widely employed as fabric and coating materials in medical devices. Although less potent than AgNPs and ZnONPs, copper oxides have antibacterial action through disrupting membranes (Beyth *et al*., 2015).

2.8.1 Zinc oxide nanoparticles

In contrast to other inorganic nanoparticles, zinc oxide nanoparticles (ZnONPs) have evolved into a versatile delivery system for pharmaceutical and herbal medicine (Agarwal *et al*., 2018). This is because ZnONPs have special properties like being electronic and optical, displaying a broad spectrum of activity against various microorganisms (Vankataraju *et al*., 2014), and having high biocompatibility. ZnO has been validated by the US Food and Drug Administration (FDA) as a food and drug precursor (Zhang *et al*., 2013). According to Fig. 14, when nanoparticles enter a cell membrane, they disrupt the lipid bilayer, allowing molecules like adenosine triphosphate (ATP) and lipolysaccharides to discharge out of the cell, blocking the transport of potassium ions (K$^+$), which results in cell death (Slavin *et al*., 2017; Yin *et al*., 2019), or affecting bacterial cell integrity by lowering negatively charged potential.
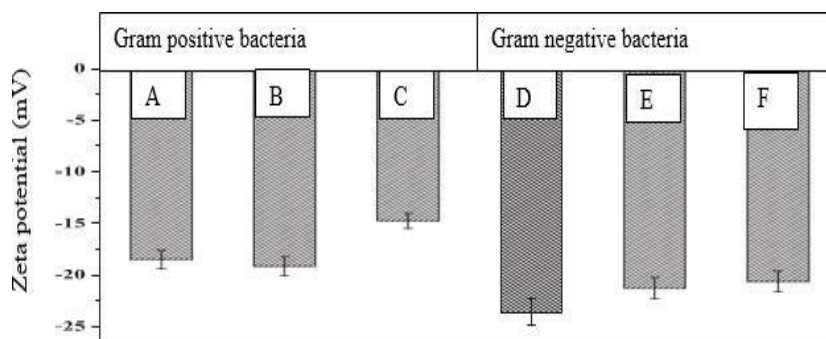
Figure 14: Zeta potentials of Gram positive and Gram-negative bacteria as reported by Arakha *et al*. (2015): *Bacillus subtilis (A); Staphylococcus aureus (B); Bacillus thuringiensis(C); Escherichia coli (D); Proteus vulgaris (E); Shigella flexneri (F)*

Zn^{2+} is produced when zinc oxide is dissolved in aqueous solutions; this metal attaches to the negatively charged cell wall and aids in cellular death (Siddiqi *et al*., 2018). When in contact with zinc oxide nanoparticles, UV-visible rays (Fig. 15) cause electrons to move from the valence band to the conduction band (Johar *et al*., 2015). When the holes at the valence band detach hydrogen from water to produce a hydroxyl radical, this results in the generation of ROS (Wang & Shao, 2017). A superoxide radical is produced when an electron in the conduction band binds with molecular oxygen, and hydrogen peroxide is generated when additional free radicals combine (Hubenko *et al*., 2018). In contrast to other radicals, hydrogenperoxide has the ability to penetrate the cell membrane, where it reacts with a biological component and damages the cell (Wang & Shayo, 2017).
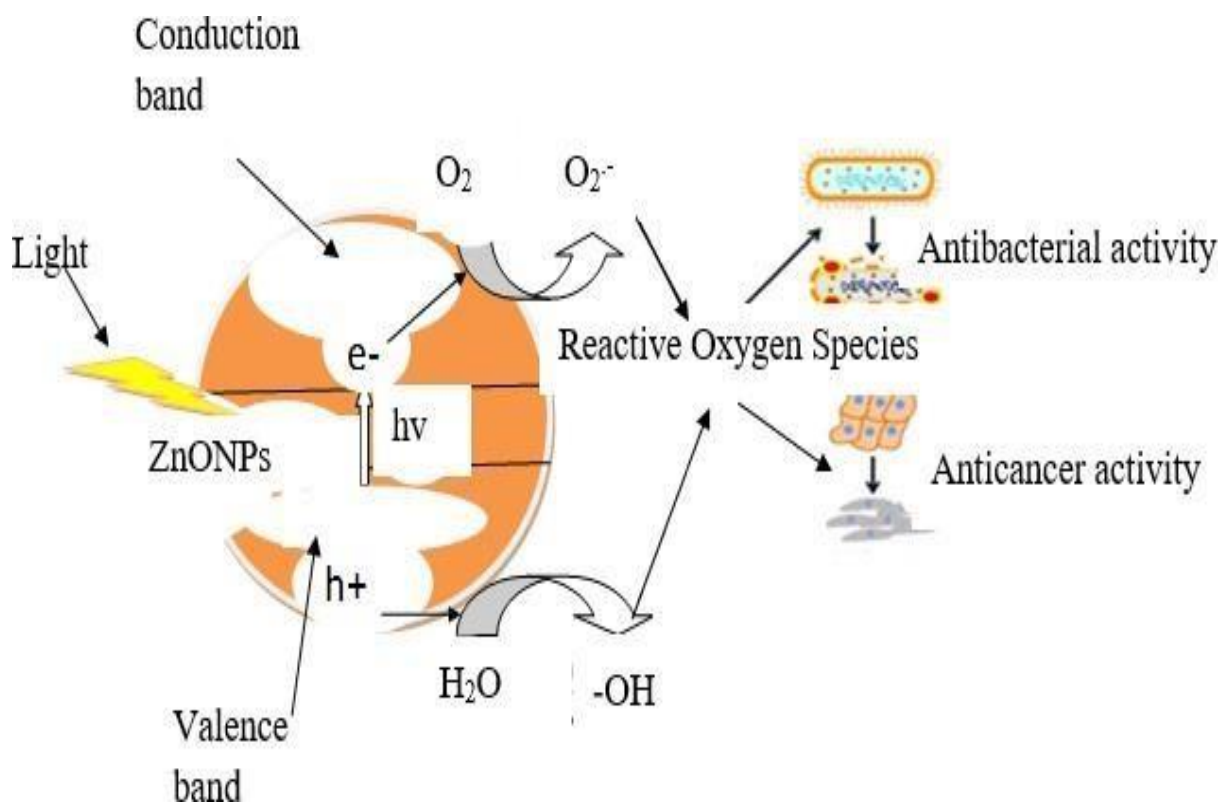
Figure 15: Production of ROS by ZnO nanoparticle (Sivakumar *et al.*, 2018)

According to Slavin *et al*. (2017) and Lobo *et al*. (2010), free radicals can oxidatively damage bacterial molecules like DNA, lipids, and proteins. Due to its improved ability to deliver therapeutic compounds to their intended targets, ZnONP surface engineering has recently attracted a lot of attention (Sadhukhan *et al*., 2019). According to Grigoletto *et al*. (2021; Yetisgin *et al*., 2020), the conjugation with a natural therapeutic agent makes it easier to transport the therapeutic agent to the biological target. For instance, curcumin was given to MCF-7 breast cancer cells utilizing synthesized phenylboronic acid (PBA)-ZnONPs. ZnONPs

in this combination made it easier for curcumin to reach the breast cancer cell membrane's sialic acid, which was overexpressed (Kundu *et al*., 2019). In addition to the ZnONPs' pH- sensitive assistance in drug delivery, ZnO-NPs' changing surface charges have significant effects on payload delivery.

Shome *et al*. (2021) evaluated the change in ZnONPs surface charge and size of the generated curcumin-ZnONPs and reported that the hydrodynamic size of the curcumin changed from 410 nm to 224 nm and the zeta potential of the curcumin changed from -25 mV to -15.9 mV when the curcumin-ZnONPs nanocomposites were formed. The improvement of antibacterial activity was caused by a rise in positive charges and a fall in hydrodynamic size (Ardean *et al*., 2021; Han *et al*., 2022). While the reduction in size makes it easier for the active principle to enter the bacterial cell and increase the antibacterial activity against *E. coli* and *S. aureus*, the increase in positive potential enables electrostatic binding of nanoformulations to negatively charged bacterial cellular surfaces (Forest *et al*., 2015; Wieszczycka *et al*., 2021; Zhang *et al*., 2023; Ghalandarlaki *et al*., 2014).

Caffeic acid has no antibacterial action, while fabrication of ZnO@Caffeic acid was found to exhibit better antibacterial activity against a wider spectrum of bacteria than when ZnO and Caffeic Acid were treated alone (Choi *et al*., 2017). In other research, it was discovered that functionalized curcumin with ZnO showed improved antibacterial activity to that of the widely used antibiotic amoxicillin (Varaprasad *et al*., 2019). In this study, zinc nitrate and curcumin were used as precursors to produce zinc oxide-curcumin (ZnO-Cum) core shell nanoparticles using the ultrasonication method (Fig. 24). Strong antibacterial activity was demonstrated against Gram-negative bacteria (*E. coli*) and methicillin-resistant S. aureus. An XRD pattern of zinc oxide at Caffeic acid (ZnO at CA) nanoparticles reveals a mean crystallite size of about 20 nm (Ebin *et al.*, 2012).

2.8.2 Inorganic nanoparticle: Functionalization and delivery of natural therapeutics

According to Sanità *et al*. (2020), functionalization is the conjugation of several compounds that results in changed surfaces in terms of their physical, chemical, and biological properties. The improved features considerably reduce chemical reactivity, oxidation, as well as rapid agglomeration, and they also give nanoparticles stability in colloidal environments (Guerrini *et al*., 2018). Modified surfaces also show evidence of drug transport to the biological target and control drug release. (Ojha, 2020). It has been suggested that inorganic nanoparticle

functionalization can enhance the medicinal potential of natural compounds (Luchini & Vitiello, 2019). Some biomolecules, including polyphenols, flavones, and quinones, have undergone functionalization to increase their anti-pathogen therapeutic action.

Nanoantibacterial materials with a variety of uses include inorganic nanoparticles. Several inorganic nanoparticles are employed as antibacterial agents. Due to their reduced toxicity, biocompatibility, and capacity to function as an essential component of the human body system, ZnO nanoparticles are preferred for developing of inorganic nanodelivery systems. ZnO nanoparticles produce Zn^{+2} in an aquos environment, which also serves as an immunomodulator, micronutrient, and a substance that prevents the growth of broad-spectrum infections.

CHAPTER THREE

MATERIAL AND METHOD

3.1   Material

3.1.1   Reagents

Sodium triphosphate (Sigma Aldrich, Missouri, USA), Sodium hydroxide (B&M Scientific Cape town, South Africa), Zinc acetate (Sigma Aldrich, Missouri, USA), Chitosan (Sigma Aldrich), Nutrient broth (Biolab MERCK No 1024537), α-L-Phosphatidly choline (Sigma Aldrich), Invitrogen Alamar Blue (DAL1025 873186), Glacial Acetic acid (Cameron Chemical Consultances). Sodium cholate, pepsin, pancreatin, Triton X-100, purchased from chemical & school supplies Limited (Nairobi, Kenya).

3.1.2   Equipments

Centrifuge machine (Heraeus sepatech), Vortex (Benchmarks, Bench mixer), Magnetic stirrer (FMH-Instruments), Homogenizer (IKAT18 digital VLTRA TURRAX), PH-Meter (Xs instruments E utech Instruments pH 2700 Wirsam), Bath Sonicator (Scientech ultra sonic cleaner), Weigh balance (Adventure OHAus), Perkin Elmer Spectrum 400ET-IR-NIR-Spectrometer, Oven (Ecotherm LaboTec), Probe sonicator (Bandelin Sonopuls), Zeta potentiometer (Malven 2590), Plate reader (POLAR star Omega Plate reader), Shaker (The Belly dancer STOVALL LIFE SCIENCE Greenboro NC USA), Orbital Shaker Incubator (YIHDER LM-530), Biosafety Cabinet (LaboTec),Incubator (Forma Scientific), Virtis Bench Top2K, 4K,and 6K freeze dryers. Tescan MIRA 3 SEM (Tescan, Brno, Czech Republic)

3.2   CsP phytochemical extraction and screening

3.2.1   Collection and preparation of medicinal plant

Between May and June of 2019, the leaves of CsP were collected in Loliondo (Tanzania). The leaves were placed in plastic bags and delivered to the laboratory at the Nelson Mandela African Institution of Science and Technology (NM-AIST) for further processing. The leaves were dried under shade for a month at the NM-AIST laboratory. The leaves were turned into powder using a blender when they had completely dried. The CsP powder was then kept in a desiccator until it was utilized for extraction.

3.2.2 The CsP extraction

The extraction procedure was carried out at the African Technical Research Center's (ATRC) analytical laboratory in Arusha, Tanzania. The powder of *Carrisa spinarum* (200 g) were soaked in 500 ml of methanol and macerated for two days. The macerated leaves underwent rotary evaporation after two days to produce a crude solvent extract. To get rid of any remaining coarse particles, the unfiltered extract was filtered through filter paper (Whatman No. 1). A rotary evaporator was used to concentrate the filtered product, which was then kept refrigerated at 4 °C. Water, petroleum ether, and chloroform were used to replicate this technique, but the water extract was concentrated using a freeze-dryer.

3.2.3 Qualitative phytochemical analysis

Phytochemical analysis was performed to determine the presence of phytoconstituents such as alkaloids, flavonoids, phenols, terpenoids, steroids, Coumarins, resins, tannins, xanthoproteins, quinines, carboxylic acid, oxyalates, carbohydrates, glycosides, proteins, and saponins using the method developed by Shafodino *et al*. (2022).

3.3 Microwave Assisted Extraction (MAE) of polyphenols

A magnetic stirrer and a water condenser were integrated into a normal family microwave. In a 500 ml round-bottomed flask, 50 g of powdered *Carrissa spinarum* leaves were soaked in 200 ml of distilled water. The flask was then microwaved at 70 degrees Celsius for 30 minutes. After that, the extract was filtered using Whatmann No. 1 filter paper. In order to concentrate polyphenols in a methanol extract, the filtrate was fixed in a rotary evaporator. Water-based extract was freeze-dried.

3.4 Estimation of total phenolic content of *Carissa spinarum* leaves

The Folin-Ciocalteu technique (Genwali *et al*., (2013) was slightly modified to determine total phenolic content. To summarize, 5 milligrams of extract were diluted in 5 mL of distilled water to produce a *Carissa spinarum* leaf aqueous extract concentration of 1 mg/mL. 5 mL of the 1% Folin-Ciocalteu reagent was mixed with 1 mL of the extract. After that, 5 mL of 7.5% sodium carbonate was added to the mixture. The absorbance at 760 nm of the combination was measured after a 20-minute incubation at 25 °C. GAE mg/g was reported as the phenolic content:

Y = 0.005X + 0.347, R^2 = 0.981.

3.5 Synthesis of liposomes and encapsulation of Cs- polyphenols (CsP)

The production of liposomes and encapsulating Cs-polyphenols (CsP) was carried out by adapting and modifying the method utilized by Cheng *et al*. (2017). In summary, 15 ml of 100% ethanol was mixed with 50 mg of phosphatidyl choline. Then, 20 mg of polyphenol-enriched Carissa spinarum leaves extract was added to 20 ml of pre-heated distilled water at 60 ^{0}C. Phosphatidyl choline in ethanol was gently added to an aqueous solution containing extract and agitated for 40 minutes at 60 degrees Celsius. After 40 minutes, the ethanol was removed by rotary evaporation, and the lipid suspension was sonicated and homogenized for 30 minutes. The LipCsP that resulted was stored at 4 ^{0}C for further investigation.

3.6 Preparation of LipCsP coated chitosan

The LipCsP-chitosan was prepared using a modified process developed by Mady and Darwish (2010). To produce a lipid-ethanol mixture, 100 mg of phosphatidyl choline was mixed with 15 ml of ethanol. Chitosan (40 mg), sodium triphosphate (10 mg), and *Carissa spinarum* extract (20 mg) were diluted in 1% acetic acid and then sonicated in a water bath. Drop by drop, ethanol was added to this mixture. For 30 minutes, probe sonication at 50 amplitudes was performed. LipCsP-chitosan pellets were produced by centrifuging the sonicated mixture at 24652 g for 15 minutes at 4 ^{0}C. The pellets that resulted were freeze-dried and kept at 4 ^{0}C for further use.

3.7 Encapsulation Efficiency Measurement

Lip-CsP (20 mg/ml) suspension was centrifuged at 24 652 g for 15 minutes at 4 ^{0}C to generate supernatants and nanopellets (Liposome loaded polyphenols). After removing the supernatant, the total phenolic content was determined using the Ciocalteu technique (Genwal *et al*., 2013). The total phenolic content of nanopellets was evaluated by rupturing liposomes with 1 ml of 0.06% Triton X-100 before performing the Folin-Ciocalteu technique. The identical technique was carried out using LipCsP-chitosan. The encapsulation efficiency was determined using the following equation:

$$\textbf{EE (\%)} = \frac{\text{Phenol in liposome}}{(\text{Phenol in liposome} + \text{ phenol in supernatant})} x100 \ (1)$$

EE (%) represent encapsulation efficiency; Phenol inside implies CsP polyphenols inside the liposome and phenols outside represent the CsP polyphenols in supernatant

3.8 Preparation of ZnO nanoparticles

The co-precipitation technique was used to make ZnO nanoparticles by using the method developed by Ahamad & Kumar (2016) with slightly modification. Briefly, 50 ml of distilled water were used to dissolve 0.5 g of zinc acetate. An alkaline solution was prepared by dissolving 0.2 g of NaOH in 25 ml of distilled water. The alkaline solution was gradually added, drop by drop, while being stirred for an hour. The precipitation was filtered twice, washed in ethanol, and then dried in an oven for an entire night at 60 °C

3.9 Preparation of ZnO-capped Chitosan

Preparation of ZnO-chitosan was conducted following the method developed by AbdEly,2012 with slightly modification. Briefly, the 10 ml of distilled water was added after 30 mg of chitosan had been dissolved in 2 ml of 1% acetic acid. The 0.5 g of zinc acetate that had previously been dissolved in 50 ml of distilled water was then added to the chitosan solution. 0.2 g of sodium hydroxide, which had been dissolved in 25 ml, was gradually added to the chitosan-zinc acetate mixture and stirred for an hour. To prepare the precipitate for further examination, it was filtered, twice washed with ethanol, and then dried in an oven at 60 °C.

3.10 Preparation of (LipCsP/ZnO)-CT

In order to generate Dual Nanohybrid Delivery system:((LipCsP-ZnONPs)-CT), a suspension of LipCsP-chitosan was mixed with the ZnO-chitosan solution in a ratio of 1:1. The mixture was thoroughly agitated for 30 minutes at room temperature and finally freeze-dried for 24 hours. The powder was collected and stored for further analysis.

3.11 Characterization of nanoformulations

3.11.1 Particle size and ζ-potential measurements

Using a zeta sizer NANO SERIES, the mean particle size and zeta potential of the LiPCsP, LipCsP-Chitosan, ZnONPs, ZnO -Chitosan, and (LipCsP-ZnO)-CT preparations were measured. The suspensions were examined in triplicate after being diluted with distilled water (1:10). The results are presented as the mean and standard deviation of nine measurements.

3.11.2 Fourier Transform Infrared Spectroscopy (FT-IR)

To identify the functional groups of ZnONPs, LiPCsP, LipCsP-Chitosan, CsP, LiPCsP, LiPCsP-LipCsP, and (LipCsP-ZnO)-CT. A Perkin Elmer Spectrum 400 ET-IR-NIR-Spectrometer was used to conduct the FTIR analysis. Before analysis, an open bean background spectrum of clean crystal was recorded. To avoid any moisture effect, 1 gram of each sample was freeze-dried before analysis. The spectrum from 4400 to 400 cm^{-1} was then collected using 24 scans at a resolution of 2 cm$^{-1.}$

3.11.3 Scanning electron microscope (SEM).

The surface morphology of the generated nanoparticles was examined using a scanning electron microscope (TESCAN, Brno, Czech Republic). The materials were lyophilized with a freeze dryer before being examined for morphology. The shape of the nanoparticles was produced with the image-processing software Image J.

3.11.4 Release of Cs-polyphenol (CsP) from Liposomes

In the investigation of polyphenol release from liposome systems, the technique described by Omwonyo *et al*. (2014) was employed, however it underwent a little modification. The pellets of the liposome formulation were made by centrifuging 10 ml of a 20 mg/ml suspension of the nanoformulation at 15 000 rpm for 30 minutes, removing the supernatant, and leaving the pellets in an eppindoff's tube that had been buffered to pH 7.4 and kept at physiological temperature (37 °C). For the purpose of determining the total phenolic content, each epindoff was removed at the appropriate period (1, 2, 3, 5, 6, 7, 8, 12, 24 h), and release kinetics were reported as the cumulative percentage released over time.

3.11.5 Mathematical modelling

In order to investigate the drug release kinetics, the zero-order, first-order, Higuchi, Hixson-Crowell, and Korsemeyer-Peppas models were used. Using the correlation coefficient (R^2) and the release exponent (n), the best-fit kinetic model and the drug release mechanism were found.

Table 6: Mathematical model to study the drug release kinetics

Kinetic model	Equation
First order model	$\log C = \log C_0 - K\,t/2.303$
Zero order model	$C_t = C_0 + K_0\,t$
Higuchi model	$C_t = KH \times t^{1/2}$
Korsemeyer-Peppas Model	$\log(C_t/C) = \log K_{kp} + n\log t,$

Note: Initial amount of polyphenols before released by nanoformulation (C0); Higuchi constant (K_H); rate constant (k); time (t); Cumulative amount of polyphenol released by nanoformulation after elapsed time, t; Exponential factor which predict Korsmeyer-Peppas model.

3.12   Nanoformulation Suspension storage stability

The stability of the nanoformulations (ZnONPs, ZnO-chitosan, LipCsP, LipCsP-chitosan, and (LiPCsP/ZnO)-CT) were assessed by monitoring the zeta potential at 20 C for 5, 10, 15, 30, and 45 days using a Malvern Instruments Zetasizer Nanoseries Nano-Z equipment. The suspensions were kept at 4 °C in a dark, oxygen, and light-free environment.

3.13   Gastrointestinal digestion

3.13.1 Simulated Mouth Fluid (SMF)

The suspensions of Lip-CsP and LipCsP-chitosan, each at a concentration of 20 mg/ml, were prepared, and their bioaccessibility and release studies were each examined individually. Following the procedure developed by Pool *et al*. (2012), a simulated saliva fluid containing mucin (30 mg/mL) was generated. Each sample (3 ml) was mixed with 3 mL of preheated, 37 °C-simulated saliva fluid. To simulate oral conditions, the resultant fluid was agitated at 90 rpm for 10 minutes at 37 °C after having its pH adjusted to 6.8 with 50 mM NaOH.

3.13.2 Simulated Gastric Fluid (SGF)

Pepsin (3.2 mg/mL), 0.03 M NaCl, and 0.16 M HCl were combined to produce simulated stomach fluid, which was then incubated at 37 °C. Three milliliters of the sample from the simulated oral fluid were mixed with simulated gastric fluid. To mimic stomach digestion, the liquids were shaken at 100 rpm for two hours with a pH adjustment to 2.5.

3.13.3 Simulated Intestinal Fluid (SIF)

After being diluted with phosphate-buffered saline (10 mM, 12 mL, pH 6.5), samples from the simulated stomach model were shaken at 37 °C for 10 min. The pH of the solution was then raised to 7.0. The digested samples were combined with simulated small intestine fluid that contained pancreatin (24 mg/ml, 2 mL), bile extract solution (50 mg/ml, 2.8 mL), and saline solution (0.5 M CaCl2 and 7.5 M NaCl, 1.2 mL). The resulting combination was then incubated for four (4) hours. The addition of 50 mM NaOH kept the pH of each digestion sample at pH 7.0.

3.13.4 Determination of the bioaccessibility of *Carissa spinarum* polyphenols

The 200 µL of raw digest were removed at various stages of digestion (gastric and intestinal phases) and utilized for the determination of total phenolic content. Samples were diluted with a solution containing 1% Triton X-100 and pH-adjusted to 5 in order to completely rupture the liposome membranes. The sample was then centrifuged for 30 minutes at 4 °C and 13 400 rpm. The "micelle" fraction, or supernatant, was carefully collected and considered to contain the solubilized bioactive compounds. The Folin-Cicalteu method was used to measure the amount of the bioactive present, and the following formula was used to determine the bioaccessibility:

$$\text{Bioaccessibility (\%)} = \frac{C_{digesta}}{C_i} x 100 \quad (2)$$

Where C digesta and Ci are the concentrations of the CsP in the mixed micelle phase and the initial concentration, respectively.

3.13.5 Release kinetics of polyphenols in simulated gastro-intestinal environment

200 µL of dissolution media from each digestion phase were taken out at predetermined time intervals after 10 min during simulated oral digestion and every 1 h during simulated gastric and intestinal digestion. These media were then instantly snap frozen in liquid nitrogen and then kept at -86 C until further analysis. The materials were centrifuged at 13 400 rpm for 30 min at 4 °C in preparation for a quantitative analysis. For quantitative analysis, the samples were centrifuged at 13 400 rpm for 30 min at 4 °C. The supernatant was carefully collected, and the total phenolic content of the samples measured is considered the total amount of compound release. The release percentages of polyphenols were calculated as per the formula below. *In vitro* release was plotted as a function of time.

$$\text{Cumulative release (\%)} = \frac{(Ct)}{Ci} x100 \quad (3)$$

Where Ct is the sample concentration for each time point, and Ci is the initial concentration.

3.14   Nanoformulation Stability in simulated gastrointestinal environment

The simulated mouth fluid (SMF), simulated gastric fluid (SGF), and simulated intestinal fluid (SIF) were added to the nanoformulation suspension samples at a final concentration of 10% (v/v), and they were then incubated at 37 °C. Samples were taken based on how long they should stay in simulated media (mouth phase for 10 minutes, stomach phase for 2 hours, and intenstinal phase for 6 hours). To remove aggregates such pancreatin in medium, samples were centrifuged for 5 minutes at 13,500x. Using a zeta sizer from the NANO SERIES, the zeta potential of Lip-CsP-chitosan (LiPCsP/ZnO)-CT preparations was assessed in order to evaluate their stability in various simulated mediums. The suspensions were examined in triplicate after being diluted with distilled water (1:10). Nine measurements were made, and the data are presented as the average and standard deviation.

3.15   Antimicrobial activity

3.15.1 Collection and preparation of inoculums

The *Klebsiella pneumoniae* and *S. aureus* strains were given as a courtesy donation on behalf of the Department of Biotechnology at the University of the Western Cape by the American Type Culture Collection (ATCC; Manassas, VA, USA). The microorganism was plated on agar nutritional agar and cultured at 37 °C for 24 hours. In order to conduct an antimicrobial test after incubation, the plates were kept in a refrigerator at 4 °C. The inoculated bacterium was removed from the nutrient agar using a wire loop, introduced to the nutrient broth, and calibrated to the 0.5 McFarad standard (0.08-0.1 at 600 nm).

3.15.2 Agar well diffusion assay

The antibacterial activity of nanoformulations and CsP extract was examined in agar diffusion studies on nutrient agar plates. The bacteria were grown until they reached a concentration of 0.5 McFarad, and then they were diluted to a concentration of roughly 10^6 colony forming units/ml in new nutritional broth. Nanoformulations with a concentration of 20 mg/mL were made in sterile distilled water. On the surface of the nutritional agar plates, 8 mm diameter

wells were bored. The diluted colonies were uniformly dispersed across 100 µl of nutrient agar plates. The CsP extracts and 70 µl of the nanoformulations were added to the treatment wells. 10 g/ml of ciprofloxacin was present in the positive controls. After 24 hours of incubation at 37 °C, each plate underwent a zone of inhibition analysis. The zones of inhibition against test microorganisms were measured in order to determine the antibacterial activity. Three times the experiment was conducted. Equation 3 was used to express the antibacterial activity as a percentage relative inhibition zone diameter (RIZD), as previously discussed (Rubaka *et al.*, 2014):

$$\% \text{ RIZD} = (\text{IZD sample} - \text{IZD negative control})x \frac{100}{(\text{IZD antibiotic standard})} \text{ (4)}$$

3.15.3 The micro plate AlamarBlue assay (MABA)

MABA was used to assess the susceptibility of two microorganisms (*Klebsiella pneumoniae* and *Staphylococcus aureus*) to the nanoformulations. In a 96-well plate, the concentrations of the nanoformulations (ZnONPs, LipCsP, LipCsP-chitosan, and (LiPCsP/ZnO)-CT) were serially diluted from 500 mg/ml to 31.25 mg/ml. Each well received 100 µl of microbe at a concentration of 1×10^6 CFU/ml, and the plates underwent a 24-hour incubation period at 37 °C. The Alamar Blue dye reagent was then added to each well, which was then incubated for 3 hours at 37 °C. The growth of the microorganisms was assessed using the BMG microplate reader's absorbance at 570 nm, and the viability of the cells was calculated using equation 5:

$$\% \text{Viability} = \frac{\text{Absorbance of nanoformulation treated cells}}{(\text{Absorbance of control cells})} x100 \text{ (5)}$$

MIC was taken as the lowest concentration of drug that reduces the viability of microorganism by more than 50%.

3.15.4 Antimicrobial interaction

The antimicrobial activity of plant extract combinations was determined by calculating the fractional inhibitory concentration (FIC) index as previously described (Rubaka *et al.*, 2014)

$$\text{FIC of compound a(FICa)} = \frac{\text{MIC of compound a in combination}}{\text{MIC of compound a alone}} \quad (4)$$

$$\text{FIC of compound b(FICb)} = \frac{\text{MIC of compound b in combination}}{\text{MIC of compound b alone}}$$

Then, FIC index= FICa+ FICb.

For FIC index≤0.5 the combination was regarded as synergistic; for FIC index >0.5 and< 4 it was regarded as additive and antagonism for>4 (Rubaka *et al*., 2014)

3.15.5 Time-kill assay

Three sterile Elenmeyer flasks containing 50 mL of nutritional broth each received the (LiPCsP/ZnO)-CT solution before being serially diluted to create the (MIC, 0.5 MIC, and 2 MIC) concentrations. Each MIC concentration received an inoculum containing 1×10^8 cells per milliliter. The three flasks were then incubated at 37 °C in an orbital shaker incubator at intervals of 1, 2, 3, 4, 5, 6, 7, 8, and 9 hours. A 150 µl sample of the mixture was taken out and put through the MABA assay to measure the time-dependent viability at various concentrations. Positive controls included untreated microorganisms.

3.16 Statistical analysis

Analysis of variance (ANOVA) was utilized in the statistical analysis, with computations carried out using Origin2019 (64-bit) software, and the fisher's least significant difference (L.S.D.) used to compare treatment means at a p-value ofP < 0.05 level of significance.

CHAPTER FOUR

RESULTS AND DISCUSSION

4.1   Results

4.1.1   Phytochemical analysis and total phenolic content

Table 7 provides a summary of the phytochemical analysis' results, which indicated several phytochemicals present in it. The total phenolic content for methanol and water extracts varied with the concentration of extracts and was 362.00 ± 1.00 mg GAE/g and 348.00 ± 1.53 mg GAE/g, respectively, at the maximum concentration (1.00 mg/mL) of *Carissa spinarum* extract tested (Table 8). At the lowest concentration of extract.

Table 7: Phytochemical Screening of *Carissa spinarum* leaves extract

		ME	AE	PE	CE
Alkaloids	Mayer's Test	+	+	-	-
	Wagner's Test	+	-	-	-
Flavanoids	Ammonia Reduction Test	+	+	-	-
Phenol	Ferric Chloride Test	+	+	-	-
Terpenoids	Salkowski's Test	+	-	-	-
Steroids	Salkowski's Test	+	+	-	-
Coumarins	NaOH Test	+	+	-	-
Resins	Copper Sulphate Test	-	-	-	-
Tannins	Ferric Chloride Test	+	+	-	+
Xanthoproteins	Nitric Acid +Ammonia Test	-	-	-	-
Quinones	Alc. KOH Test	-	-	-	-
Carboxylic acid	Effervescence Test	-	-	-	-
Oxylates	Acetic Acid Test	+	-	-	-
Carbohydrates	Fehling's Test	+	+	-	-
Glycosides	Keller-Killiani Test	+	-	-	+
Proteins	Ninhydrin Test	-	-	-	-
Saponins	Froth Test	+	+	-	-

+ indicates the presence; - indicates the absence, methanol extract (ME), aquous extract (AE), petroleum ether extract (PE) and chroloform extract (CE)

Table 8: Total phenolic content of methanolic and aquous extract of *Carissa spinarum* leaves

Samples	0.25 mgmL^{-1}	0.5mgmL^{-1}	1mgmL^{-1}
Methanol extract	365.00^c ± 1.00	368.00^b ± 1.20	373.00^a ± 1.52
Water extract	350.5^f ± 0.50	354.33^e ± 0.58	357.50^d ± 0.50

*Note: Total Phenolic Content of *Carissa spinarum* leaves extract. Values reported as mean ± SD; n = 3. Values reported as mean ± SD; n = 3. Means followed by dissimilar letter in a row are significantly different from each other at P < 0.05 according to Fischer's Least Significant Difference (LSD).

4.1.2 Particle size, Zeta potential, PDI and encapsulation efficiency

The characteristics of nanoliposomal systems were investigated, and the results are shown in Table 9 in terms of particle size, polydispersity index, zeta potential, and encapsulation efficiency. In the chitosan-coated liposome and the uncoated liposome, respectively, the hydrophilic liposome core entrapped polyphenols at 81.07 ± 2.5% and 66.11 ± 1.11%, respectively (Lip-CsP). The average diameter of the nanoliposome CsP increased from 176.17 ± 1.05 nm to 365.22 ± 0.70 nm. In nanoliposomal systems, the polydipersity index value remained below 0.4. The charge of the uncoated system changed from a negative value of -45.3 ± 0.78 mV to a positive value of +34.43 ± 1.36 mV. The zeta potential of ZnONPs was changed from +9.36 ± 4.08 mV to +34.43 ± 1.36 mV. The size of ZnONP was also reduced from 91.17 ± 1.191 nm to 78.82 ± 1.20 nm. However, it's higher than 0.4 in uncoated zinc oxide. In the nanohybrid system, which constitutes LipCsP-Chitosan and ZnO nanoparticles, the positive potential (+37.5 ± 5.10) was preserved.

Table 9: Particle size, Polydipersity Index and zeta potential of nanoformulations

S/N	Formulations	Size(nm)	PDI	Z$_P$ (mV)	EE%
1	ZnO-Chitosan	78.82 ± 1.20	0.323 ±0.00	+34.43±1.36	-
2	LipCsP-Chitosan	365.22 ± 0.70	0.351 ±0.00	+45.3±0.78	81.07 ± 2.5%
3	LipCsP	176.17 ± 1.05	0.345 ± 0.00	-45.3 ± 0.78	66.11 ± 1.11%.
4	ZnONPs	91.17 ± 1.191	0.540 ±0.00	+9.36 ± 4.08	-
6	(LiPCsP/ZnO)-CT	-	-	+37.5± 5.10	-

Particle size, Polydispersity Index and zeta potential of nanoformulations: Liposome loaded Carissa spinarum polyphenols (LipCsP), LipCsP coated chitosan (LipCsP-Chitosan), Zinc Oxide nanoparticles (ZnONPs), ZnO coated chitosan (ZnO-Chitosan), nanohybrid (LiPCsP/ZnO)-CT). (Values reported are mean ± SD; n = 3)

4.1.3 Optical analysis

Optical analysis of ZnONPs and ZnO-chitosan was carried out, and the UV-visible spectrum was obtained (Fig. 16). There was a significant blueshift in excitonic absorption of the prepared ZnO-Chitosan (337 nm) compared to that of the ZnOnNPs (366 nm). The optical band gap of ZnONPs determined from the absorption spectra was 3.1 eV (Fig. 17), which is slightly higher than that of ZnO-Chitosan (3.0 eV) (Fig. 18).
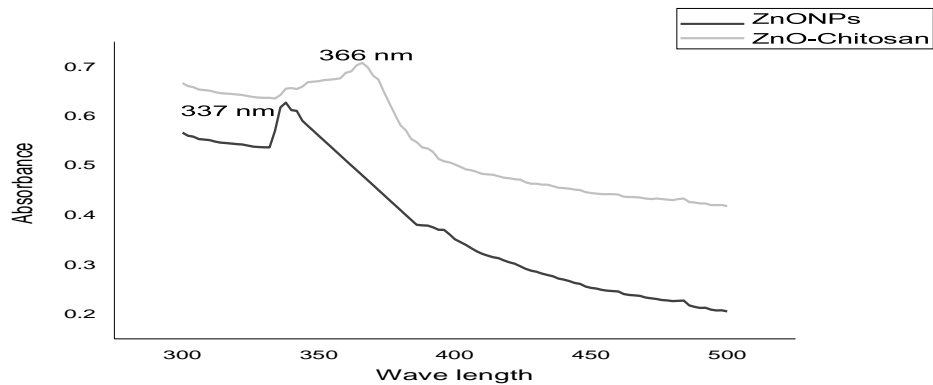
Figure 16: Optical analysis of Zinc oxide nanoparticles (ZnONPs), ZnO nanoparticles coated with chitosan (ZnO-Chitosan)
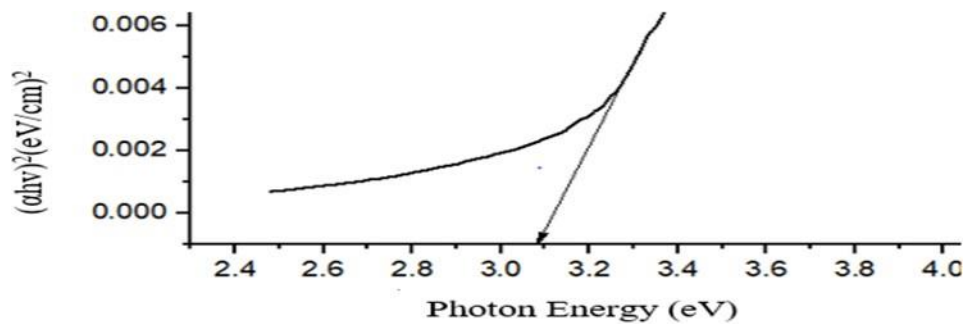
Figure 17: Plots of (αhv)2 versus photon energy (eV) of the ZnO nanoparticles for evaluating of optical band gap energy (Eg) value
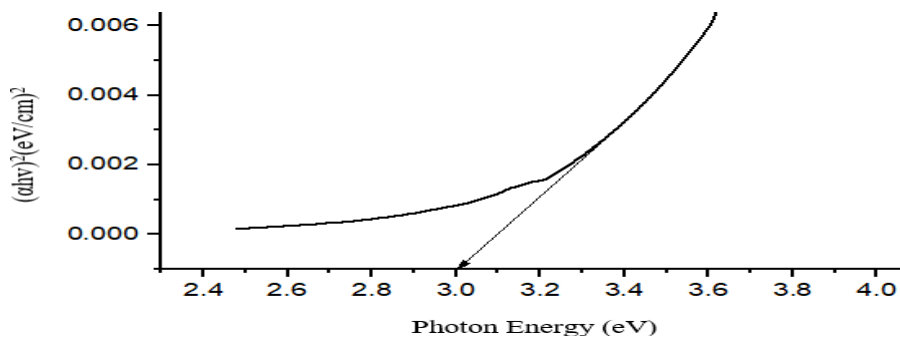
Figure 18: Plots of (αhv)2 versus photon energy (eV) of the ZnO -chitosan for evaluating of optical band gap energy (Eg) value

44

4.1.4   Fourier Transform Infrared (FTIR) spectroscopy analysis

The various spectra of the nanoformulations were obtained by performing a Fourier Transform Infrared (FTIR) spectroscopic study on CsP, liposomes, chitosan, and LipCsP-chitosan (Fig. 19 and Table 10). An absorption peak at 1653 cm^{-1} that corresponds to C = O stretching in amide I vibration was seen in the chitosan spectra shown in Fig. 19 a. Additionally, discrete absorption bands around 2870 cm^{-1} caused by C-H stretching and bands related to O-H and N-H stretching around the region 3352 cm^{-1} that are normally seen in polysaccharide IR spectra were found. The bending vibration frequency at wave number 1578 cm^{-1} confirmed the presence of the primary amine functional group. The existence of absorption bands at 2919 cm^{-1}, which are clearly visible in the liposomes in Fig. 19c, depicts the C-H stretching vibration. In addition, peaks at 1236 cm^{-1} were caused by P = O stretching vibration. A strong signal also occurred at 1739 cm^{-1}, which is related to C = O stretching vibration.

Abosabaa *et al*. (2021) obtained similar results. The IR spectra of CsP is shown in Figure 19d. The phenolic hydroxyl groups are responsible for the absorption spectra at 3276 cm^{-1} that reflects OH stretching and vibrating (Lisperguer *et al*., 2016; Liang *et al*., 2011). At 1602 cm^{-1} and 1439 cm^{-1}, the C-C of the aromatic ring and the flavonoid C = O functional groups were identified, whilst the 1054 cm^{-1} appearance of the C-O stretching vibration was noted. The LipCsP-Chitosan FTIR spectra are displayed in Figure 19b. The interaction of liposomes with chitosan was revealed by the disappearance of N-H primary amine (bending) in chitosan, which was previously reported (Abosabaa *et al*., 2021). Along this stretch, the vibration frequency of OH and NH shifted from 3352 cm^{-1} to lower vibration frequency of 3331 cm^{-1} due to hydrogen bonding between the liposome and chitosan. Additionally, the liposome's C = O vibration frequency changed from 1739 cm^{-1} to a lower frequency at 1732 cm^{-1}. The interaction between the polyphenolic components of the CsP and the liposomes was demonstrated by changes in the absorbance bands of the P = O group of liposomes from 1236 cm^{-1} to a lower frequency of 1226 cm^{-1}.

Table 10: Fourier Transform Infrared (FTIR) spectroscopy analysis

Formulation	Absorption peak	Function group
Chitosan	1653	C=O stretching in amide I Vibration
	3352	O-H and N-H stretching
	2870	C-H stretching
	1578	Primary amine function group
Liposome	2919	C-H stretching
	1739	C=O stretching vibration
	1236	P=O, stretching vibration
CsP	3276	-OH, stretching vibration in phenolic hydroxyl group
	1602	Flavonoid C=O function group
	1439	C-C aromatic ring
	1054	C-O, stretching vibration
LipCsP-Chitosan	3351	OH, N-H, shifted vibration frequency of chitosan
	1732	C=O Shifted vibration frequency of liposome
	1226	Shifted absorption band of P=O of liposome

*Note: CsP- *Carissa spinarum* polyphenols, LipCsP - Liposome loaded CsP polyphenols, LipCsP-Chitosan - LipCsP coated chitosan.
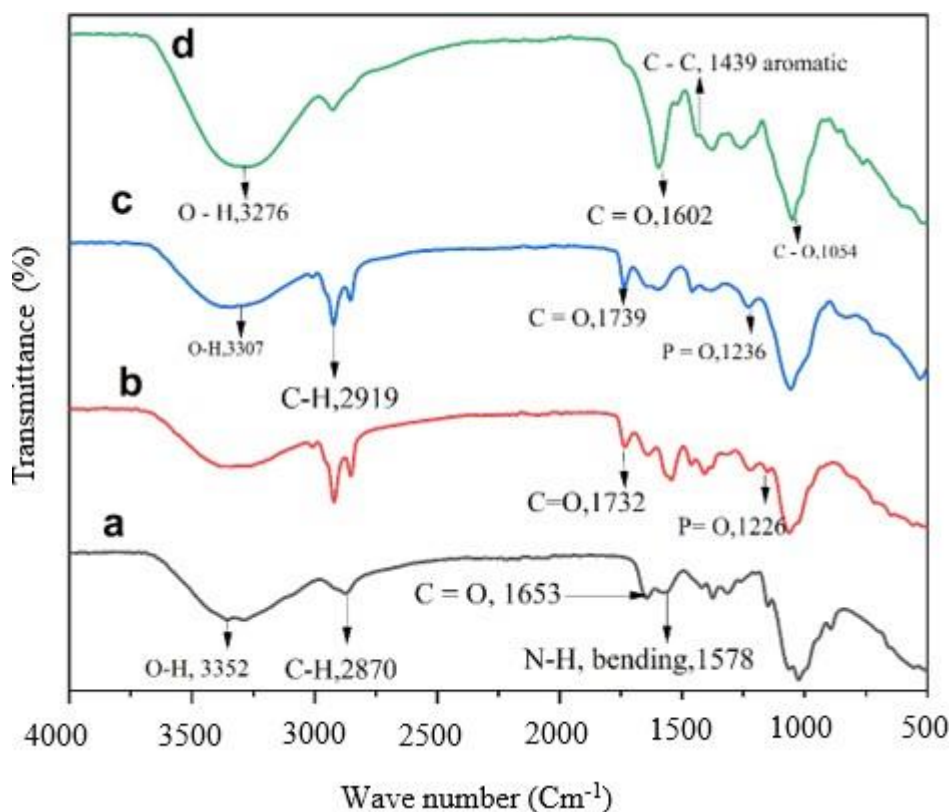
Figure 19: FTIR analysis of Liposome (Lip)- (c), Chitosan- (a), *Carissa spinarum* Polyphenol (CsP)-(d), LipCsP coated chitosan (b)

The FTIR analysis of inorganic nanoparticles (ZnONPs and ZnO-chitosan) was also carried. An absorption band with wave number, 1020 cm^{-1}, 1551 cm^{-1} and 3359 cm^{-1} were obtained in ZnO-chitosan. In FTIR analysis of chitosan the absorption bands observed were 3352 cm^{-1} corresponding, 1013 cm^{-1} and ZnONPs generated the absorption bands of 467 cm^{-1}.
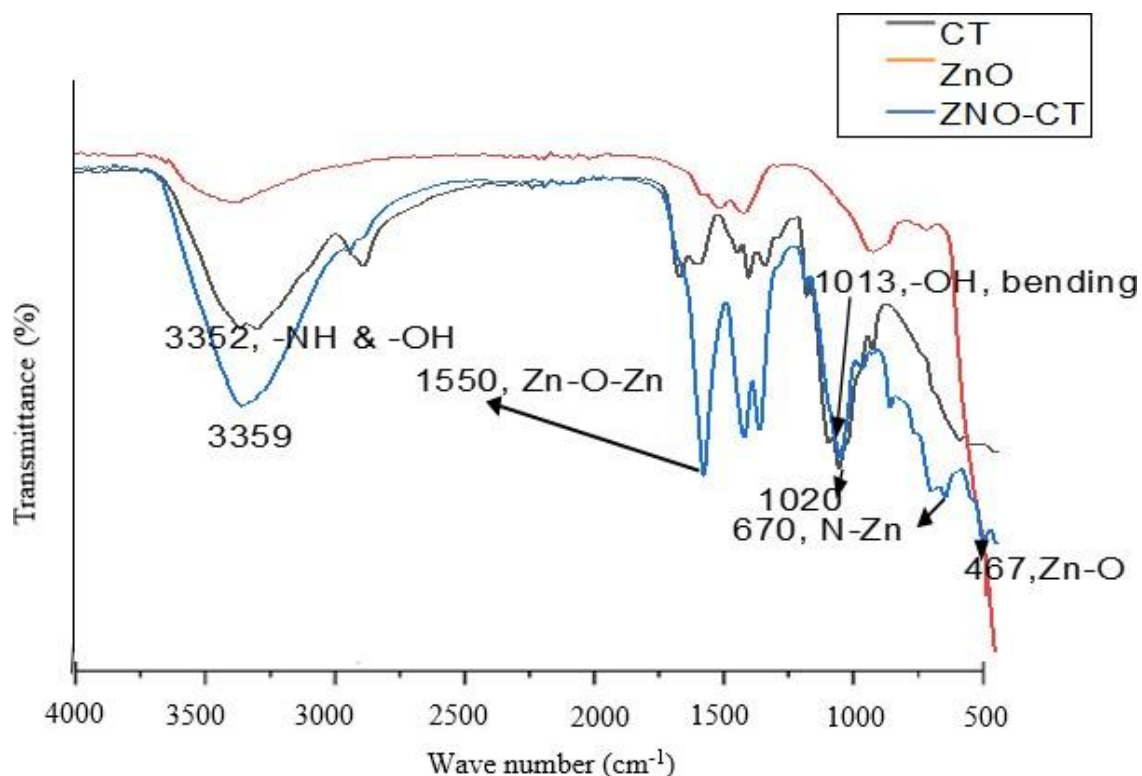
Figure 20: FTIR analysis of chitosan, ZnONPs and ZnO-CT nanoparticles

4.1.5 Scanning electron microscope

The SEM images of the pure chitosan (A), ZnO nanoparticles (B), and their hybrid nanocomposite were obtained when scanned using a scanning electron microscope. The results of SEM images varied in shape, as indicated in Fig. 21. Images varied in shape, as indicated in Fig. 21.
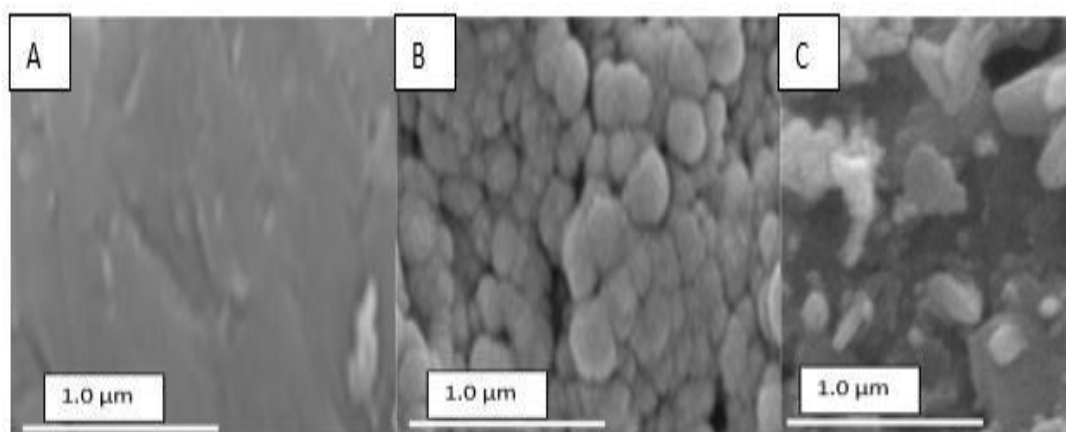
Figure 21: Surface topography of pure chitosan (A), ZnO nanoparticles (B), and that of their hybrid nanocomposite (ZnO-Chitosan) evaluated by Scanning Electron Microscope

48

4.1.6 Bioaccessibility

Bioaccessibility of free CsP and when encapsulated in nanoformulations (LipCsP, LipCsP-chitosan, and LipCsP/ZnO)-CT, when subjected to a simulated Gastrointestinal environment, was carried out, and the results are indicated in Table 11 and Fig. 22. LipCsP/ZnO)-CT exhibited significantly higher ($P < 0.05$) bioaccessibility of polyphenol: $82.14 \pm 0.80\%$ and $71.60 \pm 0.86\%$ in SGF and SIF, respectively, as compared to CsP, LipCsP, and LipCsP-chitosan. The bioaccessibility of polyphenols after the intestinal phase differed significantly ($P < 0.05$) from that during the gastric phase.

Table 11: Bioaccessibility of polyphenols loaded in nanoformulations in simulated Gastric phase and intestinal phase

	Simulated Gastric Fluid (SGF)	Simulated Intestinal Fluid (SIF)
CsP	$39.38^h \pm 0.34$	$31.50^g \pm 0.50$
LipCsP	$51.53^f \pm 0.46$	$43.87^e \pm 0.15$
LipCsP-Chitosan	$74.54^d \pm 0.45$	$63.67^b \pm 0.34$
(LiPCsP/ZnO)-CT	$82.14^c \pm 0.80$	$71.60^a \pm 0.86$

*Note: *Carissa spinarum* polyphenols (CsP), Liposome loaded *Carissa spinarum* polyphenols (LipCsP), LipCsP coated chitosan (LipCsP-Chitosan), Zinc Oxide nanoparticles (ZnO), ZnO, Chitosan (CT), Values reported as mean $\pm$ SD; n = 3. Means followed by dissimilar letter are significantly different from each other at $P = 0.05$ according to Fischer's Least Significant Difference (LSD).
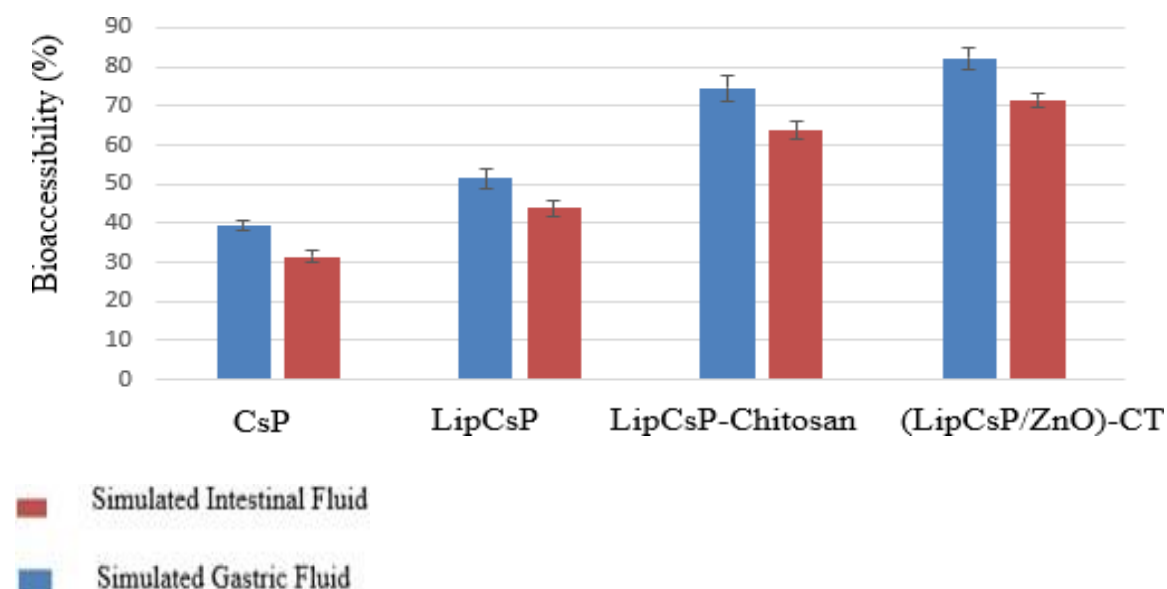
Figure 22: The bioaccessibility of Carissa spinarum –polyphenol (CsP)

Liposome loaded *Carissa spinarum* polyphenol (Lip-CsP) and liposome loaded *Carissa spinarum* polyphenol coated with chitosan. The (LipCsP- Chitosan) and Dual Nanohybrid Drug System (LipCsP/ZnO)-CT in gastric and intestinal fluid. (Values reported are mean ± SD; n = 3).

4.1.7 CsP release in Gastro-Intestinal phase by nanoformulations

The results for the release kinetics of polyphenols from Lip-CsP-chitosan and Lip-CsP nanoformulations in a simulated gastric digestion phase were obtained (Fig. 23). The results showed that polyphenol release from nanoformulations in a simulated GI environment differed significantly ($P < 0.05$). After 2 h, a polymeric-coated formulation (LipCsP-Chitosan) was released at 7.73 ± 0.50 % into Simulated Gastric Fluid (SGF). Uncoated formulations (LipCsP) released 10.53 ± 0.40 % into SGF, while (LipCsP/ZnO)-CT released 5.68 ± 0.5 %. A formulation with a polymeric coating (LipCsP) released 16.15 ± 0.7 % of polyphenols into simulated intestinal fluid (SIF) after 6 hours. 18.65 ± 0.60 % of polyphenols were discharged into the SIF from the uncoated formulations (LipCsP), while the nanohybrid (LiPCsP/ZnO)-CT released $14.27 \pm 0.6\%$ % polyphenols into the SIF. Nanohybrid Delivery System was significantly different ($P < 0.05$) as compared to the release exhibited by LipCsP and LipCsP-Chitosan alone, exhibiting the slowest and most continuous release pattern of CsP.
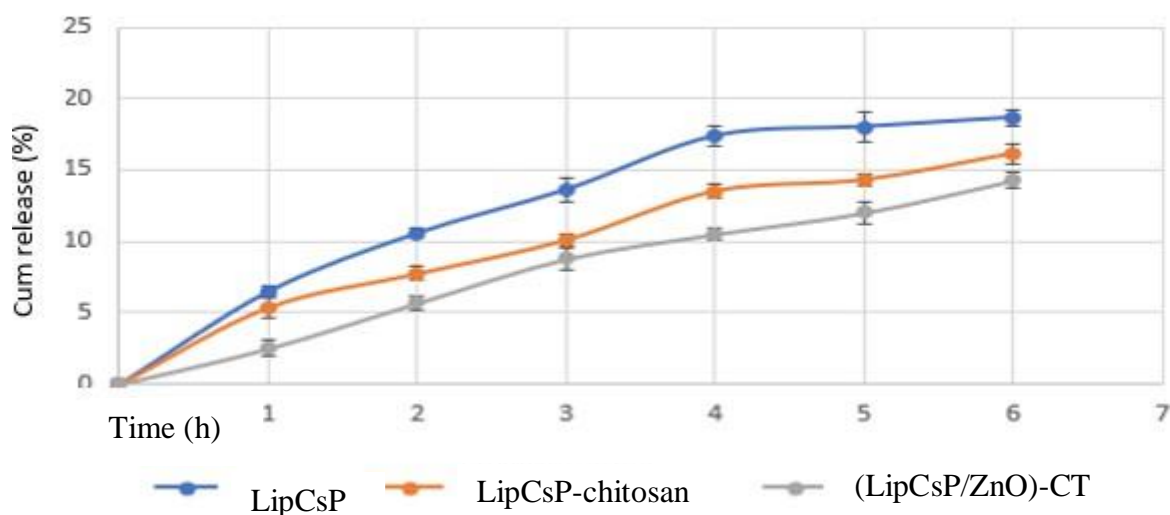
Figure 23: CsP release in Gastro-Intestinal phase by nanoformulations

Chitosan coated nanoliposomes (LipCsP-Chitosan), un coated liposome loaded polyphenols (LipCsP) and Dual Nanohybrid Delivery System (LipCsP/ZnO)-CT. (Values reported are mean ± SD; n = 3).

4.1.8   Release kinetics in Gastro-Intestinal phase by nanoformulations

The best fit model was revealed by highest correlation coefficient (R2) by consulting the equations for the kinetics models. The release factor (N) was assessed by using Korsmeyer Peppas model LipCsP-chitosan and (LipCsP/ZnO)-CT demonstrating non-Fickian diffusion (Table 12). However, non- coated system (LipCsP) demonstrated Fickian diffusion.

Table 12: Different kinetic model fitted to investigate the mechanism of polyphenols release from LipCsP-Chitosan

Nanoformulation	Kinetic model	R^2	K	Mechanism
LipCsP	Zero order	0.9390	2.0097	Fickian diffusion
	First order	0.9013	-0.013	
	Higuchi	0.9230	6.000	
	Korsmeyer Peppas	0.7640	0.181	
LipCsP-Chitosan			N = 0.181	Non- Fickian diffusion
	Zero order	0.9634	1.8471	
	First order	0.8969	-0.04	
	Higuchi	0.9701	13.6190	
	Korsmeyer Peppas	0.6431	0.7594	
(LipCsP/ZnO)-CT			N = 0.7594	Non-Fickian diffusion
	Zero order	0.9425	1.456	
	First order	0.7894	-0.0100	
	Higuchi	0.9624	11.5670	
	Korsmeyer Peppas	0.6678	0.6565	
			N = 0.6565	

4.1.9   Storage stability of nanoformulations

The storage stability of nanoformulations was investigated (Table 13). No significant variation in the zeta potential of ZnO-chitosan was observed after 30 days of storage ($P > 0.05$). After 45 days of storage, there was a noticeable shift in the storage stability of ZnO-Chitosan. For uncoated ZnONPs, the first 10 days of storage did not result in any changes in zeta potential ($P > 0.05$), but after 15 days, the alterations were noticeable. LipCsP-chitosan stabilized in 15 days, but the zeta potential significantly differed ($P < 0.05$) after 30 days. In the absence of chitosan, as depicted by LipCsP, the stable system was significantly changed ($P < 0.05$) after 15 days. In 45 days of storage of the Dual Nanohybrid Delivery System (LiPCsP/ZnO)-CT, there was no significant difference ($P > 0.05$) in zeta potential.

Table 13: Storage stability of nanoformulations

Nanoformulation	DAY5	DAY10	DAY15	DAY30	DAY45
ZnO-Chitosan	+34.43[e]±1.36	+34.60[e]±1.23	+34.56[e]±1.35	+33.57[e]±0.58	+27.83[g]±0.76
LipCsP-Chitosan	+40.10[ab]±0.85	+39.23[ab]±0.93	+39.13[ab]±0.81	+38.13[cb]±0.81	+34.20[e]±1.25
LipCsP	-44.13[l]±1.00	-45.37[l]±1.27	-41.00[k]±1.00	-39.00[kj]±1.23	-37.00[j]±0.50
ZnONPs	+9.50[g]±1.30	+7.41[h]±0.52	+6.42[ih]±0.52	+5.70[i]±0.76	+5.03[i]±0.55
(LiPCsP/ZnO)-CT	+38.67[a]±0.76	+37.23[a]±0.40	+37.43[a]±0.42	+37.48[a]±0.55	+37.08[a]±0.14

Storage stability of nanoformulations: Liposome loaded Carissa spinarum polyphenols (LipCsP), LipCsP coated chitosan (LipCsP-Chitosan), Zinc Oxide nanoparticles (ZnONPs), ZnO coated chitosan (ZnO-Chitosan) and nanohybrid, LiPCsP/ZnO)-CT: Values reported as mean ± SD; n = 3. Means followed by dissimilar letter in a row are significantly different from each other at $P < 0.05$ according to Fischer's Least Significant Difference (LSD).

4.1.10 Stability study in simulated gastro intenstinal environment

A stability study in a simulated gastrointenstinal environment was conducted, and the results are indicated in Table 14. In the different stages of the digestion process, a significant difference ($P < 0.05$) between the zeta potential values of the nanoformulation was seen. More stable charge retains were observed in LiPCsP/ZnO)-CT.

Table 14: Stability in zeta potentials of nanoformulations in simulated environment

	Initial	SMF	SGF	SIF
LipCsP	-45.37 d ± 0.78	-45.80 d ±0.26	-42.67 b ± 0.58	-48.83 c ± 0.762
LipCsP-Chitosan	+39.00 f ± 0.50	+39.10 f ±0.17	+41.67 a ± 1.52	+36.67 e ± 0.76
(LiPCsP/ZnO)-CT	+37.17 fe ± 0.76	+37.17 fe ±1.75	+37.30 fe ± 2.06	+36.33fe ± 0.57

Variation of nanoformulations zeta potentials in simulated environment: Liposome formulation loaded *Carissa spinarum* polyphenol (Lip-CsP) and the formulation coated with chitosan (Lip-CsP-Chitosan) nanohybrid, LiPCsP/ZnO)-CT: Values reported as mean ± SD; n = 3. Means followed by dissimilar letter in a row are significantly different from each other at $P < 0.05$ according to Fischer's Least Significant Difference (LSD).

4.1.11 Antimicrobial effect of nanoformulations on bacterial pathogens

The antibacterial activity of *Carissa spinarum* polyphenols (CsP), liposome-loaded *Carissa spinarum* polyphenols (LipCsP), LipCsP coated chitosan (LipCsP-Chitosan), Zinc Oxide nanoparticles (ZnONPs), ZnO coated chitosan (ZnO-Chitosan), and LiPCsP/ZnO-CT was tested against *S. aureus* and *K. pneumoniae*. The agar diffusion assay results shown in Table 15 revealed that the tested formulations exhibited a significant difference ($P < 0.05$) in antibacterial activity against the tested pathogens. Concentrations and the time-dependent viability effect of nanoformulations against pathogens are indicated in Figs. 24 and 25. (LiPCsP/ZnO)-CT exhibited a significant ($P < 0.05$) viability reduction effect against pathogens at the lowest concentrations as compared to other nanoformulations.

The values for the Minimum Inhibition Concentration (MIC) of the nanoformulation are indicated in Fig. 26. The lowest MIC value (31.25 mg/mL) was observed in (LiPCsP/ZnO)-CT against *K. pneumoniae,* which inhibits the growth of *K. pneumoniae* by 4 folds as compared to LipCsP-Chitosan; 8 folds as compared to ZnO-Chitosan; and 16 folds as ZnONPs. However, the lowest MIC value exhibited by (LiPCsP/ZnO)-CT against *S. aureus* was 125 mg/mL, which inhibited the growth of *S. aureus* by 2 folds as compared to LipCsP-chitosan and by 4 folds as compared to ZnO-chitosan and ZnONPs. Synergistic interactions were exhibited by the nanohybrid (LiPCsP/ZnO)-CT against *K. pneumoniae* and additive interactions against *S. aureus* (Fig. 27).

ZnONPs exhibited antibacterial activity against tested pathogens, however, at a lower level as compared to ZnO-chitosan. The kinetic inhibition of growth of the nanohybrid system against *K. pneumoniae* is shown in Fig. 28. The inhibition kinetic profile was concentration-time dependent, and the effect ranked as 2MIC >MIC>0.5MIC against *K. pneumoniae*. Untreated microorganisms exhibited a normal growth pattern and exhibited a high optical density after 12 h as compared to the microorganisms treated with different concentrations of (LipCsP/ZnO-CT. The antimicrobial activity of LipCsP nanoformulations was significantly higher ($P < 0.05$) than that exhibited by free extract (CsP). When LipCsP/ZnO)-CT tested against *K. pneumoniae,* it exhibited a bacteriostatic effect (Fig. 31) against *K. pneumoniae* and *S. aureus.*

Table 15: Antibacterial activities (mm of zone inhibition) of nanoformulations against tested pathogens

Formulation	Conc (mg/mL)	Zone of inhibition (mm)		% RIZD	
		K. pneumoniae	*S. aureus*	*K. pneumoniae*	*S. aureus*
CsP	20	$4.00^j \pm 1.00$	$6.00^k \pm 1.00$	$12.00^M \pm 1.00$	$23.07^L \pm 0.60$
ZnO-Chitosan	20	$15.67^e \pm 1.15$	$13.89^f \pm 0.84$	$68.13^E \pm 0.75$	$53.42^G \pm 0.88$
LipCsP	20	$7.22^i \pm 0.69$	$8.65^h \pm 0.77$	$31.39^K \pm 2.00$	$33.27^J \pm 0.76$
LipCsP-Chitosan	20	$18.00^d \pm 0.50$	$15.47^e \pm 0.21$	$84.33^C \pm 2.51$	$59.50^F \pm 0.87$
ZnONPs	20	$9.67^h \pm 1.26$	$11.83^g \pm 0.76$	$42.04^H \pm 0.59$	$45.50^I \pm 0.85$
(LiPCsP/ZnO)-CT	20	$20.61^c \pm 0.35$	$17.86^d \pm 0.30$	$89.60^B \pm 1.32$	$68.69^D \pm 0.28$
Ciprofloxacin	20	$23.00^b \pm 0.50$	$26.50^a \pm 0.50$	$100.00^A \pm 0.00$	$100.00^A \pm 0.00$
Media(water)	20	$0.00^l \pm 0.00$	$0.00^l \pm 0.00$	$0.00^N \pm 0.00$	$0.00^N \pm 0.00$
Liposome	20	$0.00^l \pm 0.00$	$0.00^l \pm 0.00$	$0.00^N \pm 0.00$	$0.00^N \pm 0.00$

*Note: *Carissa spinarum* polyphenols (CsP), Liposome loaded *Carissa spinarum* polyphenols (LipCsP), LipCsP coated chitosan (LipCsP-Chitosan), Zinc Oxide nanoparticles (ZnONPs), ZnO coated chitosan (ZnO-Chitosan), Percentage Relative Inhibition Zone Diameter (%RIZD), (Values reported are mean ± SD; n = 3). Means followed by dissimilar letter in a row and column are significantly different from each other at P = 0.05 according to Fischer's Least Significant Difference (LSD
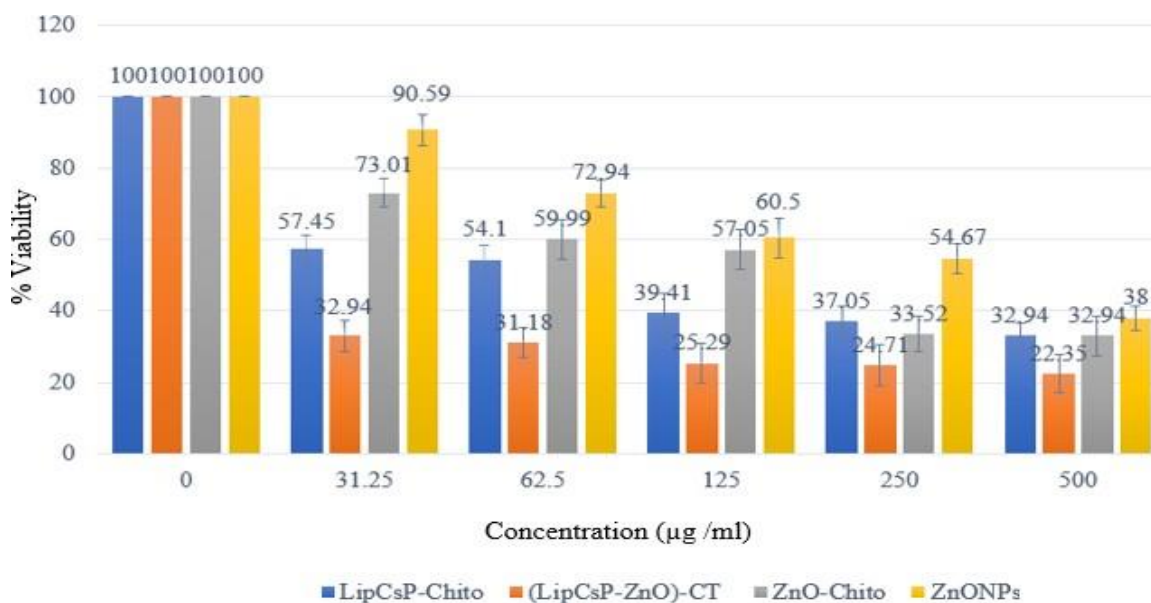
Figure 24: **Concentration dependent viability reduction effect of nanoformulations against *Klebsiela pneumonia***

LipCsP coated chitosan (LipCsP-Chitosan), Zinc Oxide nanoparticles (ZnONPs), ZnO coated chitosan (ZnO-Chitosan), Dual Nanohybrid Delivery System, (LipCsP/ZnO)-CT were tested against *Klebsiela pneumoniae* (Values reported are mean ± SD; n = 3)
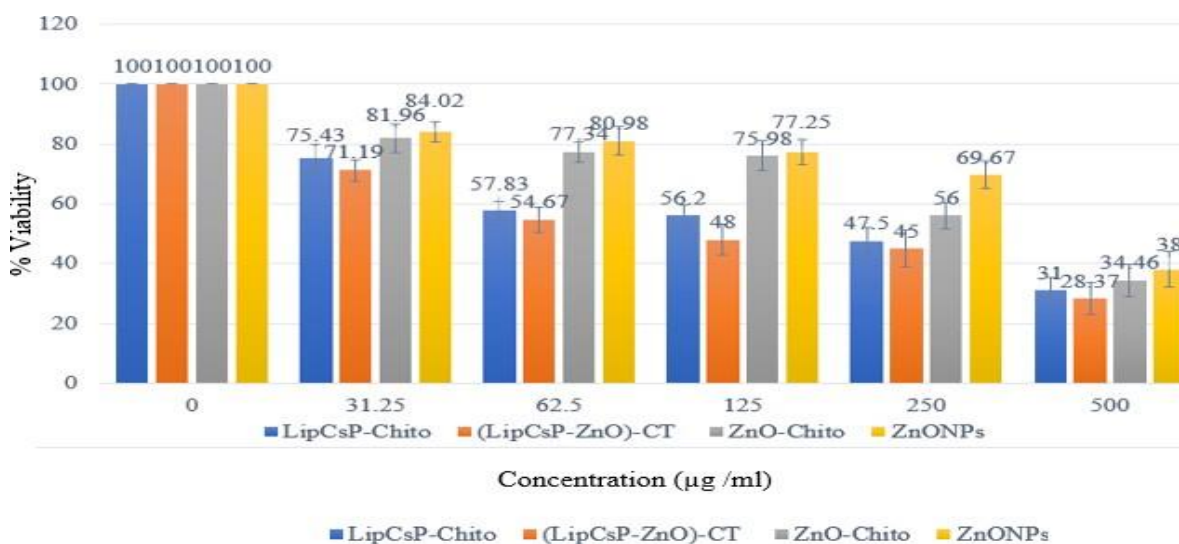
Figure 25: **Concentration dependent viability reduction effect of nanoformulations against *Staphylococcus aureus***

LipCsP coated chitosan (LipCsP-Chitosan), Zinc Oxide nanoparticles (ZnONPs), ZnO coated chitosan (ZnO-Chitosan), Dual Nanohybrid Delivery System (LipCsP/ZnO)-CT were tested against *Staphylococcus aureus* (Values reported are mean ± SD; n = 3)
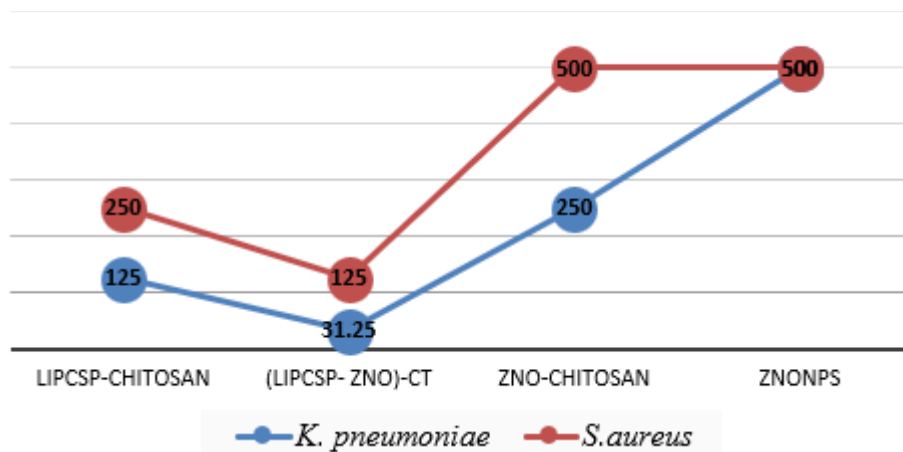
Figure 26: Minimum inhibitory concentrations (MIC50) of nanoformulations

LipCsP coated chitosan (LipCsP-Chitosan), Zinc Oxide nanoparticles (ZnONPs), ZnO coated chitosan (ZnO-Chitosan) and Dual Nanohybrid Delivery System (LipCsP/ZnO)-CT were tested against *S. aureus* and *K. pneumoniae*.
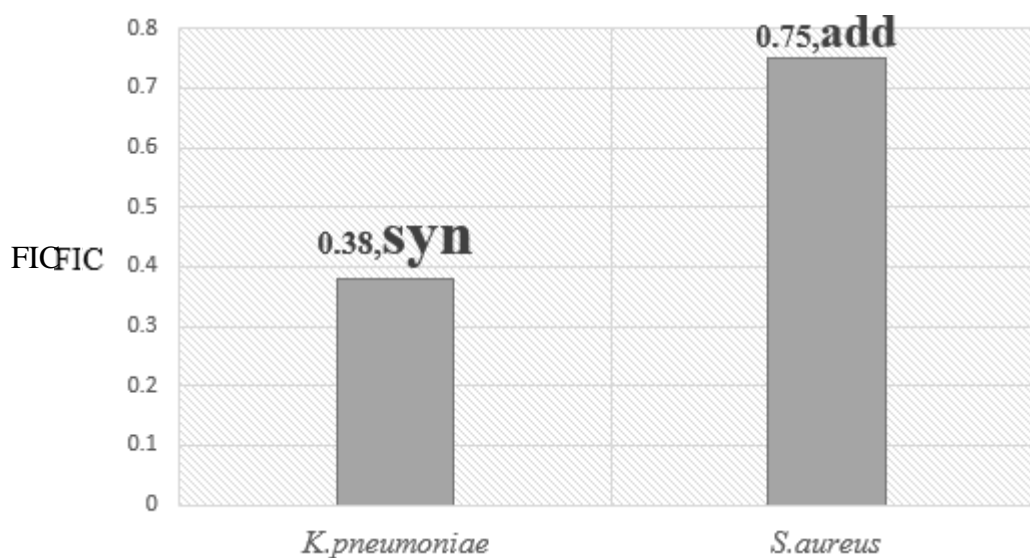
Figure 27:   Antimicrobial interaction analysis against *Klebsiella pneumoniae and Staphylococcus aureus*

Note: Synergy (Syn), additive (add), Klebsiella pneumoniae (K. pneumoniae) and Staphylococcus aureus (S. aureus) and fractional inhibition concentration (FIC).
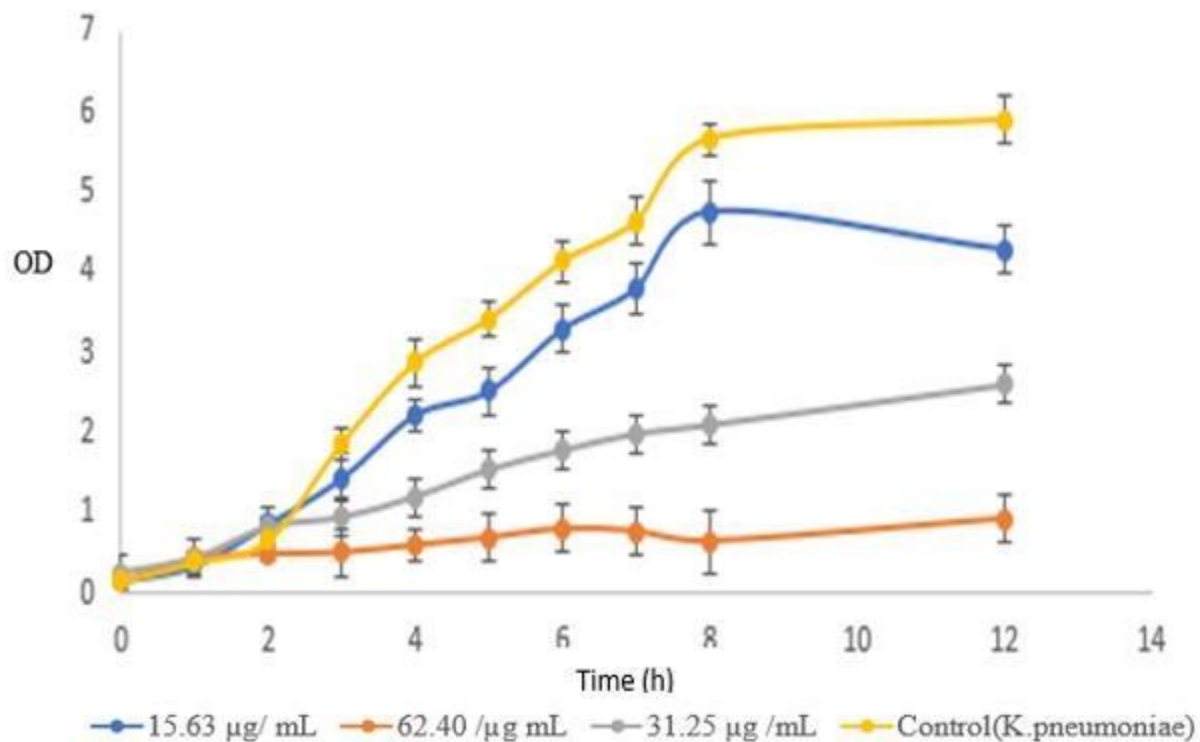
Figure 28: Time-concentration dependent viability reduction effect of Dual Nanohybrid Delivery System (LipCsP/ZnO)-CT against *Klebsiela pneumoniae* (*K. pneumoniae*); OD represent optical density
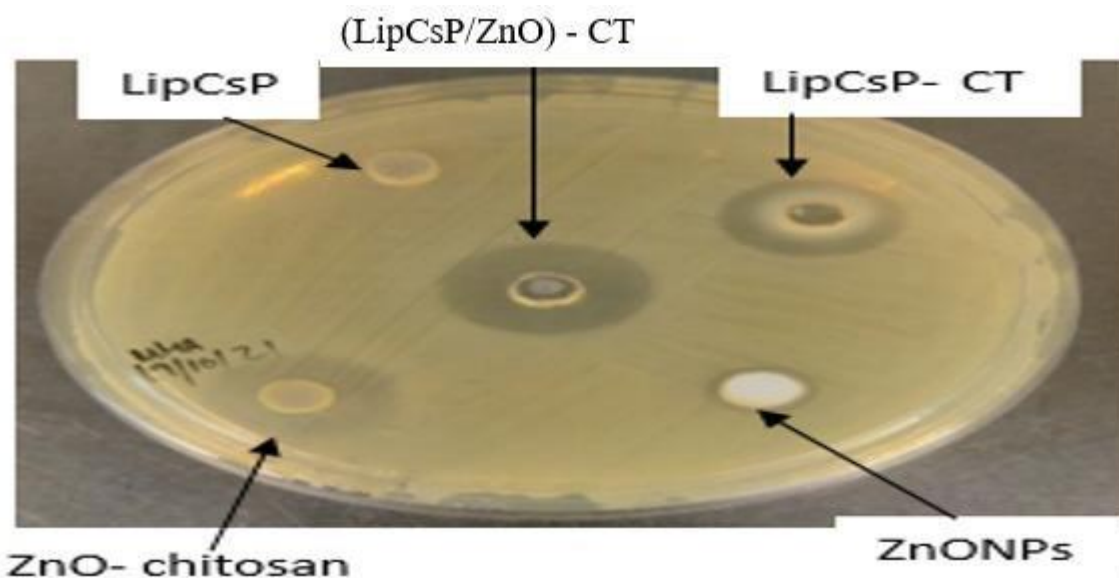
Figure 29: Antibacterial activities (mm of zone inhibition) of nanoformulations against tested *Klebsiela pneumoniae*

Liposome loaded *Carissa spinarum* polyphenols (LipCsP), LipCsP coated chitosan (LipCsP-Chitosan), Zinc Oxide nanoparticles (ZnONPs), ZnO coated chitosan (ZnO-Chitosan) and Dual Nanohybrid Delivery System (LipCsP/ZnO)-CT were tested against *Klebsiela pneumoniae (K. pneumoniae)*
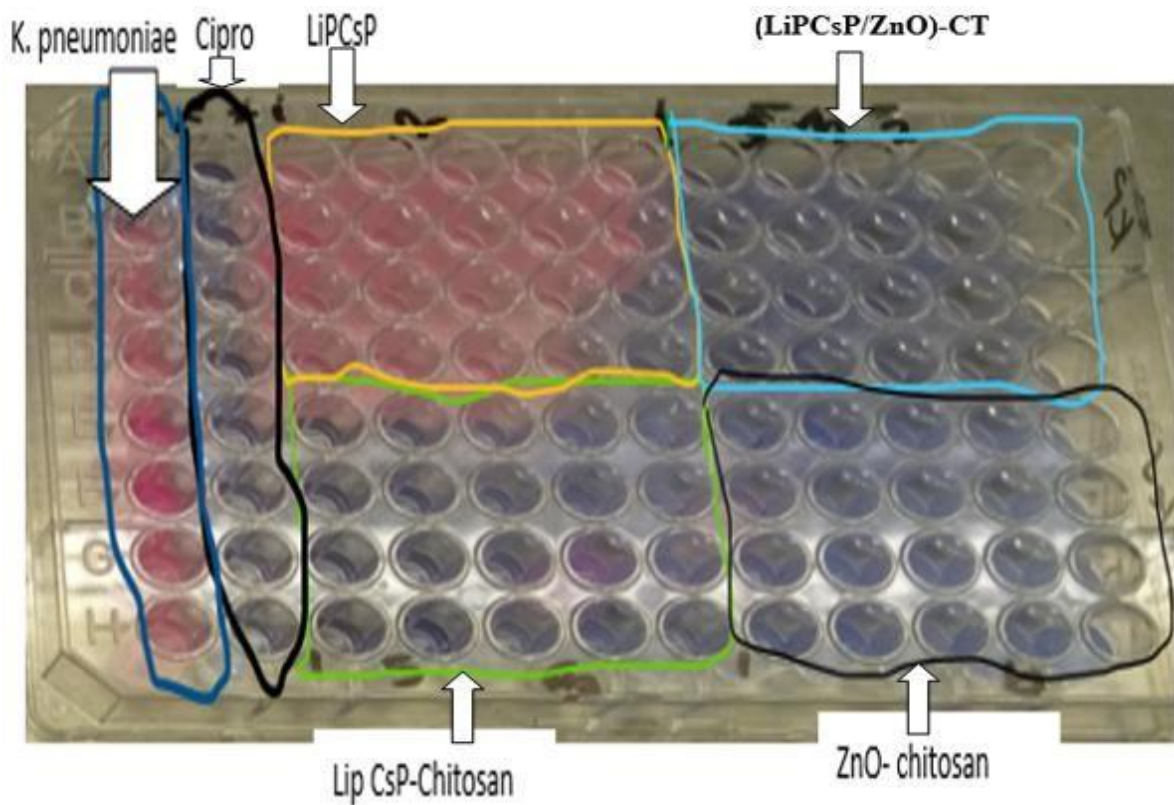
Figure 30: Concentration dependent viability reduction effect of nanoformulations

Liposome loaded *Carissa spinarum* polyphenols (LipCsP), LipCsP coated chitosan (LipCsP-Chitosan), Zinc Oxide nanoparticles (ZnONPs), ZnO coated chitosan (ZnO-Chitosan) and Dual Nanohybrid Delivery System (LipCsP/ZnO)-CT were tested against *Klebsiela pneumoniae*.
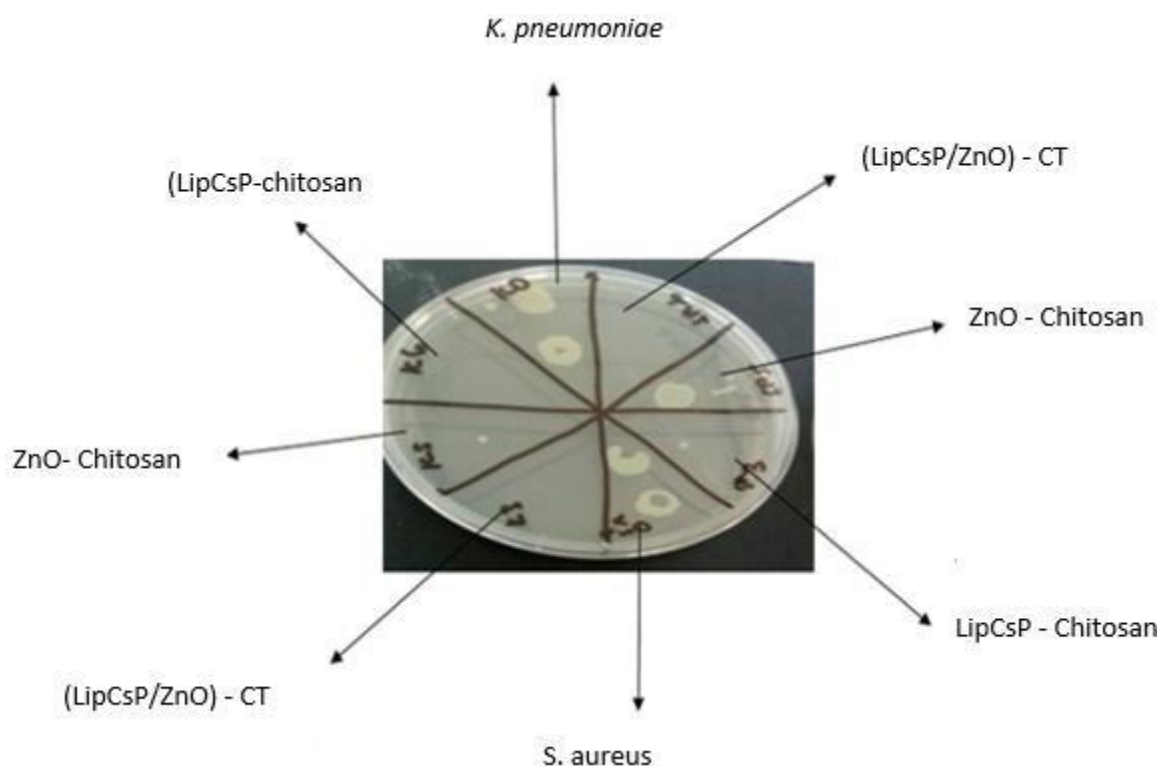
Figure 31: Bactericidal effect of nanoformulations

LipCsP coated chitosan (LipCsP-Chitosan), ZnO coated chitosan (ZnO-Chitosan) and (LipCsP/ ZnO)- CT were tested against *Klebsiela pneumoniae* (*K. pneumoniae*) and *Staphylococcus aureus* (*S. aureus*)

4.2   Discussion

4.2.1   Phytochemical analysis and total phenolic content

Preliminary screening of the presence of phytochemicals indicates that most of these phytochemicals are in the class of polyphenols, which reveals the high distribution of them in *Carissa spinarum* leaf extract. Interestingly, the appearance of flavonoid C = O functional groups and C-C of aromatic rings at 1602 cm^{-1} and 1439 cm^{-1} absorption bands in FTIR analysis complement the information for polyphenol distributions in *Carissa spinarum.* According to the regression equation of the calibration curve (Y = 0.005x+0.347; R2 = 0.981), which supports quantification of polyphenols in aqueous and methanol extracts, the polyphenols are more highly distributed in methanol extracts than in water extracts. This is due to the additional dispersion factors that exist in methanols, which are not present in water; nevertheless, the dielectric constant of water favors the extraction of polyphenols when the MAE method is used.

59

For the issue of toxicity prevention, polyphenol-based aqueous extract is the best option for encapsulating these compounds in nanoformulations. Integrations of the polyphenols with nanoformulations have an advantage for improving their health benefits, particularly in the treatment of diseases (Ansari & Patil, 2018). For instance, terpenoids are thought to have antibacterial properties elicited by rupturing cell membranes and inhibiting the activity of ion channels (Na^+, K^+, Ca^{2+}, or Cl^-). Thymol, a terpenoid frequently present in essential oils, is said to form a hydrogen bond with the active site of specific enzymes, which then renders the enzyme inactive (Guimaraes *et al*., 2019). The ability of tannins to precipitate proteins and prevent metabolic activities like oxidative phosphorylation is what gives them their antibacterial properties (Fraga-Corral *et al*., 2020).

Anti-inflammatory, antibacterial, and antioxidant properties are reportedly elicited by flavanoids. Flavanoids' hydroxyl group is thought to provide antioxidant and chelating effects that boost their ability to fight microbes (Adamczak *et al*., 2020). The capacity of saponins to create a pore in the cell membrane, which allows hazardous substances unrestricted access to the cell, has been attributed to their bioactivity as an antibacterial agent (Kregiel *et al*., 2017). Alkaloids are thought to be a good source of many drugs and can kill microbes by intercalating their DNA (Rubaka *et al*., 2014).

4.2.2 Particle size, Zeta potential, PDI and encapsulation efficiency

The nanoformulations display different zeta potentials. Remarkably, the chitosan-capped nanosystems (LipCsP-chitosan, ZnO-chitosan, and (LipCsP/ZnO)-CT) have positive potentials, while the non-capped system has negative potentials (LipCsP). The non-capped inorganic nanoparticles (ZnONPs) display positive potential. Except ZnONPs, all nanoformulations have a potential greater than or equal to ±30 mV, which suggests their steady dispersion and absence of aggregation. The zeta potential of ZnONPs is less than ±30mV which indicates low dispersion in colloid systems, which increases the chance of agglomeration in colloid systems. This effect does not appear in ZnO-chitosan due to the presence of a capping agent (chitosan). The effect of cationic capping introduces positive charges, which repeal and improve the dispersions in colloidal systems.

Zeta potential values greater than or equal to ±30 mV was found to suggest steady dispersion, as reported by Baranauskaite *et al*. (2018). All nanoformulations except ZnO nanoparticles have a polydispersity index lower than 0.4, which indicates a less pronounced tendency to

aggregation in the absence of a capping agent. The positively charged ammine group of the chitosan interacts with the negatively charged phosphate group of the liposome by electrostatic attraction and is adsorbed on the surface of the liposome. The adsorption of chitosan amplified the density of the positive charge and made the Zeta potential positive (Gibis *et al*., 2016). Recently, Abosabaa *et al*. (2021) reported that an increased Zeta potential for chitosan liposomes due to their cationic character can be used as an indication of successful coating. Zeta potential (ζ potential) is thus a measure of the surface electrical charge of particles, and has often been used to characterize colloidal drug delivery systems.

The size of the zeta potential provides a clue as to the colloidal system's possible stability. A more stable colloidal dispersion will result from increased particle repulsion as the zeta potential rises. There won't be a tendency for the particles to aggregate if every particle in suspension has a significant negative or positive zeta potential since they will tend to repel one another (Mady & Darwish, 2010). The nanoformulations show different sizes depending on the nature of the nanoparticles or the capping effects. The increases in size of LipCsP-chitosanare attributed to the additional polymeric layers (chitosan) on the lipid bilayer of the liposome.This is contrary to the reduction of the size of polymeric-coated ZnONPs, which is due to the capping effect of chitosan on ZnONPs, which prevents aggromeration of nanoparticles and thus limits their growth into large sizes. The increased amount of polyphenol loaded in LipCsP-chitosan is due to some of the polyphenols being trapped in the chitosan layer, which adds to the amount loaded in the liposomal core.

4.2.3   Optical analysis

ZnONPs were confirmed to have formed when their optical examination revealed a unique absorption peak at 366 nm. The quantum confinement property of the ZnONPs is evident from the blue shift in excitation absorption. As the particle size decreased in the quantum confinement range, the absorption edge shifted to a lower wavelength as a result of an increase in the particle's band gap. It has been found that ROS generation and nanoparticle energy band gaps are associated. According to Arakha *et al*. (2017), the formation of ROS is triggered by a decrease in the band energy gap.

4.2.4 Fourier Transform Infrared (FTIR) spectroscopy analysis

Fourier Transform Infrared (FTIR) spectra show different absorption bands. The variation of the finger print region in the analyzed spectra reveals the interaction of chitosan with liposomes, zinc oxide, or polyphenols. Indeed, the shifting of the vibration frequency to high or lower frequencies also describes the interactions of the molecules in fabricated nanoformulations. The interaction of liposomes with chitosan reveals the disappearance of N-H primary amine (bending) in chitosan, which was previously reported (Abosabaa *et al.*, 2021). Along this line, the shifting of the stretch vibration frequency of OH and NH from 3352 cm^{-1} to a lower vibration to a frequency of 3331 cm^{-1} is due to hydrogen bonding between the liposome and chitosan.

Furthermore, the C = O vibration frequency of the liposome shifted from 1739 cm^{-1} to lower frequency at 1732 cm^{-1}. The changes in the absorption bands of the P = O group of liposomes from 1236 cm^{-1} to a lower frequency of 1226 cm^{-1} reveals the interaction between the CsP polyphenol components and the liposomes. Further more some spectrum justifies the presence of classes of polyphenols in *Carissa spinarum* extract. For example, the absorption spectrum at 3276 cm^{-1} reflecting OH stretching and vibrating is ascribed to phenolic hydroxyl groups (Lisperguer *et al.,* 2016; Liang *et al.,* 2011). The presence of C = O functional groups and C-C of aromatic ring at 1602 cm^{-1} and 1439 cm^{-1}. suggests the presence of flavonoids.

The shifting of -OH vibration frequency of chitosan from 3359 cm^{-1} to 3359 cm^{-1} upon coating the chitosan suggests signifies the formation of a hydrogen bond between these groups and ZnONPs. The new absorption peaks at 670 cm^{-1} and 465cm^{-1} are due to the attachment of the amide group and the stretching mode of ZnO, which is consistent with the findings reported by AbdElhady *et al.* (2012). The OH bending vibration frequency at 1013 cm^{-1} shifted to 1020 cm^{-1}.

4.2.5 Scanning electron microscope

The alteration of surface topography as a result of coating chitosan over the surface of chitosan reveals the successful coating of chitosan on the surface of ZnO nanoparticles.

4.2.6 Bioaccessibility

Polymeric coatings provide versatile protection against polyphenol degradation in gastro-intestinal environments (Jung *et al.,* 2014). According to a previous publication by Hasan *et al.* (2019), the coated chitosan on the liposome delivery system can resist the gastrointestinal (GI) enzyme's digestion environment, which further increases the bioavailability of active substances. This phenomenon was also reported by Panya *et al.* (2010), who reported that coating chitosan on the surface of liposomes reduces lipid oxidation. However, they incorporated rosmarinic acid as an antioxidant, which combined with chitosan to enhance the reduction of the oxidative degradation of liposomes. Due to the chitosan coatings in LipCsP-chitosan, oxidative degradation is overwhelmed, hence bioaccessibility is increased. Our results are consistent with the earlier study by Ydjedd *et al.* (2017), which reported on the microencapsulation of carob polyphenols from carob pulp extracts.

This study focused on the protective role of the delivery system. In their study, carob polyphenols were reported to effectively protect against pH changes and enzymatic activities during digestion, thereby promoting bioaccessibility in the gut. However, the coated system was not included in their study. In the present study, it was also noted that the integration of inorganic oxide in a dual nanodelivery system improves bioaccessibility. Among all formulations tested, the dual nanohybrid system LipCsP/ZnO)-CT exhibits higher bioaccessibility, which reflects its large potential to protect polyphenol degradation. This significant increase could be due to the combination of chitosan and metal oxide, which create stable systems in acidic and alkaline media and are essential in minimizing the degradation of polymeric membranes.

When charged species in the stomach electrolyte bond to the surfaces of liposomes, they help to reduce the negative charge of the liposomes by changing the ionic strength and pH in the gastric environment. The negative potential increases in the duodenum, which may indicate the adsorption of anionic species (such as free fatty acids, bile salts, or lipase) on liposome surfaces or the uptake of tiny negatively charged ions from the electrolyte solution in the small intestine. The bioaccessibility of polyphenols after the intestinal phase differed significantly ($P < 0.05$) from that during the gastric phase. This behavior is attributed to the presence of a mixture of pancreatic enzymes and bile salts that destroy the liposomal membrane, which was also reported by Hasan *et al.* (2019)

4.2.7 CsP release in Gastro-Intestinal phase by nanoformulations

The release of polyphenols from LipCsP-Chitosan is slower and more sustained than in the uncoated system (LipCsP). This is attributed to the ability of the polymeric coat to protect the degradation of membrane bilayers, which agrees with the findings reported by Hasan *et al.* (2019). Chitosan-coated liposomes released curcumin more sustainably than uncoated nanoliposomes in their study. Furthermore, they suggested that the ability of the coated liposome system to sustain the release of cargo is attributed to the prevention of lipid digestion by coated polymers such as chitosan.

Dual Nano Hybrid System (LiPCsP/ZnO)-CT exhibits the slowest and most continuous release pattern of CsP as compared to the release exhibited by LipCsP and LipCsP-chitosan. This is attributed to the presence of chitosan-Zn (II) in the nanohybrid construct, which reduces the degradation of the chitosan layer at high pH and also contributes to a more stable polymeric layer, thus slowing and controlling the release of polyphenols from the liposome core. Based on the aforementioned pH-responsiveness of the chitosan-Zn (II) complex in controlling the sustained release of polyphenols from the liposome core, the release of polyphenols from the liposome core in the presence of the chitosan-Zn (II) complex in the Dual Nanohybrid Delivery System is significantly different (P<0.05) as compared to the release exhibited by LipCsP and LipCsP-Chitosan alone.

The smart fabrication of the delivery system into a dual nanohybrid delivery system critically controlled the release of the drug, which is essential in maintaining the therapeutic window and reducing toxicity. The LipCsP/ZnO system executes the sustained release of polyphenols more efficiently, which reduces the burst release as compared to the release of polyphenols by LipCsP and LipCsP-chitosan. Because burst releases may result in drug concentrations in vivo that are close to or over hazardous levels, researchers try to prevent them (Huang & Brazel, 2001). According to Huang and Brazel (2001), any substance released during the burst stage may also be digested and eliminated without being fully used. However, in some situations, the burst release is crucial. For instance, when treating a wound for the first time, the initial burst immediately relieves the pain, and then a prolonging release helps to encourage slow healing (Geraili & Mequanint, 2021).

The fabrication of nanohybrid materials enables the incorporation of different nanomaterials with different delivery functions. In the LipCsP/ZnO-CT system, some of the nanomaterials

can be used to control the release of drugs by maintaining the degradation of the nanosystem. In this study, the inclusion of ZnO-chitosan as one of the components of (LipCsP/ZnO-CT controls the release of polyphenols by its pH-responsive properties, reducing the rate of degradation, minimizing the burst release, and ultimately controlling and sustaining the release of polyphenols.

4.2.8 Release of CsP mechanism in Gastro-Intestinal phase by nanoformulations

Non-Fickian diffusion is demonstrated by LipCsP-chitosan and LipCsP/ZnO-CT. Such mechanisms show that both erosion and diffusion mechanisms were under control of release. Polymers first expand and create a gelatinous mass, which causes them to relax and then erode. Diffusion then occurred after the polymer became soluble and porous. However, the LipCsP system that was not coated displayed diffusion processes.

4.2.9 Storage stability of nanoformulations

Uncoated ZnONPs destabilize the zeta potential earlier as compared to coated ZnONPs (ZnO-chitosan), due to their tendency to agglomerate in the absence of capping agents. Capping agents facilitate the repulsion force and minimize the electrostatic force, thus reducing the agglomeration of nanoparticles to improve stability. Conversely, the early destabilization of LipCsP as compared to LipCsP is due to the rapid degradation of the naked liposome due to changes in pH, temperature, and air oxidation. The prominent storage stability of (LipCsP/ZnO) is due to the repulsion force and additional steric hindrance that exist in the Chitosan-Zinc (II) complex. These two factors hinder the degradation of the Dual Nanohybrid Delivery System, as a result of pH, temperature fluctuation, and air oxidation.

The Dual Nanohybrid Delivery System (LiPCsP/ZnO)-CT withstands the Fluctuation of zeta potential as compared to all formulations. The reason that makes the LiPCsP/ZnO)-CT withstand the fluctuation of zeta potential is due to the presence of a large magnitude of zeta potential, which creates a great repulsion force between LipCsP-Chitosan and ZnO-Chitosan. The repulsion forces tend to minimize the electrostatic force of attraction between nanoparticles, which maintains the charges of the nanoparticles. Over recent years, hybrid materials based on polymer-metallic ions constructed on chitosan have attracted attention due to the excellent properties of individual components and their outstanding synergistic effects simultaneously (Abdelhadi, 2012).

It has been reported that the combination of chitosan and metal oxide creates unique properties such as photocatalysis and the creation of stable systems in acidic and alkaline media (Al-Nemrawi *et al.,* 2022). Based on these aforementioned grounds, this study focused on the fabrication of an improved stable nanohybrid system that involves combined repulsion force and pH responsiveness against degradation effects and steric hindrance to maintain stable Dual Nanohybrid systems.

4.2.10 Stability study in simulated environment

The results demonstrate that there is no significant change in zeta potential in the oral phase despite the variations in charge potential seen in the stomach and intestinal stages. It's possible that the brief contact with the nanoformulation won't be sufficient to noticeably change the zeta potential. The stability of the Zeta potential in a simulated gastrointestinal environment is impacted by the presence of HCl in the stomach phase because it alters the phosphatidylcholine head's ionization state and charge distribution. These results matched those of Toro-Uribe et al. (2018), who remarked about how simulated gastrointestinal fluid affected the zeta potential of liposomes. They found that the electrical charge of liposomes varied according to variations in the solution conditions (pH and ionic strength) on the adsorption of charged species from gastric electrolyte solution on liposome surfaces during the early stomach stage (gastric phase).

The anionic bile salts in the intestinal phase adsorb on the liposome's surface and raise the liposome's negative potentials (He *et al.*, 2019). He *et al*. (2019) suggests that the acid, bile salts, and pancreatic enzymes present in the gastro-intestinal environment have a major detrimental effect on conventional liposomes. Due to their breakdown and subsequent payload leakage, which is then exposed and destroyed, the charge potentials fluctuate as shown in LipCsP. Due to its low phase transition temperature, phosphatidylcholine possesses a lipid bilayer that is easily dissolved by bile salt. Phospholipids are hydrolyzed by lipolytic enzymes found in pancreatic fluid, which break down the structure of liposomes. To combat the effects of gastrointestinal fluid's breakdown, liposomes can be coated on their surface (Lee, 2020; Hasan & El Khoury, 2019; Zamani-Ghaleshahi *et al.,* 2020).

According to Sebaaly *et al*. (2021), the presence of a chitosan layer, which forms a wall to prevent swelling and the release of encapsulated components, causes the polymeric coated nanoformulation (LipCsP-chitosan) to exhibit a more stable charge than the non-coated system (LipCsP). Additionally, the electrostatic interaction between chitosan and the lipid bilayer

helps to reinforce the structural integrity of the lipid membranes. It was found that chitosan-coated liposomes were significantly more stable in simulated stomach fluid than uncoated liposomes (Filipovic-Grcic *et al.*, 2001). However, according to Pimentel *et al.* (2016), using pH-sensitive polymers prevents them from being broken down by digestive enzymes and makes it easier for bioactive substances to be released in gastrointenstinal environment. In the presence of the gastrointestinal environment, the combination of repulsion force, pH responsiveness to reduce the degrading effect, and steric hindrance promotes the stability of the Dual Nanohybrid Delivery System. The noteworthy charge stabilization was more obvious in (LipCsP/ZnO)-CT.

4.2.11 Antimicrobial effect of nanoformulations on bacterial pathogens

LipCsP nanoformulations exhibit much more antibacterial activity (P < 0.05) than free extract (CsP) does. The liposomes' capacity for transport is what causes the discrepancy in antibacterial activity. According to other studies (Wang *et al.*, 2016; Bozzuto &Molinari, 2015), the capacity of the lipid bilayer structure to fuse with an infectious pathogen can be associated to its increased antibacterial efficacy in comparison to free extract. However, Noudoost *et al.* (2015) highlighted that the cellular transport and release of the active component inside the bacterial cell is made possible via nanoliposomes' intermembrane transfer, contact release, absorption, fusion, and phagocytosis. Other studies have revealed that the fusion with bacterial membrane structure caused by the fluidity of the lipid bilayer contributes to high antimicrobial doses inside bacteria.

According to Wang *et al.* (2020), the bacterial cell membrane and the liposomal phospholipid bilayer have a mimetic feature that makes it easier for bacteria to fuse with bacterial walls. In addition to enhancing liposome stability, cationic surface modification also makes it easier for them to engage in antibacterial activity. In comparison to CsP and LipCsP, the coated liposome system (LipCsP-chitosan) displays increased activity. The disparity in charge potential is what causes the difference in antibacterial activity between the coated (LipCsP-Chitosan) and uncoated (LipCsP) systems. A positively charged coating system has a strong attraction force with the bacterial cell's negative membrane, causing cell damage. The improvement of antibacterial activity by positively charged liposome systems is similar to the findings of Lee *et al.* (2022). However, different materials for surface modification of lipid nanoparticles were used.

In their research, synthetic lipid-coated hybrid nanoparticles (LCHNPs), made of a poly (lactic-co-glycolic acid) (PLGA) core and a dioleoyl-3-trimethylammonium propane (DOTAP) lipid shell, were generated and loaded with the antibiotic vancomycin (van), resulting in positively charged liposome systems (van-LCHNPs) with a Zeta potential of +36.13 mV. In order to produce negatively charged nanosystems (van-PLGANPs) with a Zeta potential of -36.83 mV, vancomycin was loaded into poly (lactic-co-glycolic acid) (PLGA). Van-LCHNPs eliminated up to 99.99% of the underlying biofilm cells when applied to cure bacterial biofilms; this result was not seen with Free-Van or Van-PLGANPs. Imam *et al*. (2022) observed that the cationic charge of chitosan can interact with negatively charged cell membranes to open tight epithelial junctions, which is consistent with this explanation. Ammonia ions (NH_3^+) damage bacterial cell walls and cause macromolecule leaks by electrostatically adhering to microorganism cell walls (Imam *et al*., 2022).

Mady and his coworker (2010) suggested that the mucoadhesive feature of chitosan is made possible by a positively charged surface that favors adhesions to cell membranes, which are typically negatively charged. ZnONPs have antibacterial action against the studied pathogens, but at a lower activity than ZnO-chitosan. ZnONPs increase the positive charge of the chitosan amino group and improve interactions with the negatively charged microbial cell wall According to Farouk *et al*. (2012), there are several mechanisms that can cause damages to bacteria, including the generation of active oxygen species, penetration through the cell membrane, interaction between the active oxygen species and the cell, and damage to the cell wall caused by particles adhering to the bacteria's surface due to electrostatic forces. By producing ROS such hydrogen peroxide and hydroxyl radicals, ZnONPs have an antimicrobial effect.

According to Taylor and Webster (2011), the hydroxyl radical can depolymerize polysaccharides, damage DNA, render enzymes inactive, and start lipid peroxidation. ZnO is also capable of damaging the cytoplasmic membrane by dissolving in water and releasing Zn^{2+} ions. The Zn^{2+} ion functions as an inhibitor of the glycolytic enzyme through thiol group oxidation because of its affinity for the sulfur group. Electrostatic forces are used by the chitosan in the ZnO-Chitosan composite to interact with the bacterial cell wall's negative charge. These interactions impair the ability of the microbial cell membrane to function, such as allowing internal substances to leak out, and they also stop nutrients from being transformed, which causes the bacteria to die (Farouk *et al*., 2012). The nanoparticles' surface was coated

with chitosan, which resulted in steric stability and decreased agglomeration (Guerrini *et al*., 2018), consequently raising the effective concentration of the nanoparticles and improving the binding forces between the positive charges of chitosan and the negative charges of the bacteria (Yilmaz, 2020; Ke *et al*., 2021).

The electron transition from the valence band to the conduction band caused an electron-hole pair with the electron (e^-) being reductive and the hole (h^+) being oxidative when ZnO nanoparticles were exposed to light, which was the mechanism that controlled the production of ROS (Abdelhadi, 2012). Superoxide anion (O^-_2), hydroxyl radicals, and perhydroxyl radicals (HO_2^-) were produced as a result of the hole's reaction with the surface of ZnO nanoparticles (Lallo da Silva *et al*., 2019; Mendes *et al*., 2022). These extremely potent free radicals and the deadly hydrogen peroxide (H_2O_2), which are created from and, can harm bacterial cells, causing breakdown and total internal destruction.

The surface area of nanoparticles influences the generation of reactive oxidation species (ROS). Fabrication of chitosan with ZnO nanoparticles leads to changes in the chemical composition of the surface of the nanoparticles, which consequently change their biological characteristics. The generation of ROS is correlated with the energy band gap of nanoparticles. ROS are produced as the band energy gap narrows (Arakha *et al*., 2017; Khalid *et al*., 2021). Compared to the Tauc plot of ZnONPs, the ZnO-Chitosan nanoparticles plot showed a reduced energy band gap. It was anticipated that a decrease in band energy would boost ROS production and boost antibacterial activity. The results of Aga *et al*. (2022), who decreased the energy band gap of ZnONPs by doping with sulfur atoms, are consistent with this observation. Improved antibacterial activity against *Staphylococcus aureus* was shown by sulfur-doped ZnONPs.

Reduction of band gap improves visible light absorption and the generation of ROS, thus improving antibacterial activities (Agar *et al.,* 2022; Rekha *et al.,* 2010). The interaction of antibacterial substances in LipCsP/ZnO-CT contributed to the high antibacterial activity as compared to when LipCsP-chitosan, ZnO-chitosan were treated alone against a pathogen. Dual Nanohybrid Delivery System (DN-DS) is based on biomimetic-inorganic hybrid materials that are smart-fabricated to deliver herbal antibacterial (polyphenol) and inorganic antibacterial (zinc oxide) simultaneously against *Klebsiella pneumoniae and S. aureus*. The two antibacterial substances, polyphenol and zinc oxide, essentially combined to improve antibacterial activity against *Klebsiella pneumoniae* and *S. aureus* by the mechanism depicted

in Fig. 1 (LipCsP/ZnO)-CT. Improve stability, bioavailability, and antibacterial performance more than separated systems (LipCsP, LipCsP-chitosan, and ZnO-chitosan).

(LiPCsP/ZnO)-CT exhibits synergistic interactions against *K. pneumoniae* and additive interactions against *S. aureus*. Synergistic interactions occur when the combined activity of the drugs is greater than the sum of their individual effects (Rubaka *et al.* 2014). Synergism can be contributed by the sequential blocking of metabolic pathways, the facilitation of the entry of one drug into a microorganism by the other drug, or when one drug prevents the inactivation of another drug by microbial enzymes. On the other hand, additive interaction occurs when the activity of the combined action is equivalent to the sum of the activity of each drug when used alone. In an antagonistic interaction, the combined action is less effective than the more effective agent when used alone. Antagonism is discouraged for clinical uses, and it occurs when a bacteriostatic drug is given with a bactericidal drug. Antagonism occurs mainly if a bacteriostatic drug reaches the site of infection before the bactericidal drug (Rubaka *et al.*, 2014).

The synergistic approach, whereby the combined action of both agents is more effective than the action of a single agent, has been the focus of most combination treatments, as this interaction type has understandably been known to be the most effective. Additivity, on the other hand, is less preferred compared to synergism, wherein the interaction between two drugs is mutually exclusive to each other, resulting in a less significant reduction of applied dosages when used singly or combined. The inhibition kinetic profile was concentration-time dependent, and the effect ranked as 2MIC >MIC>0.5MIC against *K. pneumoniae*. Untreated microorganisms exhibited a normal growth pattern and exhibited a high optical density after 12 h as compared to the microorganisms treated with different concentrations of LipCsP/ZnO-CT. The study reveals the nanohybrid system is a potential delivery system for attaining sustained release of polyphenols and is prominent in exhibiting a bactericidal effect against *K. pneumoniae*.

Gram-negative bacteria suffer greater damage to their cell walls as a result of the physical contact between nanoparticles and the cell wall because they lack the thick peptidoglycan layer present in Gram-positive bacteria, which may serve as a protective coating. The fact that Gram-negative bacteria are covered in lipopolysaccharide molecules, which have a negative charge, may further contribute to their vulnerability to NPs (Slavin *et al.*, 2017). Because these negatively charged molecules have a stronger affinity for the positive ions that are primarily

released along with the nanoparticles, there is a buildup and greater uptake of ions that eventually cause intracellular damage. A mosaic of anionic surface domains rather than a continuous layer is found in the cell wall of Gram-negative bacteria like Salmonella typhimurium, according to another research (Magnusson & Bayer, 1982). Consequently, due to the comparatively high NP concentrations in these regions, the potential binding of a large number of NPs on these negative anionic domains may increase the focal toxicity. Additionally, it was discovered that *E. coli* is more negatively charged and stiff than *S. aureus* through the use of mathematical calculations and electrophoretic mobility tests (Sonohara *et al.*, 1995).

In the present study, the focus was on creating high repulsion forces between two cationic nanosytems to improve stability in a colloidal environment. The charge stability as indicated by storage time and gastrointestinal phases contributes to the understanding of nanoparticle stability in a colloidal environment. A stable charge also makes it easier for nanoformulations to bind to the bacterial cell wall. Electrostatic binding with the bacterial cell wall is considered one of the mechanisms for destroying the bacterial cell wall that allows the discharge of ZnO ions in the cell. On the other hand, fusion, phagocytosis, and adherence of cationic liposomes to the surface of bacteria allow cellular transport and release of the polyphenols inside the bacterial cell.

The two bioactive principles, polyphenols and zinc oxide nanoparticles, exhibited synergistic effects against the tested microbes. Polyphenols also have antibacterial activity by inactivating metabolism through hydrogen binding of the phenolic compound with vital proteins such as microbial enzymes (Bourab-Chibane *et al.*, 2019), whereas ZnONPs generate ROS. This synergy effect of the LipCsP/ZnO-CT system contributed to the significant increase in antibacterial activities as compared to other formulations.

CHAPTER FIVE

CONCLUSION AND RECOMMENDATIONS

5.1   Conclusion

This study successful reveals, Dual Nanohybrid Delivery System is potential antibacterial material for delivery of *Carissa spinarum* polyphenols against bacteria strain particularly *K. pneumoniae*. Therefore, the fabricated nanohybrid is reliable material for treatment of pneumococcal infections. Polyphenols and Zinc oxide nanoparticles were dual delivered by nanohybrid system to enhance antibacterial activity against bacterial strain facilitated by prominent electrostatic attraction exhibited by DN-DS with bacterial cell wall. Indeed, the bioavailability of polyphenols was improved as revealed by high bioaccessibility of polyphenols protected by DN-DS in simulated GI fluid.

Surface modification of delivery material is prominent approach for improvement of physiochemical properties and antibacterial activity of nanomaterials. Chitosan coated nanosystem (LipCsP-Chitosan and ZnO-Chitosan) which are components constitutes Dual Nanohybrid Delivery System, provided improved antibacterial activity, physiochemical properties and bioavailability of polyphenols as compared to uncoated systems. Dual drug delivery system co- functionalized with cationic capping agent gain multitude of advantages, such as improved stability as indicated by stability data and antibacterial activity.

Targeting the bacterial surface is of paramount interest in the development of new antimicrobials. Surface acting agent have been found to display a remarkable bactericidal effect and has simultaneously revealed a low tendency to triggers resistance. (LipCsP/ZnO)-CT is reliable surface acting agent against bacterial strain, with high potential of eradicating pneumonia pathogen such as *Klebsiella pneumoniae*.

This study successful provide the utility of nanohybrid as potential antibacterial material against *K. pneumoniae*. Therefore, the fabricated nanohybrid is an efficacy material for treatment of pneumococcal infections.

5.2   Recommendations

Dual Nano Hybrid Delivery System fabricated in this study is potential material for treatment of bacterial pneumococcal infection. We recommend in further study regarding in vivo study

using animal model to be carried as an advance step for developing nanohybrid system as potential candidate for treatment of pneumococcal infections. Further study involves the measurement of concentration of ROS generated by inorganic nanoparticles should be carried to assess the ability of inorganic nanomaterial to generate optimal concentration of ROS essentially for destruction of bacterial cellular wall. The variation of protein amount as a result of destruction of bacterial cell by nanohybrid and Inhibition of metabolic process such as protein synthesis should be carried to reveal the ability of the antibacterial substance in nanohybrid such as polyphenols and ZnONPs to perform their antibacterial activity at molecular level.

REFERENCES

AbdElhady, M. M. (2012). Preparation and Characterization of Chitosan/Zinc Oxide Nanoparticles for Imparting Antimicrobial and UV Protection to Cotton Fabric. *International Journal of Carbohydrate Chemistry*, *2012*, 1-7. https://doi.org/10. 1155/2012/840591

Abdul, G. K., Kumar, G. A., Zaman, M., Skwarczynski, M., & Toth, I. (2014). Liposomes as nanovaccine delivery systems. *Current Topics in Medicinal Chemistry*, *14*(9), 1194-1208.

Abeylath, S. C., & Turos, E. (2008). Drug delivery approaches to overcome bacterial resistance to beta-lactam antibiotics. *Expert Opinion on Drug Delivery*, *5*(9), 931-949. https://doi.org/10.1517/17425247.5.9.931

Abosabaa, S. A., Arafa, M. G., & ElMeshad, A. N. (2021). Hybrid chitosan-lipid nanoparticles of green tea extract as natural anti-cellulite agent with superior in vivo potency: Full synthesis and analysis. *Drug Delivery*, *28*(1), 2160-2176. https://doi.org/10.1080/ 10717544.2021.1989088

Adamczak, A., Ożarowski, M., & Karpiński, T. M. (2020). Antibacterial activity of some flavonoids and organic acids widely distributed in plants. *Journal of Clinical Medicine*, *9*(1), 1-17.

Adibkia, K., Khorasani, G., Payab, S., & Lotfipour, F. (2016). Anti Pneumococcal Activity of Azithromycin-Eudragit RS100 Nano-Formulations. *Advanced Pharmaceutical Bulletin*, *6*(3), 455-459. https://doi.org/10.15171/apb.2016.059

Ag Seleci, D., Seleci, M., Walter, J. G., Stahl, F., & Scheper, T. (2016). Niosomes as Nanoparticular Drug Carriers: Fundamentals and Recent Applications. *Journal of Nanomaterials*, *2016*, 1-14. https://doi.org/10.1155/2016/7372306

Aga, K. W., Efa, M. T., & Beyene, T. T. (2022). Effects of Sulfur Doping and Temperature on the Energy Bandgap of ZnO Nanoparticles and Their Antibacterial Activities. *ACS Omega*, *7*(12), 10796-10803. https://doi.org/10.1021/acsomega.2c00647

Agarwal, H., Menon, S., Kumar, S. V., & Rajeshkumar, S. (2018). Mechanistic study on antibacterial action of zinc oxide nanoparticles synthesized using green route. *Chemico-Biological Interactions*, *286*, 60-70.

Ahamed, A. J., & Kumar, P. V. (2016). Synthesis and characterization of ZnO nanoparticles by co-precipitation method at room temperature. *Journal of Chemical and Pharmaceutical Research*, *8*(5), 624-628.

Ahmed, F., Soliman, F. M., Adly, M. A., Soliman, H. A. M., El-Matbouli, M., & Saleh, M. (2019). Recent progress in biomedical applications of chitosan and its nanocomposites in aquaculture: A review. *Research in Veterinary Science*, *126*, 68-82. https://doi.org/https://doi.org/10.1016/j.rvsc.2019.08.005

Aisha, A. F., Majid, A. M. S. A., & Ismail, Z. (2014). Preparation and characterization of nano liposomes of Orthosiphon stamineusethanolic extract in soybean phospholipids. *BMC Biotechnology*, *14*(1), 1-11.

Al-Nemrawi, N. K., Alkhatib, R. Q., Ayyad, H., & Alshraiedeh, N. (2022). Formulation and characterization of tobramycin-chitosan nanoparticles coated with zinc oxide nanoparticles. *Saudi Pharmaceutical Journal, 30*(4), 454-461. https://doi.org/10.1016/j.jsps.2022.01.016.

Alrbyawi, H., Poudel, I., Annaji, M., Boddu, S. H. S., Arnold, R. D., Tiwari, A. K., & Babu, R. J. (2022). pH-Sensitive Liposomes for Enhanced Cellular Uptake and Cytotoxicity of Daunorubicin in Melanoma (B16-BL6) Cell Lines. *Pharmaceutics*, *14*(6),1-17. https://doi.org/10.3390/pharmaceutics14061128.

Álvarez-Martínez, F. J., Rodríguez, J. C., Borrás-Rocher, F., Barrajón-Catalán, E., & Micol, V. (2021). The antimicrobial capacity of Cistus salviifolius and Punica granatum plant extracts against clinical pathogens is related to their polyphenolic composition. *Scientific Reports*, *11*(1), 1-12. https://doi.org/10.1038/s41598-020-80003-y

Amin, M. K., & Boateng, J. S. (2022). Enhancing Stability and Mucoadhesive Properties of Chitosan Nanoparticles by Surface Modification with Sodium Alginate and Polyethylene Glycol for Potential Oral Mucosa Vaccine Delivery. *Marine Drugs*, *20*(3), 1-22. https://doi.org/10.3390/md20030156

Amina, S. J., & Guo, B. (2020). A Review on the Synthesis and Functionalization of Gold Nanoparticles as a Drug Delivery Vehicle. *International Journal of Nanomedicine*, *15*, 9823-9857. https://doi.org/10.2147/ijn.s279094

Anaya-Esparza, L. M., Villagrán-de la Mora, Z., Rodríguez-Barajas, N., Sandoval-Contreras, T., Nuño, K., López-de la Mora, D. A., Pérez-Larios, A., & Montalvo-González, E. (2020). Protein–TiO2: A Functional Hybrid Composite with Diversified Applications. *Coatings*, *10* (12), 1-29. https://doi.org/10.3390/coatings10121194

Andrea, L., Marica, I., & Anamarija, R. (2017). Lysozyme-Induced Degradation of Chitosan: The Characterisation of Degraded Chitosan Scaffolds. *Journal of Tissue Repair and Regeneration*, *1*(1), 12-22. https://doi.org/https://doi.org/10.14302/issn.2640-6403.jtrr-17-1840

Ansari, I., & Patil, D. T. (2018). A brief review on phytochemical and pharmacological profile of *Carissa spinarum* l. *Asian Journal of Pharmaceutical and Clinical Research*, *11*(9), 12-18. https://doi.org/10.22159/ajpcr.2018.v11i9.26316

Arakha, M., Roy, J., Nayak, P. S., Mallick, B., & Jha, S. (2017). Zinc oxide nanoparticle energy band gap reduction triggers the oxidative stress resulting into autophagy-mediated apoptotic cell death. *Free Radical Biology and Medicine*, *110*, 42-53. https://doi.org/https://doi.org/10.1016/j.freeradbiomed.2017.05.015

Arakha, M., Saleem, M., Mallick, B. C., & Jha, S. (2015). The effects of interfacial potential on antimicrobial propensity of ZnO nanoparticle. *Scientific Reports*, *5*, (1), 1-10.

Aranaz, I., Alcántara, A. R., Civera, M. C., Arias, C., Elorza, B., Heras Caballero, A., & Acosta, N. (2021). Chitosan: An Overview of Its Properties and Applications. *Polymers (Basel)*, *13*(19), 1-27. https://www.mdpi.com/2073-4360/13/19/3256

Arato, V., Raso, M. M., Gasperini, G., Berlanda Scorza, F., & Micoli, F. (2021). Prophylaxis and treatment against *Klebsiella pneumoniae*: Current insights on this emerging anti-microbial resistant global threat. *International Journal of Molecular Sciences*, *22*(8), 1-20.

Ardean, C., Davidescu, C. M., Nemeş, N. S., Negrea, A., Ciopec, M., Duteanu, N., Negrea, P., Duda-Seiman, D., & Musta, V. (2021). Factors Influencing the Antibacterial Activity of Chitosan and Chitosan Modified by Functionalization. *International Journal of Molecular Sciences*, *22*(14), 1-28. https://doi.org/10.3390/ijms22147449

Ardean, C., Davidescu, C. M., Nemeş, N. S., Negrea, A., Ciopec, M., Duteanu, N., Negrea P., Duda-Seiman, D., & Musta, V. (2021). Factors Influencing the Antibacterial Activity of Chitosan and Chitosan Modified by Functionalization. *International Journal of Molecular Sciences*, *22*(14), 1-28. https://doi.org/10.3390/ijms22147449

Arias, L. S., Pessan, J. P., Vieira, A. P. M., Lima, T. M. T. D., Delbem, A. C. B., & Monteiro, D. R. (2018). Iron oxide nanoparticles for biomedical applications: A perspective on synthesis, drugs, antimicrobial activity, and toxicity. *Antibiotics*, *7*(2), 1-32.

Ashok, B., Arleth, L., Hjelm, R. P., Rubinstein, I., & Önyüksel, H. (2004). In vitro characterization of PEGylated phospholipid micelles for improved drug solubilization: Effects of PEG chain length and PC incorporation. *Journal of Pharmaceutical Sciences*, *93*(10), 2476-2487. https://doi.org/https://doi.org/10.1002/ jps.20150

Auer, G. K., & Weibel, D. B. (2017). Bacterial Cell Mechanics. *Biochemistry*, *56*(29), 3710-3724. https://doi.org/10.1021/acs.biochem.7b00346

Ayala, A., Muñoz, M. F., & Argüelles, S. (2014). Lipid Peroxidation: Production, Metabolism, and Signaling Mechanisms of Malondialdehyde and 4-Hydroxy-2-Nonenal. *Oxidative Medicine and Cellular Longevity*, 2014,1-31. https://doi.org/ 10.1155/2014/360438

Badhwar, R., Mangla, B., & Neupane, Y. R. (2021). Quercetin loaded silver nanoparticles in hydrogel matrices for diabetic wound healing. *32*(50),1-17.

Bakić, M. T., Pedisić, S., Zorić, Z., Dragović-Uzelac, V., & Grassino, A. N. (2019). Effect of microwave-assisted extraction on polyphenols recovery from tomato peel waste. *Acta Chimica Slovenica*, *66*(2), 367-377.

Baranauskaite, J., Duman, G., Corapcıoğlu, G., Baranauskas, A., Taralp, A., Ivanauskas, L., & Bernatoniene, J. (2018a). Liposomal Incorporation to Improve Dissolution and Stability of Rosmarinic Acid and Carvacrol Extracted from Oregano (*O. onites* L.). *BioMed Research International*, *2018*, 1-11. https://doi.org/10.1155/2018/6147315

Barhoumi, A., Liu, Q., & Kohane, D. S. (2015). Ultraviolet light-mediated drug delivery: Principles, applications, and challenges. *Journal of Controlled Release*, *219*, 31-42. https://doi.org/https://doi.org/10.1016/j.jconrel.2015.07.018

Beheshti, F., Shabani, A. A., Akbari Eidgahi, M. R., Kookhaei, P., Vazirian, M., & Safavi, M. (2021). Anticancer Activity of <i>Ipomoea purpurea</i> Leaves Extracts in Monolayer and Three-Dimensional Cell Culture. *Evidence-based Complementary and Alternative Medicine*, *2021*, 1-14. https://doi.org/10.1155/2021/6666567

Beltran-Huarac, J. C., Singh, S. P., Tomar, M. S., Peña, S., Rivera, L., & Perales-Perez, O. J. (2010). Synthesis of Fe3O4/ZnO core-shell nanoparticles for photodynamic therapy applications. *MRS Online Proceedings Library, 1257*, 6-14.

Berhanu, G., Atalel, D., & Kandi, V. (2020a). A Review of the Medicinal and Antimicrobial Properties of <i>Carissa spinarum </i>L. *American Journal of Biomedical Research*, *8*(2), 54-58. https://doi.org/10.12691/ajbr-8-2-5

Berhanu, G., Atalel, D., & Kandi, V. (2020b). A Review of the Medicinal and Antimicrobial Properties of *Carissa spinarum* L. *American Journal of Biomedical Research*, *8*(2), 54-58.

Berhanu, G., Babele, D., & K. V. R. (2020). Review of the Medicinal and Antimicrobial Properties of Carissa spinarum L. *American Journal of Biomedical Research*, *8*, 54-58. https://doi.org/10.12691/ajbr-8-2-5

Beyth, N., Houri-Haddad, Y., Domb, A., Khan, W., & Hazan, R. (2015). Alternative antimicrobial approach: Nano-antimicrobial materials. *Evidence-based Complementary and Alternative Medicine*, *2015,* 1-17.

Bnyan, R., Cesarini, L., Khan, I., Roberts, M., & Ehtezazi, T. (2020). The effect of ethanol evaporation on the properties of inkjet produced liposomes. *DARU Journal of Pharmaceutical Sciences*, *28*(1), 271-280. https://doi.org/10.1007/s40199-020-00340-1

Bouarab Chibane, L., Degraeve, P., Ferhout, H., Bouajila, J., & Oulahal, N. (2019). Plant antimicrobial polyphenols as potential natural food preservatives. *Journal of the Science of Food and Agriculture*, *99*(4), 1457-1474. https://doi.org/10.1002/jsfa.9357

Bouarab-Chibane, L., Forquet, V., Lantéri, P., Clément, Y., Léonard-Akkari, L., Oulahal, N., Degraeve, P., & Bordes, C. (2019). Antibacterial Properties of Polyphenols: Characterization and QSAR (Quantitative Structure-Activity Relationship) Models. *Frontiers in Microbiology*, *10*, 829-829. https://doi.org/10.3389/fmicb.2019.00829

Bozzuto, G., & Molinari, A. (2015). Liposomes as nanomedical devices. *International Journal of Nanomedicine*, *10*, 975-999. https://doi.org/10.2147/IJN.S68861

Breijyeh, Z., & Karaman, R. (2023). Design and Synthesis of Novel Antimicrobial Agents. *Antibiotics (Basel, Switzerland)*, *12*(3), 1-62.

Brezoiu, A. M., Bajenaru, L., Berger, D., Mitran, R. A., Deaconu, M., Lincu, D., Stoica Guzun, A., Matei, C., Moisescu, M. G., & Negreanu-Pirjol, T. (2020). Effect of Nanoconfinement of Polyphenolic Extract from Grape Pomace into Functionalized Mesoporous Silica on Its Biocompatibility and Radical Scavenging Activity. *Antioxidants*, *9*(8), 1-24. https://doi.org/10.3390/antiox9080696

Brown, A. N., Smith, K., Samuels, T. A., Lu, J., Obare, S. O., & Scott, M. E. (2012). Nanoparticles functionalized with ampicillin destroy multiple-antibiotic-resistant isolates of Pseudomonas aeruginosa and Enterobacter aerogenes and methicillin-resistant *Staphylococcus aureus*. *Applied and Environmental Microbiology*, *78*(8), 2768-2774. https://doi.org/10.1128/AEM.06513-11

Bruna, T., Maldonado-Bravo, F., Jara, P., & Caro, N. (2021). Silver Nanoparticles and Their Antibacterial Applications. *International Journal Molecular Sciences*, *22*(13), 1-21. https://doi.org/10.3390/ijms22137202

Buszewski, B., Rafińska, K., Pomastowski, P., Walczak, J., & Rogowska, A. (2016). Novel aspects of silver nanoparticles functionalization. *Colloids and Surfaces A: Physicochemical and Engineering Aspects*, *506*, 170-178. https://doi.org/10.1016/j.colsurfa.2016.05.058

Caneiras, C., Lito, L., Melo-Cristino, J., & Duarte, A. (2019). Community- and Hospital-Acquired Klebsiella pneumoniae Urinary Tract Infections in Portugal: Virulence and Antibiotic Resistance. *Microorganisms*, *7*(5), 1-14. https://doi.org/10.3390/microorganisms7050138

Cao, D., Shu, X., Zhu, D., Liang, S., Hasan, M., & Gong, S. (2020). Lipid-coated ZnO nanoparticles synthesis, characterization and cytotoxicity studies in cancer cell. *Nano Convergence*, *7*, 1-18.

Cao, S. J., Xu, S., Wang, H. M., Ling, Y., Dong, J., Xia, R. D., & Sun, X.-h. (2019). Nanoparticles: Oral delivery for protein and peptide drugs. *AAPS PharmSciTech*, *20*(5), 1-11.

Cao, Y., Dong, X., & Chen, X. (2022). Polymer-Modified Liposomes for Drug Delivery: From Fundamentals to Applications. *Pharmaceutics*, *14*(4), 1-27. https://doi.org/10.3390/pharmaceutics14040778.

Catalá, A. (2013). Five decades with polyunsaturated Fatty acids: Chemical synthesis, enzymatic formation, lipid peroxidation and its biological effects. *Journal of Lipids*, *2013*,1-21. https://doi.org/10.1155/2013/710290

Cazares-Cortes, E., Cabana, S., Boitard, C., Nehlig, E., Griffete, N., Fresnais, J., Wilhelm, C., Abou-Hassan, A., & Ménager, C. (2019). Recent insights in magnetic hyperthermia: From the "hot-spot" effect for local delivery to combined magneto-photo-thermia using magneto-plasmonic hybrids. *Advanced Drug Delivery Reviews*, *138*, 233-246.

Cazzola, M., Corazzari, I., Prenesti, E., Bertone, E., Vernè, E., & Ferraris, S. (2016). Bioactive glass coupling with natural polyphenols: Surface modification, bioactivity and anti-oxidant ability. *Applied Surface Science*, *367*, 237-248.

Celia, C., Trapasso, E., Locatelli, M., Navarra, M., Ventura, C. A., Wolfram, J., Carafa, M., Morittu, V.M., Britti, D., Di Marzio, L., & Di Marzio, L. (2013). Anticancer activity of liposomal bergamot essential oil (BEO) on human neuroblastoma cells. *Colloids and Surfaces B: Biointerfaces*, *112*, 548-553.

Checkouri, E., Reignier, F., Robert-Da Silva, C., & Meilhac, O. (2020). Evaluation of Polyphenol Content and Antioxidant Capacity of Aqueous Extracts from Eight Medicinal Plants from Reunion Island: Protection against Oxidative Stress in Red Blood Cells and Preadipocytes. *Antioxidants*, *9*, 1-21. https://doi.org/10.3390/antiox9100959

Chen, L., Yang, J., Li, X., Liang, T., Nie, C., Xie, F., Liu, K., Peng, X., & Xie, J. (2020). Carbon nanoparticles enhance potassium uptake via upregulating potassium channel expression and imitating biological ion channels in BY-2 cells. *Journal of Nanobiotechnology*, *18*(1), 1-14. https://doi.org/10.1186/s12951-020-0581-0

Chen, S., Hao, X., Liang, X., Zhang, Q., Zhang, C., Zhou, G., Shen, S., Jia, G., & Zhang, J. (2016). Inorganic nanomaterials as carriers for drug delivery. *Journal of Biomedical Nanotechnology*, *12*(1), 1-27.

Chen, W., Duša, F., Witos, J., Ruokonen, S. K., & Wiedmer, S. K. (2018). Determination of the Main Phase Transition Temperature of Phospholipids by Nanoplasmonic Sensing. *Scientific Reports*, *8*(1), 1-11. https://doi.org/10.1038/s41598-018-33107-5

Chen, W., Zou, M., Ma, X., Lv, R., Ding, T., & Liu, D. (2019). Co-encapsulation of EGCG and quercetin in liposomes for optimum antioxidant activity. *Journal of Food Science*, *84*(1), 111-120.

Cheng, C., Peng, S., Li, Z., Zou, L., Liu, W., & Liu, C. (2017). Improved bioavailability of curcumin in liposomes prepared using a pH-driven, organic solvent-free, easily scalable process [10.1039/C7RA02861J]. *RSC Advances*, *7*(42), 25978-25986. https://doi.org/10.1039/C7RA02861J

Cheung, R. C. F., Ng, T. B., Wong, J. H., & Chan, W. Y. (2015). Chitosan: An Update on Potential Biomedical and Pharmaceutical Applications. *Marine Drugs*, *13*(8), 5156-5186. https://doi.org/10.3390/md13085156

Cho, N. J., Hwang, L. Y., Solandt, J. J. R., & Frank, C. W. (2013). Comparison of Extruded and Sonicated Vesicles for Planar Bilayer Self-Assembly. *Materials (Basel, Switzerland)*, *6*(8), 3294-3308. https://doi.org/10.3390/ma6083294

Cho, S. G. (2017). The role of reactive oxygen species (ROS) in the biological activities of metallic nanoparticles. *International Journal of Molecular Sciences*, *18*(1), 1-21.

Cho, Y. S., Lee, D. S., Kim, Y.-M., Ahn, C. B., Kim, D. H., Jung, W. K., & Je, J. Y. (2013). Protection of hepatic cell damage and antimicrobial evaluation of chitosan-catechin conjugate. *Journal of the Korean Society for Applied Biological Chemistry*, *56*(6), 701-707. https://doi.org/10.1007/s13765-013-3168-8

Choi, K. H., Nam, K. C., Lee, S. Y., Cho, G., Jung, J. S., Kim, H. J., & Park, B. J. (2017). Antioxidant potential and antibacterial efficiency of caffeic acid-functionalized ZnO nanoparticles. *Nanomaterials*, *7*(6), 1-11

Nkanga,C.I., Bapolisi,A.M.,Okafor,N.I.,Krause,R.W.(2020). General Perception of Liposome: Formation, Manufacturing and Applicaton. *Liposome-Advances and Perspectives*, 14(9): 1194-1208. https://doi.org/10.5772 /intechopen.84255

Control, C. F. D., & Prevention. (2010). *Klebsiella pneumoniae in healthcare settings.* https://www.cdc.gov/hai/organisms/klebsiella/klebsiella. html

Cooke, I. R., & Deserno, M. (2006). Coupling between lipid shape and membrane curvature. *Biophysics Journal*, *91*(2), 487-495. https://doi.org/10.1529/biophysj.105.078683

Cory, H., Passarelli, S., Szeto, J., Tamez, M., & Mattei, J. (2018). The Role of Polyphenols in Human Health and Food Systems: A Mini-Review. *Frontiers in Nutrition*, *5*, 1-9. https://doi.org/10.3389/fnut.2018.00087

Cotea, V., Luchian, C., Bilba, N., & Marius, N. (2012). Mesoporous silica SBA-15, a new adsorbent for bioactive polyphenols from red wine. *Analytica Chimica Acta*, *732*, 180-185. https://doi.org/10.1016/j.aca.2011.10.019

Cutrim, C. S., & Cortez, M. A. S. (2018). A review on polyphenols: Classification, beneficial effects and their application in dairy products. *International Journal of Dairy Technology*, *71*(3), 564-578. https://doi.org/10.1111/1471-0307.12515

Da, R., Nayak, M., Sahoo, G. C., Pandey, K., Chawla-Sarkar, M., Das, V., & Madhukar, M. (2019). Iron oxide nanoparticles based antiviral activity of H1N1 influenza A virus. *Journal of Infection and Chemotherapy*, *25*(5), 325-329.

Dai, W., Ruan, C., Zhang, Y., Wang, J., Han, J., Shao, Z., Sun, Y., & Liang, J. (2020). Bioavailability enhancement of EGCG by structural modification and nano-delivery: A review. *Journal of Functional Foods*, *65*, 1-9. https://doi.org/10.1016/j.j ff.2019. 103732

Daraee, H., Etemadi, A., Kouhi, M., Alimirzalu, S., & Akbarzadeh, A. (2016). Application of liposomes in medicine and drug delivery. *Artificial Cells, Nanomedicine, and Biotechnology*, *44*(1), 381-391.

Das, B., Khan, M. I., Jayabalan, R., Behera, S. K., Yun, S. I., Tripathy, S. K., & Mishra, A. (2016). Understanding the antifungal mechanism of Ag@ ZnO core-shell nanocomposites against Candida krusei. *Scientific Reports*, *6*, (1), 1-12.

De Gaetano, G. V., Lentini, G., Famà, A., Coppolino, F., & Beninati, C. (2023). Antimicrobial Resistance: Two-Component Regulatory Systems and Multidrug Efflux Pumps. *Antibiotics*, *12*(6), 1-35.

Dessie, T., Jemal, M., Maru, M., & Tiruneh, M. (2021). Multiresistant Bacterial Pathogens Causing Bacterial Pneumonia and Analyses of Potential Risk Factors from Northeast Ethiopia. *International Journal of Microbiology*, *2021*, 1-9. https://doi.org/10.1155/ 2021/6680343

Dhatwalia, J., Kumari, A., Verma, R., Upadhyay, N., Guleria, I., Lal, S., Thakur, S., Gudeta, K., Kumar, V., Chao, J. C. J., & Sharma, S., & Amarowicz, R. (2021). Phytochemistry, Pharmacology, and Nutraceutical Profile of Carissa Species: An Updated Review. *Molecules*, *26*(22), 1-34. https://doi.org/10.3390/molecules 26227010

Di Salle, A. (2016). Polyphenols Nanoencapsulation for Therapeutic Applications. *Journal of Biomolecular Research and Therapeutics*, *05*(2), 1-13 . https://doi.org/10.4172/2167-7956.1000139

Dixit, S., & Rana, S. (2018). Investigation of Immunomodulation Activity in the Leaves of Dalbergia dissoo. *Global Journal of Pharmacy and Pharmaceutical Sciences*, *5*(1), 23-28.

Doshi, G., Chaskar, P. K., & View, M. (2017). Antiinflammatory and antibacterial potential of Carissa carandas and Carissa spinarum nanoemulsions. *International Journal of Pharmaceutical Sciences and Research*, *8*(12), 5137-5145.

Dossou-Yovo, K. M., Diallo, A., Lawson-Evi, P., Kantati, Y. T., Darré, T., Bakoma, B., & Eklu-Gadégbéku, K. (2021). A 90-Day Oral Toxicity of Hydroethanolic Root Extract of <i>Carissa spinarum</i> in Wistar Rats. *Journal of Toxicology*, *2021*, 1-6. https://doi.org/10.1155/2021/5570206

Dua, J., Rana, A., & Bhandari, A. (2012). Liposome: methods of preparation and applications. *International Journal of Pharmaceutical Studies Research*, *3*(2), 14-20.

Ebin, B., Arıg, E., Ozkal, B., & Gurmen, S. (2012). Production and characterization of ZnO nanoparticles and porous particles by ultrasonic spray pyrolysis using a zinc nitrate precursor. *International Journal of Minerals Metallurgy and Materials*, *19*(7), 651-656. https://doi.org/10.1007/s12613-012-0608-0

Elieh-Ali-Komi, D., & Hamblin, M. R. (2016). Chitin and Chitosan: Production and Application of Versatile Biomedical Nanomaterials. *International Journal of Advanced Research (Indore)*, *4*(3), 411-427.

Farouk, A., Moussa, S., Ulbricht, M., & Textor, T. (2012). ZnO Nanoparticles-Chitosan Composite as Antibacterial Finish for Textiles. *International Journal of Carbohydrate Chemistry*, *2012*, 1-9. https://doi.org/10.1155/2012/693629

Fathalla, D., Soliman, G., & Fouad, E. (2015). Development and in vitro/in vivo evaluation of liposomal gels for the sustained ocular delivery of latanoprost. *Journal of Clinical and Experiemental Ophthalmology*, *6*(390), 1-9.

Fatima, A., Singh, P. P., Agarwal, P., Irchhaiya, R., Alok, S., & Verma, A. (2013). Treatment of various diseases by Carissa spinarum L.: A promising shrub. *International Journal of Pharmaceutical Sciences and Research*, *4*(7), 2489-2495.

Fatullayeva, S., Tagiyev, D., Zeynalov, N., Mammadova, S., & Aliyeva, E. (2022). Recent advances of chitosan-based polymers in biomedical applications and environmental protection. *Journal of Polymer Research*, *29*(7), 2-19. https://doi.org/10.1007/s10965-022-03121-3

Fernandes, M. M., Francesko, A., Torrent-Burgués, J., Carrión-Fité, F. J., Heinze, T., & Tzanov, T. (2014). Sonochemically processed cationic nanocapsules: Efficient antimicrobials with membrane disturbing capacity. *Biomacromolecules*, *15*(4), 1365-1374.

Ferraris, S., Zhang, X., Prenesti, E., Corazzari, I., Turci, F., Tomatis, M., & Vernè, E. (2016). Gallic acid grafting to a ferrimagnetic bioactive glass-ceramic. *Journal of Non-Crystalline Solids*, *432*, 167-175.

Filipović-Grcić, J., Skalko-Basnet, N., & Jalsenjak, I. (2001). Mucoadhesive chitosan-coated liposomes: Characteristics and stability. *Journal of Microencapsulation*, *18*(1), 3-12. https://doi.org/10.1080/026520401750038557

Forest, V., Cottier, M., & Pourchez, J. (2015). Electrostatic interactions favor the binding of positive nanoparticles on cells: A reductive theory. *Nano Today*, *10*(6), 677-680. https://doi.org/https://doi.org/10.1016/j.nantod.2015.07.002 Fan, X., Chen, K., He, X., Li, N., Huang, J., Tang, K., Li, Y., & Wang, F. (2016). Nano-TiO2/collagen-chitosan porous scaffold for wound repairing. *International Journal of Biological Macromolecules, 91*, 15-22. https://doi.org/10.1016/j.ijbiomac.2016.05. 094

Fraga-Corral, M., García-Oliveira, P., Pereira, A. G., Lourenço-Lopes, C., Jimenez-Lopez, C., Prieto, M. A., & Simal-Gandara, J. (2020). Technological application of tannin-based extracts. *Molecules*, *25*(3), 1-27.

Fu, Y., & Kao, W. J. (2010). Drug release kinetics and transport mechanisms of non-degradable and degradable polymeric delivery systems. *Expert Opinion on Drug Delivery*, *7*(4), 429-444.

Gao, P., Nie, X., Zou, M., Shi, Y., & Cheng, G. (2011). Recent advances in materials for extended-release antibiotic delivery system. *The Journal of Antibiotics*, *64*(9), 625-634. https://doi.org/10.1038/ja.2011.58

Gao, W., Hu, C. M. J., Fang, R. H., & Zhang, L. (2013). Liposome-like nanostructures for drug delivery. *Journal of Materials Chemistry B*, *1*(48), 6569-6585.

Gatica, S., Fuentes, B., Rivera-Asín, E., Ramírez-Céspedes, P., Sepúlveda-Alfaro, J., Catalán, E. A., Bueno, S. M., Kalergis, A. M., Simon, F., Riedel, C, A., & Melo-Gonzalez, F. (2023). Novel evidence on sepsis-inducing pathogens: From laboratory to bedside. *Frontiers in Microbiology*, *14,* 1-24. https://doi.org/10.3389/fmicb.2023.1198200

Genwali, G. R., Acharya, P. P., & Rajbhandari, M. (2013). Isolation of gallic acid and estimation of total phenolic content in some medicinal plants and their antioxidant activity. *Nepal Journal of Science and Technology*, *14*(1), 95-102.

Geraili, A., Xing, M., & Mequanint, K. (2021). Design and fabrication of drug-delivery systems toward adjustable release profiles for personalized treatment. *View*, *2*(5), 1-24. https://doi.org/https://doi.org/10.1002/VIW.20200126.

Ghaffari, S. B., Sarrafzadeh, M. H., Fakhroueian, Z., Shahriari, S., & Khorramizadeh, M. R. (2017). Functionalization of ZnO nanoparticles by 3-mercaptopropionic acid for aqueous curcumin delivery: Synthesis, characterization, and anticancer assessment. *Materials Science and Engineering: C*, *79*, 465-472.

Ghalandarlaki, N., Alizadeh, A. M., & Ashkani-Esfahani, S. (2014). Nanotechnology-applied curcumin for different diseases therapy. *BioMedical Research International*, *2014*, 1-24 https://doi.org/10.1155/2014/394264

Gharib, A., Faezizadeh, Z., & Godarzee, M. (2012). In vitro and in vivo activities of ticarcillin-loaded nanoliposomes with different surface charges against Pseudomonas aeruginosa (ATCC 29248). *DARU Journal of Pharmaceutical Sciences*, *20*(1), 1-7.

Gibis, M., Ruedt, C., & Weiss, J. (2016). In vitro release of grape-seed polyphenols encapsulated from uncoated and chitosan-coated liposomes. *Food Research International*, *88*(Pt A), 105-113. https://doi.org/10.1016/j.foodres.2016.02.010

Gibis, M., Vogt, E., & Weiss, J. (2012). Encapsulation of polyphenolic grape seed extract in polymer-coated liposomes. *Food and Function*, *3*(3), 246-254.

Górniak, I., Bartoszewski, R., & Króliczewski, J. (2019). Comprehensive review of antimicrobial activities of plant flavonoids. *Phytochemistry Reviews*, *18*(1), 241-272. https://doi.org/10.1007/s11101-018-9591-z

Gortzi, O., Lalas, S., Chinou, I., & Tsaknis, J. (2006). Reevaluation of antimicrobial and antioxidant activity of Thymus spp. extracts before and after encapsulation in liposomes. *Journal of Food Protection*, *69*(12), 2998-3005.

Gouda, A., Sakr, O. S., Nasr, M., & Sammour, O. (2021). Ethanol injection technique for liposomes formulation: An insight into development, influencing factors, challenges and applications. *Journal of Drug Delivery Science and Technology*, *61*, 1-15.

Gregoriou, G., Neophytou, C. M., Vasincu, A., Gregoriou, Y., Hadjipakkou, H., Pinakoulaki, E., Christodoulou, M. C., Ioannou, G. D., Stavrou, I. J., Christou, A., Kapnissi-Christodoulou, C. P., & Constantinou, A. I. (2021). Anti-Cancer Activity and Phenolic Content of Extracts Derived from Cypriot Carob *(Ceratonia siliqua* L.) Pods Using Different Solvents. *Molecules*, *26*(16), 1-22. https://www.mdpi.com/1420-3049/26 /16/5017

Grigoletto, A., Tedeschini, T., Canato, E., & Pasut, G. (2021). The evolution of polymer conjugation and drug targeting for the delivery of proteins and bioactive molecules. *WIREs Nanomedicine and Nanobiotechnology*, *13*(3),1-12.

Guardia, P., Riedinger, A., Kakwere, H., Gazeau, F., & Pellegrino, T. (2014). Magnetic nanoparticles for magnetic hyperthermia and controlled drug delivery. *Bio-and Bioinspired Nanomaterials*, *2014,* 139-172.

Guerrini, L., Alvarez-Puebla, R. A., & Pazos-Perez, N. (2018). Surface Modifications of Nanoparticles for Stability in Biological Fluids. *Materials*, *11*(7), 1-28. https://www.mdpi.com/1996-1944/11/7/1154

Guimarães, A. C., Meireles, L. M., Lemos, M. F., Guimarães, M. C. C., Endringer, D. C., Fronza, M., & Scherer, R. (2019). Antibacterial activity of terpenes and terpenoids present in essential oils. *Molecules*, *24*(13), 1-12.

Gupta, S., Undale, V. R., & Lakhadive, K. (2020). Novel Targets for Antimicrobials. *Turkey Journal of Pharmaceutical Science*, *17*(5), 565-575. https://doi.org/10.4274/tjps. galenos.2020. 90197

Gyamera, B., & Kim, Y. H. (2019). Preparation and Characterization of Liposomes Containing Green Tea and Roselle Extracts to be Used in Cosmetics. *Journal of International Development Cooperation*, *14*(2), 131-160.

Hadian, Z., Sahari, M. A., Moghimi, H. R., & Barzegar, M. (2014). Formulation, characterization and optimization of liposomes containing eicosapentaenoic and docosahexaenoic acids; a methodology approach. *Iran Journal of Pharmaceutical Research*, *13*(2), 393-404.

Han, X., Zheng, Z., Yu, C., Deng, Y., Ye, Q., Niu, F., Chen, Q., Pan, W., & Wang, Y. (2022). Preparation, characterization and antibacterial activity of new ionized chitosan. *Carbohydrate Polymers*, *290*, 1-11. /https://doi.org/10.1016/j.carbpol.2022.119490

Hangas, A., Aasumets, K., Kekäläinen, N. J., Paloheinä, M., Pohjoismäki, J. L., Gerhold, J. M., & Goffart, S. (2018). Ciprofloxacin impairs mitochondrial DNA replication initiation through inhibition of Topoisomerase 2. *Nucleic Acids Research*, *46*(18), 9625-9636. https://doi.org/10.1093/nar/gky793

Hao, F., He, Y., Sun, Y., Zheng, B., Liu, Y., Wang, X., Zhang, Y., Lee, R. J., Teng, L., & Xie, J. (2016). Improvement of oral availability of ginseng fruit saponins by a proliposome delivery system containing sodium deoxycholate. *Saudi Journal of Biological Sciences*, *23*(1), S113-S125.

Harwansh, R. K., Garabadu, D., Rahman, M. A., & Garabadu, P. S. (2010). In vitro anthelmintic activity of different extracts of root of Carissa Spinarum. *International Journal of Pharmaceutical Sciences and Research*, *1*(10), 84-88.

Hasan, M., Elkhoury, K., Kahn, C. J. F., Arab-Tehrany, E., & Linder, M. (2019b). Preparation, Characterization, and Release Kinetics of Chitosan-Coated Nanoliposomes Encapsulating Curcumin in Simulated Environments. *Molecules (Basel, Switzerland)*, *24*(10), 1-14. https://doi.org/10.3390/molecules24102023

Hatamie, A., Khan, A., Golabi, M., Turner, A. P., Beni, V., Mak, W. C., Sadollahkhani, A., Alnoor, H., Zargar, B., Nur, O., & Bano, S. (2015). Zinc oxide nanostructure-modified textile and its application to biosensing, photocatalysis, and as antibacterial material. *Langmuir*, *31*(39), 10913-10921.

Hawthorne, D., Pannala, A., Sandeman, S., & Lloyd, A. (2022). Sustained and targeted delivery of hydrophilic drug compounds: A review of existing and novel technologies from bench to bedside. *Journal of Drug Delivery Science and Technology*, *78*, 1-27. https://doi.org/https://doi.org/10.1016/j.jddst.2022.103936

He, H., Lu, Y., Qi, J., Zhu, Q., Chen, Z., & Wu, W. (2019a). Adapting liposomes for oral drug delivery. *Acta Pharmaceutica Sinica B*, *9*(1), 36-48. https://doi.org/https://doi.org/10.1016/j.apsb.2018.06.005

He, H., Lu, Y., Qi, J., Zhu, Q., Chen, Z., & Wu, W. (2019b). Adapting liposomes for oral drug delivery. *Acta Pharmaceutica Sinica B*, *9*(1), 36-48. https://doi.org/10.1016/j.apsb.2018.06.005

He, Q., Huang, Y., Lin, B., & Wang, S. (2016). A nanocomposite film fabricated with simultaneously extracted protein-polysaccharide from a marine alga and TiO2nanoparticles. *Journal of Applied Phycology*, *29*, 1541-1552.

Heneweer, C., Gendy, S. E., & Peñate-Medina, O. (2012). Liposomes and inorganic nanoparticles for drug delivery and cancer imaging. *Therapeutic Delivery*, *3*(5), 645-656.

Henriksen, I., Smistad, G., & Karlsen, J. (1994). Interactions between liposomes and chitosan. *International Journal of Pharmaceutics*, *101*(3), 227-236. https://doi.org/https://doi.org/10.1016/0378-5173(94)90218-6

Herdiana, Y., Wathoni, N., Shamsuddin, S., & Muchtaridi, M. (2022). Drug release study of the chitosan-based nanoparticles. *Heliyon*, *8*(1), 1-16. https://doi.org/10.1016/j.heliyon.2021.e08674.

Horn, S. J., Vaaje-Kolstad, G., Westereng, B., & Eijsink, V. (2012). Novel enzymes for the degradation of cellulose. *Biotechnology for Biofuels*, *5*(45).1-13.

Hosny, K. M., Ahmed, O. A., & Al-Abdali, R. T. (2013). Enteric-coated alendronate sodium nanoliposomes: A novel formula to overcome barriers for the treatment of osteoporosis. *Expert Opinion on Drug Delivery, 10*(6), 741-746. https://doi.org/10.1517/17425247.2013.799136

Hosseini, S. M., Taheri, M., Nouri, F., Farmani, A., Moez, N. M., & Arabestani, M. R. (2022). Nano drug delivery in intracellular bacterial infection treatments. *Biomedicine and Pharmacotherapy*, *146*, 1-13. https://doi.org/https://doi.org/10.1016/j.biopha. 2021. 112609

Hsieh, D. S., Lu, H. C., Chen, C. C., Wu, C. J., & Yeh, M. K. (2012). The preparation and characterization of gold-conjugated polyphenol nanoparticles as a novel delivery system. *International Journal of Nanomedicine*, *7*, 1623-1633.

Huang, C., Quinn, D., Sadovsky, Y., Suresh, S., & Hsia, K. J. (2017). Formation and size distribution of self-assembled vesicles. *Proceedings of the National Academy of Sciences*, *114*(11), 2910-2915. https://doi.org/10.1073/pnas.1702065114

Huang, X., & Brazel, C. S. (2001). On the importance and mechanisms of burst release in matrix-controlled drug delivery systems. *Journal of Controlled Release*, *73*(2), 121-136. https://doi.org/https://doi.org/10.1016/S0168-3659(01)00248-6

Hubenko, K., Yefimova, S., Tkacheva, T., Maksimchuk, P., Borovoy, I., Klochkov, V., Kavok, N., Opolonin, O., & Malyukin, Y. (2018). Reactive oxygen species generation in aqueous solutions containing GdVO 4: Eu 3+ nanoparticles and their complexes with methylene blue. *Nanoscale research letters*, *13*(1), 1-9.

Hussain, K., Ismail, Z., Sadikun, A., & Ibrahim, P. (2009). Antioxidant, anti-TB activities, phenolic and amide contents of standardised extracts of Piper sarmentosum Roxb. *Natural Product Research*, *23*(3), 238-249.

Ibrahim, H., Oyi, R., O.Joseph, E., Musa Yusuf, K., & Bright, N. (2010). Antimicrobial activity of the water extracts of the leaves and fruits of Carissa edulis Vahl (Apocynaceae). *Journal of Medicinal Plants Research*, 4(11)1028-1032.

Ickenstein, L. M., Sandström, M. C., Mayer, L. D., & Edwards, K. (2006). Effects of phospholipid hydrolysis on the aggregate structure in DPPC/DSPE-PEG2000 liposome preparations after gel to liquid crystalline phase transition. *Biochimica et Biophysica Acta (BBA) - Biomembranes*, *1758*(2), 171-180. https://doi.org/10.1016/ j.bbamem. 2006.02.016

İlyasoğlu, H., & Guo, Z. (2019). Water soluble chitosan-caffeic acid conjugates as a dual functional polymeric surfactant. *Food Bioscience*, *29*, 118-125. https://doi.org/10.1016/j.fbio.2019.04.007

Imam, S. S., Alshehri, S., Altamimi, M. A., Almalki, R. K. H., Hussain, A., Bukhari, S. I., Mahdi, W. A., & Qamar, W. (2022). Formulation of Chitosan-Coated Apigenin Bilosomes: In Vitro Characterization, Antimicrobial and Cytotoxicity Assessment. *Polymers (Basel)*, *14*(5), 1-15. https://doi.org/10.3390/polym14050921

Imran, M., Jha, S. K., Hasan, N., Insaf, A., Shrestha, J., Shrestha, J., Mohammed, Y. (2022). Overcoming Multidrug Resistance of Antibiotics via Nanodelivery Systems. *Pharmaceutics*, *14*(3), 1-25. https://doi.org/10.3390/pharmaceutics14030586

Jackson, N., Czaplewski, L., & Piddock, L. J. V. (2018). Discovery and development of new antibacterial drugs: learning from experience? *Journal of Antimicrobial Chemotherapy*, *73*(6), 1452-1459. https://doi.org/10.1093/jac/dky019

Jain, P., Jain, S., Prasad, K., Jain, S., & Vyas, S. P. (2009). Polyelectrolyte coated multilayered liposomes (nanocapsules) for the treatment of Helicobacter pylori infection. *Molecular Pharmaceutics*, *6*(2), 593-603.

Jain, S., Jain, V., & Mahajan, S. C. (2014). Lipid Based Vesicular Drug Delivery Systems. *Advances in Pharmaceutics*, *2014*, 1-12. https://doi.org/10.1155/2014/574673

Jesús, M.-S. T., Hernán, H. M. C., & Rubén, R.-N. J. (2018). An overview of the chemical modifications of chitosan and their advantages. *Green Materials*, *6*(4), 131-142. https://doi.org/10.1680/jgrma.18.00053

Jia, Z., shen, D., & Xu, W. (2001). Synthesis and antibacterial activities of quaternary ammonium salt of chitosan. *Carbohydrate Research*, *333*(1), 1-6.

Jiang, J., Pi, J., & Cai, J. (2018). The Advancing of Zinc Oxide Nanoparticles for Biomedical Applications. *Bioinorganic Chemistry and Applications*, *2018*, 1062562-1062562. https://doi.org/10.1155/2018/1062562.

Jiménez-Gómez, C. P., & Cecilia, J. A. (2020). Chitosan: A Natural Biopolymer with a Wide and Varied Range of Applications. *Molecules*, *25*(17), 1-43.

Jing, Y., Diao, Y., & Yu, X. (2019). Free radical-mediated conjugation of chitosan with tannic acid: Characterization and antioxidant capacity. *Reactive and Functional Polymers*, *135*, 16-22. https://doi.org/10.1016/j.reactfunctpolym.2018.12.005.

Jiskoot, W., Teerlink, T., Beuvery, E. C., & Crommelin, D. J. (1986). Preparation of liposomes via detergent removal from mixed micelles by dilution. The effect of bilayer composition and process parameters on liposome characteristics. *Pharmaceutisch Weekblad Scientific*, *8*(5), 259-265. https://doi.org/10.1007/bf01960070.

Johar, M. A., Afzal, R. A., Alazba, A. A., & Manzoor, U. (2015). Photocatalysis and bandgap engineering using ZnO nanocomposites. *Advances in Materials Science and Engineering*, *2015,* 1-22.

Joshi, V., & Singh, R. (2017). Antibacterial activity of Root and Leaf Extracts of Carissa spinarum against Methicillin-resistant Staphylococcus aureus (MRSA) and other Clinically Pathogenic bacterial strains. *Octa Journal of Biosciences*, *5*(2), 61-64.

Jung, I. W., & Han, H. K. (2014). Effective mucoadhesive liposomal delivery system for risedronate: Preparation and in vitro/in vivo characterization. *International Journal of Nanomedicine*, *9*, 2299-2306. https://doi.org/10.2147/IJN.S61181.

Kadiyala, U., Kotov, N. A., & VanEpps, J. S. (2018). Antibacterial Metal Oxide Nanoparticles: Challenges in Interpreting the Literature. *Current Pharmaceutical Design*, *24*(8), 896-903. https://doi.org/10.2174/1381612824666180219130659.

Kalepu, S., Sunilkumar, K., Betha, S., & Mohanvarma, M. (2013). Liposomal drug delivery system: A comprehensive review. *International Journal of Drug Development and Research*, *5*(4), 62-75.

Kama-Kama, F., Midiwo, J., Nganga, J., Maina, N., Schiek, E., Omosa, L. K., Osanjo, G., & Naessens, J. (2016). Selected ethno-medicinal plants from Kenya with in vitro activity against major African livestock pathogens belonging to the "Mycoplasma mycoides cluster". *Journal of Ethnopharmacol*, *192*, 524-534.

Kamble, V., Somkuwar, D., & Wankhade, D. S. (2016). Chemical composition, antioxidant and antisalmonella activity of *Mangifera indica* L. flower and seed kernel extracts. *International Current Pharmaceutical Journal*, *5*(10), 82-93.

Kannan, M., Muralisankar, T., Jayakumar, R., & Gandhi, C. (2021). A study on structural comparisons of α-chitin extracted from marine crustacean shell waste. *Carbohydrate Polymer Technologies and Applications*, *2*, 1-9. https://doi.org/10.1016/jcarpta. 2021.100037.

Kapadnis, G., Dey, A., Dandekar, P., & Jain, R. (2019). Effect of degree of deacetylation on solubility of low molecular weight chitosan produced via enzymatic breakdown of chitosan. *Polymer International*, *68*(6), 1054-1063. https://doi.org/10.1002/pi.5795.

Ke, C. L., Deng, F. S., Chuang, C. Y., & Lin, C. H. (2021). Antimicrobial Actions and Applications of Chitosan. *Polymers (Basel)*, *13*(6), 1-21. https://doi.org/10.3390/ polym13060904.

Keller, S., Tsamaloukas, A., & Heerklotz, H. (2005). A Quantitative Model Describing the Selective Solubilization of Membrane Domains. *Journal of the American Chemical Society*, *127*(32), 11469-11476. https://doi.org/10.1021/ja052764q.

Khalid, A., Ahmad, P., Alharthi, A. I., Muhammad, S., Khandaker, M. U., Faruque, M. R. I., Din, I. U., Alotaibi, M. A., & Khan, A. (2021). Synergistic effects of Cu-doped ZnO nanoantibiotic against Gram-positive bacterial strains. *PloS One*, *16*(5), e0251082-e0251082. https://doi.org/10. 1371/journal.pone.0251082.

Khalid, A., Ahmad, P., Alharthi, A. I., Muhammad, S., Khandaker, M. U., Faruque, M. R. I., Khan, A., Din, I. U., Alotaibi, M. A., Alzimami, K., Alfuraih, A. A., & Bradley, D. A. (2021). Enhanced Optical and Antibacterial Activity of Hydrothermally Synthesized Cobalt-Doped Zinc Oxide Cylindrical Microcrystals. *Materials (Basel, Switzerland)*, *14*(12), 1-16. https://doi.org/10.3390/ma14123223.

Khameneh, B., Iranshahy, M., Soheili, V., & Fazly Bazzaz, B. S. (2019). Review on plant antimicrobials: a mechanistic viewpoint. *Antimicrobial Resistance & Infection Control*, *8*(1), 1-28. https://doi.org/10.1186/s13756-019-0559-6.

Khare, T., Anand, U., Dey, A., Assaraf, Y. G., Chen, Z.-S., Liu, Z., & Kumar, V. (2021). Exploring Phytochemicals for Combating Antibiotic Resistance in Microbial Pathogens. *Frontiers in Pharmacology*, *12,1-18.*

Kong, D., Foley, S. R., & Wilson, L. D. (2022). An overview of modified chitosan adsorbents for the removal of precious metals species from aqueous media. *Molecules*, *27*(3), 978.

Kovach, A. K., Gambino, J. M., Nguyen, V., Nelson, Z., Szasz, T., Liao, J., Williams, L., Bulla, S., & Prabhu, R. (2016). Prospective Preliminary In Vitro Investigation of a Magnetic Iron Oxide Nanoparticle Conjugated with Ligand CD80 and VEGF Antibody As a Targeted Drug Delivery System for the Induction of Cell Death in Rodent Osteosarcoma Cells. *BioResearch Open Access*, *5*(1), 299-307. https://doi.org/10.1089/biores.2016.0020.

Kravanja, G., Primožič, M., Knez, Ž., & Leitgeb, M. (2019). Chitosan-based (Nano)materials for Novel Biomedical Applications. *Molecules*, *24*(10) 1-23. https://doi.org/10.3390/molecules24101960.

Kregiel, D., Berlowska, J., Witonska, I., Antolak, H., Proestos, C., Babic, M., Babic, L., & Zhang, B. (2017). Saponin-based, biological-active surfactants from plants. *Application and Characterization of Surfactants*, *2017,* 183-205.

Kulkarni, S., Betageri, G., & Singh, M. (1995). Factors affecting microencapsulation of drugs in liposomes. *Journal of Microencapsulation*, *12*(3), 229-246.

Kumar, N., & Goel, N. (2019). Phenolic acids: Natural versatile molecules with promising therapeutic applications. *Biotechnology Reports*, *24,*1-10.

Kumar, N., & Upadhyay, L. S. B. (2016). Facile and green synthesis of highly stable l-cysteine functionalized copper nanoparticles. *Applied Surface Science*, *385*, 225-233. https://doi.org/10.1016/j.apsusc.2016.05.125.

Kundu, M., Sadhukhan, P., Ghosh, N., Chatterjee, S., Manna, P., Das, J., & Sil, P. C. (2019). pH-responsive and targeted delivery of curcumin via phenylboronic acid-functionalized ZnO nanoparticles for breast cancer therapy. *Journal of Advanced Research*, *18*, 161-172. https://doi.org/10.1016/j.jare.2019.02.036.

Kundu, N., Banik, D., & Sarkar, N. (2018). Self-Assembly of Amphiphiles into Vesicles and Fibrils: Investigation of Structure and Dynamics Using Spectroscopy and Microscopy Techniques. *Langmuir*, *34*(39), 11637-11654. https://doi.org/10.1021/acs.langmuir.7b04355.

Ladj, R., Bitar, A., Eissa, M., Mugnier, Y., Le Dantec, R., Fessi, H., & Elaissari, A. (2013). Individual inorganic nanoparticles: Preparation, functionalization and in vitro biomedical diagnostic applications. *Journal of Materials Chemistry B*, *1*(10), 1381-1396.

Lallo da Silva, B., Abuçafy, M. P., Berbel Manaia, E., Oshiro Junior, J. A., Chiari-Andréo, B. G., Pietro, R. C. R., & Chiavacci, L. A. (2019). Relationship Between Structure and Antimicrobial Activity of Zinc Oxide Nanoparticles: An Overview. *International Journal of Nanomedicine*, *14*, 9395-9410. https://doi.org/10.2147/ijn.s216204.

Lee, H. W., Kharel, S., & Loo, S. C. J. (2022). Lipid-Coated Hybrid Nanoparticles for Enhanced Bacterial Biofilm Penetration and Antibiofilm Efficacy. *In: Research Square.* 7,35814-35824.https://doi.org/10.1021/acsomega2004008.

Lee, J. H., Ivkov, R., & Blumenthal, R. (2014). Magnetically triggered drug release from Liposome Embedded gel. *Journal of Nanomedicine & Biotherapeutic Discovery*, *4*(3), 1-6.

Lee, J., Choi, K. H., Min, J., Kim, H. J., Jee, J. P., & Park, B. J. (2017). Functionalized ZnO nanoparticles with gallic acid for antioxidant and antibacterial activity against methicillin-resistant *S. aureus*. *Nanomaterials*, *7*(11), 1-10.

Lee, M. K. (2020). Liposomes for Enhanced Bioavailability of Water-Insoluble Drugs: In Vivo Evidence and Recent Approaches. *Pharmaceutics*, *12*(3), 1-30. https://doi.org/10.3390/pharmaceutics12030264.

Lee, Y., & Thompson, D. H. (2017). Stimuli-responsive liposomes for drug delivery. *Wiley Interdiscip Rev Nanomed Nanobiotechnol*, *9*(5) 1-76. https://doi.org/10.1002/wnan.1450.

Legba, B., Dougnon, V., Chabi, Y., Gbaguidi, C., Aniambossou, A., Deguenon, E., Kpodekon, M., & Baba-Moussa, L. (2020). Evaluation of in-vivo anti-Salmonella activity of Uvaria chamae, Lantana camara and Phyllantus amarus used in Benin, West Africa. *BMC Veterinary Research*, *16*(1), 1-18. https://doi.org/10.1186/s12917-020-2266-1.

Li, H., Chen, Q., Zhao, J., & Urmila, K. (2015). Enhancing the antimicrobial activity of natural extraction using the synthetic ultrasmall metal nanoparticles. *Scientific Reports*, *5*(1), 1-13. https://doi.org/10.1038/srep11033.

Li, J., Wang, X., Zhang, T., Wang, C., Huang, Z., Luo, X., & Deng, Y. (2015). A review on phospholipids and their main applications in drug delivery systems. *Asian Journal of Pharmaceutical Sciences*, *10*(2), 81-98. https://doi.org/https://doi.org/10.1016/j.ajps.2014.09.004.

Liang, J., Li, F., Fang, Y., Yang, W., An, X., Zhao, L., Xin, Z., Cao, L., & Hu, Q. (2011). Synthesis, characterization and cytotoxicity studies of chitosan-coated tea polyphenols nanoparticles. *Colloids Surf B Biointerfaces*, *82*(2), 297-301. https://doi.org/10.1016/j.colsurfb.2010.08.045.

Lim, J., Yeap, S. P., Che, H. X., & Low, S. C. (2013). Characterization of magnetic nanoparticle by dynamic light scattering. *Nanoscale Research Letters*, *8*(1), 1-14.

Lisperguer, J., Saravia, Y., & Vergara, E. (2016). Structure and thermal behavior of tannins from Acacia dealbata bark and their reactivity toward formaldehyde. *Journal of the Chilean Chemical Society*, *61*, 3188-3190. http://dx.doi.org/10.4067/S0717-97072016000400007.

Liu, M., Gan, L., Chen, L., Xu, Z., Zhu, D., Hao, Z., & Chen, L. (2012). Supramolecular core–shell nanosilica@ liposome nanocapsules for drug delivery. *Langmuir*, *28*(29), 10725-10732.

Liu, P., Chen, G., & Zhang, J. (2022). A Review of Liposomes as a Drug Delivery System: Current Status of Approved Products, Regulatory Environments, and Future Perspectives. *Molecules*, *27*(4) 1-23. https://doi.org/10.3390/molecules27041372.

Liu, X. G., Zhang, L., Lu, S., Liu, D. Q., Zhang, L. X., Yu, X. L., & Liu, R. T. (2020). Multifunctional Superparamagnetic Iron Oxide Nanoparticles Conjugated with Aβ Oligomer-Specific scFv Antibody and Class A Scavenger Receptor Activator Show Early Diagnostic Potentials for Alzheimer's Disease. *International Journal of Nanomedicine*, *15*, 4919-4932. https://doi.org/10.2147/ijn.s240953.

Loan Khanh, L., Thanh Truc, N., Tan Dat, N., Thi Phuong Nghi, N., van Toi, V., Thi Thu Hoai, N., Quyen, T. N., Loan, T. T. T., & Thi Hiep, N. (2019). Gelatin-stabilized composites of silver nanoparticles and curcumin: characterization, antibacterial and antioxidant study. *Science and Technology of Advanced Materials*, *20*(1), 276-290. https://doi.org/10.1080/14686996.2019.1585131.

Lobo, V., Patil, A., Phatak, A., & Chandra, N. (2010). Free radicals, antioxidants and functional foods: Impact on human health. *Pharmacognosy Reviews*, *4*(8), 118-126.

Loiseau, A., Asila, V., Boitel-Aullen, G., Lam, M., Salmain, M., & Boujday, S. (2019). Silver-based plasmonic nanoparticles for and their use in biosensing. *Biosensors*, *9*(2), 1-39. https://doi.org/10.3390/bios9020078.

Lombardo, D., & Kiselev, M. A. (2022). Methods of Liposomes Preparation: Formation and Control Factors of Versatile Nanocarriers for Biomedical and Nanomedicine Application. *Pharmaceutics*, *14*(3) 1-49.

Luchini, A., & Vitiello, G. (2019). Understanding the Nano-bio Interfaces: Lipid-Coatings for Inorganic Nanoparticles as Promising Strategy for Biomedical Applications. *Frontiers in Chemistry*, *7,1-16.*

Mady, M. M., & Darwish, M. M. (2010). Effect of chitosan coating on the characteristics of DPPC liposomes. *Journal of Advanced Research, 1*(3), 187-191. https://doi.org/10.1016/j.jare.2010.05.008.

Magnusson, K. E., & Bayer, M. E. (1982). Anionic sites on the envelope of Salmonella typhimurium mapped with cationized ferritin. *Cell Biophys*, *4*(2-3), 163-175.

Maherani, B. (2012). *Encapsulation and Targeting of Biofunctional Molecules in Nanoliposomes: Study of Physico-Chemical Properties and Mechanisms of Transfer through Liposome Membrane* [Doctoral dissertation, Université de Lorraine]. https://hal.univ-lorraine.fr/tel-01749245.

Majzoub, R. N., Ewert, K. K., & Safinya, C. R. (2016). Cationic liposome–nucleic acid nanoparticle assemblies with applications in gene delivery and gene silencing. *Philosophical Transactions of the Royal Society A: Mathematical, Physical and Engineering Sciences*, *374*(2072), 1-14.

Makarewicz, M., Drożdż, I., Tarko, T., & Duda-Chodak, A. (2021). The Interactions between Polyphenols and Microorganisms, Especially Gut Microbiota. *Antioxidants (Basel)*, *10*(2), 1-70. https://doi.org/10.3390/antiox10020188.

Makhlouf, Z., Ali, A. A., & Al-Sayah, M. H. (2023). Liposomes-Based Drug Delivery Systems of Anti-Biofilm Agents to Combat Bacterial Biofilm Formation. *Antibiotics*, *12*(5), 1-32.

Malebo & Mbwambo (2011). *Technical Report on miracle Cure prescribed by Rev. Ambilikile Mwasapile in Samunge Village, Loliondo, Arusha*. https://www.scribd.com/document/53696831/Loliondo-Technical-Report#.

Manach, C., Scalbert, A., Morand, C., Rémésy, C., & Jiménez, L. (2004). Polyphenols: Food sources and bioavailability. *The American Journal of Clinical Nutrition*, *79*(5), 727-747. https://doi.org/10.1093/ajcn/79.5.727.

Manikandan, A., Divakar, D., & Poonam Singh, N. (2019). Phospholipid—the dynamic structure between living and non-living world; A much obligatory supramolecule for present and future. *AIMS Molecular Science*, *6*(1), 1-19. https://doi.org/10.3934/molsci.2019.1.1.

Mansoori, M., Agrawal, S., Jawade, S., & Khan, M. (2012). A review on liposome. *International Journal Advanced Research Pharmaceutical and Bio-sciences*, *2*(4), 453-464.

Maobe, M. A., Gitu, L., Gatebe, E., Rotich, H., & Box, P. (2012). Phytochemical analysis of phenol and flavonoid in eight selected medicinal herbs used for the treatment of diabetes, malaria and pneumonia in Kisii, Kenya. *Academic Journal of Cancer Research*, *5*, 31-39.

Marassi, V., Di Cristo, L., Smith, S. G. J., Ortelli, S., Blosi, M., Costa, A. L., Reschiglian, P., Volkov, Y., & Prina-Mello, A. (2018). Silver nanoparticles as a medical device in healthcare settings: A five-step approach for candidate screening of coating agents. *Royal Society Open Science*, *5*(1), 171113-171113.

Marín, L., Miguélez, E. M., Villar, C. J., & Lombó, F. (2015). Bioavailability of Dietary Polyphenols and Gut Microbiota Metabolism: Antimicrobial Properties. *BioMed Research International*, *2015*, 1-18. https://doi.org/10.1155/2015/905215.

Martens, U., Janke, U., Möller, S., Talbot, D., Abou-Hassan, A., & Delcea, M. (2020). Interaction of fibrinogen–magnetic nanoparticle bioconjugates with integrin reconstituted into artificial membranes [10.1039/D0NR04181E]. *Nanoscale*, *12*(38), 19918-19930. https://doi.org/10.1039/D0NR04181E.

Martínez-González, R., Estelrich, J., & Busquets, M. A. (2016). Liposomes loaded with hydrophobic iron oxide nanoparticles: Suitable T2 contrast agents for MRI. *International Journal of Molecular Sciences*, *17*(8), 1-14.

Martins, A. F., Facchi, S. P., Follmann, H. D., Pereira, A. G., Rubira, A. F., & Muniz, E. C. (2014). Antimicrobial activity of chitosan derivatives containing N-quaternized moieties in its backbone: A review. *International Journal of Molecular Sciences, 15*(11), 20800-20832. https://doi.org/10.3390/ijms151120800.

Mathew, S., Ganguly, P., Rhatigan, S., Kumaravel, V., Byrne, C., Hinder, S. J., Bartlett, J., Nolan, M., & Pillai, S. C. (2018). Cu-Doped TiO2: Visible Light Assisted Photocatalytic Antimicrobial Activity. *Applied Sciences*, *8*(11), 1-20. https://doi.org/10.3390/app8112067.

Mattingly, S. J., O'Toole, M. G., James, K. T., Clark, G. J., & Nantz, M. H. (2015). Magnetic nanoparticle-supported lipid bilayers for drug delivery. *Langmuir*, *31*(11), 3326-3332.

Mendes, C. R., Dilarri, G., Forsan, C. F., Sapata, V. D. M. R., Lopes, P. R. M., de Moraes, P. B., Montagnolli, R. N., Ferreira, H., & Bidoia, E. D. (2022). Antibacterial action and target mechanisms of zinc oxide nanoparticles against bacterial pathogens. *Scientific Reports*, *12*(1), 1-10. https://doi.org/10.1038/s41598-022-06657-y.

Mengoni, T., Adrian, M., Pereira, S., Santos-Carballal, B., Kaiser, M., & Goycoolea, F. M. (2017). A Chitosan-Based Liposome Formulation Enhances the In Vitro Wound Healing Efficacy of Substance P Neuropeptide. *Pharmaceutics*, *9*(4) 1-17. https://doi.org/10. 3390/pharmaceutics9040056.

Mikušová, V., & Mikuš, P. (2021). Advances in Chitosan-Based Nanoparticles for Drug Delivery. *International Journal of Molecular Sciencies*, *22*(17), 1-93.

Minozzo, B. R., Lemes, B., Justo, A., Lara, J., Petry, V., Fernandes, D., Belló, C., Vellosa, J. C. R., Campagnoli, E. B., Nunes, O. C., Kitagawa, R. R., & Beltrame, F. (2016). Anti-ulcer mechanisms of polyphenols extract of Euphorbia umbellata (Pax) Bruyns (Euphorbiaceae). *Journal of Ethnopharmacology*, *191,* 29-40. https://doi.org/10.1016/j.jep.2016.06.032.

Mocan, T., Mosteanu, O., Matea, C. T., Pop, T., Al-Hajjar, N., Puia, C., Furcea, L., Bura, C.. & Mocan, L. (2018). *Nano-Antimicrobial Solutions Using Synthetic-Natural Hybrid Designs. In Nanomedicines.* IntechOpen. https://www.intechopen.com/chapters/63576.

Mohammadi, Z. A., Aghamiri, S. F., Zarrabi, A., & Talaie, M. R. (2016). Liposomal Doxorubicin Delivery Systems: Effects of Formulation and Processing Parameters on Drug Loading and Release Behavior. *Current Drug Delivery*, *13*(7), 1065-1070. https://doi.org/10.2174/1567201813666151228104643.

Monteiro, N., Martins, A., Reis, R. L., & Neves, N. M. (2014). Liposomes in tissue engineering and regenerative medicine. *Journal of the Royal Society Interface*, *11*(101), 1-24.

Moorcroft, S. C., Jayne, D. G., Evans, S. D., & Ong, Z. Y. (2018). Stimuli-Responsive Release of Antimicrobials Using Hybrid Inorganic Nanoparticle-Associated Drug-Delivery Systems. *Macromolecular Bioscience*, *18*(12),1-15. https://doi.org/10.1002/mabi.201800207.

Mourya, V. K., & Inamdar, N. N. (2008). Chitosan-modifications and applications: Opportunities galore. *Reactive and Functional Polymers*, *68*(6), 1013-1051.

Mudakavi, R. J., Raichur, A. M., & Chakravortty, D. (2014). Lipid coated mesoporous silica nanoparticles as an oral delivery system for targeting and treatment of intravacuolar Salmonella infections. *RSC Advances*, *4*(105), 61160-61166.

Mukherjee, P., Harwansh, R., & Bhattacharyya, S. (2015). *Chapter 10 – Bioavailability of Herbal Products: Approach Toward Improved Pharmacokinetics.* https://doi.org/10.1016/B978-0-12-800874-4.00010-6.

Mumtaz, M. Z., Kausar, F., Hassan, M., Javaid, S., & Malik, A. (2021). Anticancer activities of phenolic compounds from Moringa oleifera leaves: In vitro and in silico mechanistic study. *Beni-Suef University Journal of Basic and Applied Sciences*, *10*(1), 1-11.

Mundaragi, A., & Thangadurai, D. (2018). Process optimization, physicochemical characterization and antioxidant potential of novel wine from an underutilized fruit Carissa spinarum L.(Apocynaceae). *Food Science and Technology*, *38*(3), 428-433.

Munita, J. M., & Arias, C. A. (2016). Mechanisms of Antibiotic Resistance. *Microbiol Spectr*, *4*(2) 1-24. https://doi.org/10.1128/microbiolspec.VMBF-0016-2015.

Mutlu, N., Liverani, L., Kurtuldu, F., Galusek, D., & Boccaccini, A. R. (2022). Zinc improves antibacterial, anti-inflammatory and cell motility activity of chitosan for wound healing applications. *International Journal of Biological Macromolecules*, *213*, 845-857. https://doi.org/10.1016/j.ijbiomac.2022.05.199.

Mworia, J., Gitahi, S., Juma, K., Njagi, J., Mwangi, B., Aliyu, U., Njoroge, W. A., Mwonjoria, K. J., Nyamai, D. W., Ngugi, M. P., & Nyamai, D. (2015). Antinociceptiv e Activities of Acetone Leaves Extracts of Carissa Spinarum in Mice. *Journal o f Medicinal and Aromatic Plants*, *1*, 2167-0412.

Nag, M., Lahiri, D., Mukherjee, D., Banerjee, R., Garai, S., Sarkar, T., Ghosh, S., Dey, A., Ghosh, S., Pattnaik, S., & Ray, R. R. (2021). Functionalized Chitosan Nanomaterials: A Jammer for Quorum Sensing. *Polymers (Basel)*, *13*(15), 1-17. https://doi.org/ 10.3390/polym13152533.

Nakhaei, P., Margiana, R., Bokov, D. O., Abdelbasset, W. K., Jadidi Kouhbanani, M. A., Varma, R. S., Marofi, F., Jarahian, M., & Beheshtkhoo, N. (2021). Liposomes: Structure, Biomedical Applications, and Stability Parameters With Emphasis on Cholesterol. *Frontiers in Bioengineering and Biotechnology*, *9*, 1-23. https://doi.org/10.3389/fbioe.2021. 705886.

Narasimhan, B., Pliska-Matyshak, G., Kinnard, R., Carstensen, S., Ritter, M. A., Von Weymarn, L., & Murthy, P. P. (1997). Novel phosphoinositides in barley aleurone cells (additional evidence for the presence of phosphatidyl-scyllo-inositol). *Plant Physiology*, *113*(4), 1385-1393.

Nele, V., Holme, M. N., Kauscher, U., Thomas, M. R., Doutch, J. J., & Stevens, M. M. (2019). Effect of formulation method, lipid composition, and PEGylation on vesicle lamellarity: A small-angle neutron scattering study. *Langmuir*, *35*(18), 6064-6074.

Neves, L. F., Duan, J., Voelker, A., Khanal, A., McNally, L., Steinbach-Rankins, J., & Ceresa, B. P. (2016). Preparation and optimisation of anionic liposomes for delivery of small peptides and cDNA to human corneal epithelial cells. *Journal of Microencapsulation*, *33*(4), 391-399.

Nguyen, T. K., Tran, T. H., Roberts, C. L., Graham, S. M., & Marais, B. J. (2017). Child pneumonia - focus on the Western Pacific Region. *Paediatric Respiratory* Reviews .*21*, 102-110. https://doi.org/10.1016/j.prrv.2016.07.004.

Nguyen, T. X., Huang, L., Gauthier, M., Yang, G., & Wang, Q. (2016). Recent advances in liposome surface modification for oral drug delivery. *Nanomedicine*, *11*(9), 1169-1185. https://doi.org/10.2217/nnm.16.9.

Noudoost, B., Noori, N., Abedini, G., Gandomi, H., Akhondzadeh Basti, A., Ashkan, J., & Ghadami, F. (2015). Encapsulation of green tea extract in nanoliposomes and evaluation of its antibacterial, antioxidant and prebiotic properties. *Journal of Medicinal Plants*, *14*, 66-78.

Nsairat, H., Khater, D., Sayed, U., Odeh, F., Al Bawab, A., & Alshaer, W. (2022). Liposomes: Structure, composition, types, and clinical applications. *Heliyon*, *8*(5), e09394. https://doi.org/10.1016/j.heliyon.2022.e09394.

Obonyo, M., Zhang, L., Thamphiwatana, S., Pornpattananangkul, D., Fu, V., & Zhang, L. (2012). Antibacterial activities of liposomal linolenic acids against antibiotic-resistant Helicobacter pylori. *Molecular Pharmaceutics*, *9*(9), 2677-2685.

Ofosu, F. K., Daliri, E. B. M., Elahi, F., Chelliah, R., Lee, B. H., & Oh, D. H. (2020). New insights on the use of polyphenols as natural preservatives and their emerging safety concerns. *Frontiers in Sustainable Food Systems*, *4*(223), 1-14. https://doi.org/10. 3389/fsufs. 2020.525810.

Ojea-Jimenez, I., Comenge, J., Garcia-Fernandez, L., Megson, Z. A., Casals, E., & Puntes, V. F. (2013). Engineered inorganic nanoparticles for drug delivery applications. *Current Drug Metabolism*, *14*(5), 518-530.

Ojha, A. (2020). Nanomaterials for removal of waterborne pathogens: Opportunities and challenges. *Waterborne Pathogens*, *2020,* 385-432.

Ojha, A., & Sharma, Y. (2018). Different approaches for delivering the drug through vesicular carriers. *International Journal* of *Research and Development* in *Pharmacy & Life Sciences*, *7*(4), 3071-3082.

Okello, D., Chung, Y., Kim, H., Lee, J., Rahmat, E., Komakech, R., Kim, Y. G., Omujal, F., & Kang, Y. (2021). Antioxidant Activity, Polyphenolic Content, and FT-NIR Analysisof Different <i>Aspilia africana</i> Medicinal Plant Tissues. *Evidence-Based Complementary and Alternative Medicine, 2021*, 1-11.

Omwoyo, W. N., Ogutu, B., Oloo, F., Swai, H., Kalombo, L., Melariri, P., Mahanga, G. M., & Gathirwa, J. W. (2014). Preparation, characterization, and optimization of primaquine-loaded solid lipid nanoparticles. *International Journal of Nanomedicine*, *9*, 3865-3874. https://doi.org/10.2147/IJN.S62630.

Pandey, K. B., & Rizvi, S. I. (2009). Plant polyphenols as dietary antioxidants in human health and disease. *Oxidative Medicine and Cellular Longevity*, *2*(5), 270-278. https://doi.org/10.4161/oxim.2.5.9498.

Pandey, P., & Dahiya, M. (2016). A brief review on inorganic nanoparticles. *Journal of Critical Review*, *3*(3), 18-26.

Pandur, Ž., Dogsa, I., Dular, M., & Stopar, D. (2020). Liposome destruction by hydrodynamic cavitation in comparison to chemical, physical and mechanical treatments. *Ultrasonics Sonochemistry*, *61*, 1-11. /https://doi.org/10.1016/j.ultsonch.2019.104826.

Panya, A., Laguerre, M., Lecomte, J., Villeneuve, P., Weiss, J., McClements, D. J., & Decker, E. A. (2010). Effects of Chitosan and Rosmarinate Esters on the Physical and Oxidative Stability of Liposomes. *Journal of Agricultural and Food Chemistry*, *58*(9), 5679-5684. https://doi.org/10.1021/jf100133b.

Pap, N., Fidelis, M., Azevedo, L., do Carmo, M. A. V., Wang, D., Mocan, A., Pereira, E. P. R., Xavier-Santos, D., Sant'Ana, A. S., Yang, B., & Granato, D. (2021). Berrypolyphenols and human health: Evidence of antioxidant, anti-inflammatory, microbiotamodulation, and cell-protecting effects. *Current Opinion in Food Science*, *42*, 167-186. /https://doi.org/10.1016/j.cofs.2021.06.003.

Pasarin, D., Ghizdareanu, A. I., Enascuta, C. E., Matei, C. B., Bilbie, C., Paraschiv-Palada, L., & Veres, P. A. (2023). Coating Materials to Increase the Stability of Liposomes. *Polymers (Basel)*, *15*(3), 1-30.

Pathomthongtaweechai, N., & Muanprasat, C. (2021). Potential Applications of Chitosan-Based Nanomaterials to Surpass the Gastrointestinal Physiological Obstacles and Enhance the Intestinal Drug Absorption. *Pharmaceutics*, *13*(6),1-22. https://doi.org/10.3390/pharmaceutics13060887.

Patil-Sen, Y., Torino, E., De Sarno, F., Ponsiglione, A. M., Chhabria, V. N., Ahmed, W., & Mercer, T. (2020). Biocompatible superparamagnetic core-shell nanoparticles for potential use in hyperthermia-enabled drug release and as an enhanced contrast agent. *Nanotechnology*. *31*(37), 1-19.

Patra, J. K, Das G., Fraceto, L. F., Campos, E. V., Rodriguez-Torres, M. D., Acosta-Torres, L. S., Diaz-Torres, L. A., Grillo, R, Swamy, M. K., Sharma, S., & Habtemariam, S. (2018). Nano based drug delivery systems: recent developments and future prospects. *Journal of Nanobiotechnology*, 16(1),1-33.

Piazzini, V., Lemmi, B., D'Ambrosio, M., Cinci, L., Luceri, C., Bilia, A. R., & Bergonzi, M. C. (2018). Nanostructured lipid carriers as promising delivery systems for plant extracts: The case of silymarin. *Applied Sciences*, *8*(7), 1-15.

Piekarska, K., Sikora, M., Owczarek, M., Jóźwik-Pruska, J., & Wiśniewska-Wrona, M. (2023). Chitin and Chitosan as Polymers of the Future— Obtaining, Modification, Life Cycle Assessment and Main Directions of Application. *Polymers (Basel)*, *15*(4), 1-31.

Pimentel Moral, S., Verardo, V., Robert, P., Segura Carretero, A., & Martinez-Ferez, A. (2016). *Nanoencapsulation strategies applied to maximize target delivery of intact polyphenols, 2016, 559-595.*https://doi.org/10.1016/B978-0-12-804307-3.00013-2.

Pool, H., Quintanar, D., Figueroa, J. D. D., H Bechara, J. E., McClements, D. J., & Mendoza, S. (2012). Polymeric nanoparticles as oral delivery systems for encapsulation and release of polyphenolic compounds: impact on quercetin antioxidant activity & bioaccessibility. *Food Biophysics*, *7*(3), 276-288. https://doi.org/10.1007/s11483-012-9266-z.

Popescu, R. C., Andronescu, E., & Vasile, B. S. (2019). Recent advances in magnetite nanoparticle functionalization for nanomedicine. *Nanomaterials*, *9*(12), 1-31.

Prakash Upputuri, R. T., & Azad Mandal, A. K. (2017). Sustained Release of Green Tea Polyphenols from Liposomal Nanoparticles; Release Kinetics and Mathematical Modelling. *Iranian Journal of Biotechnology*, *15*(4), 277-283. https://doi.org/10.15171/ ijb.1322.

Qin, Y., & Li, P. (2020). Antimicrobial Chitosan Conjugates: Current Synthetic Strategies and Potential Applications. *International Journal of Molecular Sciences*, *21*(2), 1-19. https://doi.org/10.3390/ijms21020499.

Rahman, M. M., Islam, M. R., Akash, S., Mim, S. A., Rahaman, M. S., Emran, T. B., . . . Wilairatana, P. (2022). In silico investigation and potential therapeutic approaches of natural products for COVID-19: Computer-aided drug design perspective. *Frontier in Cellular and Infection Microbiology*, *12*, 1-28.

Rajan, S. A., Khan, A., Asrar, S., Raza, H., Das, R. K., & Sahu, N. K. (2019). Synthesis of ZnO/Fe(3)O(4)/rGO nanocomposites and evaluation of antibacterial activities towards *E. coli* and *S. aureu*s. *IET Nanobiotechnol*, *13*(7), 682-687. https://doi.org/10. 1049/iet-nbt.2018.5330.

Raju, A., De, S. S., Ray, M. K., & Degani, M. S. (2021). Antituberculosis activity of polyphenols of Areca catechu. *International Journal of Mycobacteriology*, *10*(1), 13-18. https://doi.org/10.4103/ijmy.ijmy_199_20.

Raliya, R., Singh Chadha, T., Haddad, K., & Biswas, P. (2016). Perspective on nanoparticle technology for biomedical use. *Current Pharmaceutical Design*, *22*(17), 2481-2490.

Rashid, S., Shen, C., Yang, J., Liu, J., & Li, J. (2018). Preparation and properties of chitosan–metal complex: Some factors influencing the adsorption capacity for dyes in aqueous solution. *Journal of Environmental Sciences*, *66*, 301-309.

Rastogi, S., Jabal, J., Zhang, H., Gibson, C., Haler, K., You, Q., Aston, D. E., & Branen, A. (2011). Antibody@Silica Coated Iron Oxide Nanoparticles: Synthesis, Capture of E.coli and Sers Titration of Biomolecules with Antibacterial Silver Colloid. *Journal of Nanomedicine and Nanotechnology*, *2*, (7), 1-8.

Rekha, K., Nirmala, M., Nair, M. G., & Anukaliani, A. (2010). Structural, optical, photocatalytic and antibacterial activity of zinc oxide and manganese doped zinc oxide nanoparticles. *Physica B: Condensed Matter*, *405*(15), 3180-3185. /https://doi.org/10.1016/j.physb.2010.04.042.

Renne, M. F., & de Kroon, A. (2018). The role of phospholipid molecular species in determining the physical properties of yeast membranes. *FEBS Lett*, *592*(8), 1330-1345. https://doi.org/10.1002/1873-3468.12944.

Riccucci, G., Ferraris, S., Reggio, C., Bosso, A., Örlygsson, G., Ng, C. H., & Spriano, S. (2021). Polyphenols from Grape Pomace: Functionalization of Chitosan-Coated Hydroxyapatite for Modulated Swelling and Release of Polyphenols. *Langmuir*, *37*(51), 14793-14804. https://doi.org/10.1021/acs.langmuir.1c01930.

Rochín-Medina, J. J., Sotelo-Castro, J. A., Salazar-Salas, N. Y., López-Valenzuela, J. A., & Ramírez, K. (2019). Antioxidant and anti-Salmonella activities of eggplant peel compounds obtained by solvent-free calcium-based extraction. *CyTA - Journal of Food*, *17*(1), 873-881. https://doi.org/10.1080/19476337.2019.1675762.

Rodrigues, A. R. O., Matos, J. O., Nova Dias, A. M., Almeida, B. G., Pires, A., Pereira, A. M., Araújo, J. P., Queiroz, M. J. R., Castanheira, E. M., & Coutinho, P. J. (2019). Development of multifunctional liposomes containing magnetic/plasmonic MnFe2O4/Au core/shell nanoparticles. *Pharmaceutics*, *11*(1), 1-19.

Rosická, D., & Šembera, J. (2013). Changes in the nanoparticle aggregation rate due to the additional effect of electrostatic and magnetic forces on mass transport coefficients. *Nanoscale research letters*, *8*(1),1-9. https://doi.org/10.1186/1556-276X-8-20.

Rubaka, C., Ndakidemi, P., Malebo, H. M., & Shahada, F. (2014c). Analysis of Phytochemical and Antibacterial Activity of Carissa spinarum Linn Crude Extracts. *European Journal of Medicinal Plants*, *4*, 937-945.

Rubaka, C., Ndakidemi, P., Malebo, H., & Shahada, F. (2014b). Individual and Combined Antibacterial Activity of Crude Extracts from Medicinal Plants Carissa spinarum Linn and Carica papaya Linn. *European Journal of Medicinal Plants*, *4*(12), 1513-1523. https://doi.org/10.9734/EJMP/2014/10599.

Rudramurthy, G. R., Swamy, M. K., Sinniah, U. R., & Ghasemzadeh, A. (2016). Nanoparticles: Alternatives Against Drug-Resistant Pathogenic Microbes. *Molecules*, *21*(7), 1-30. https://doi.org/10.3390/molecules21070836.

Sadhukhan, P., Kundu, M., Chatterjee, S., Ghosh, N., Manna, P., Das, J., & Sil, P. C. (2019). Targeted delivery of quercetin via pH-responsive zinc oxide nanoparticles for breast cancer therapy. *Materials Science and Engineering: C*, *100*, 129-140. https://doi.org/https://doi.org/10.1016/j.msec.2019.02.096.

Sadžak, A., Mravljak, J., Maltar-Strmečki, N., Arsov, Z., Baranović, G., Erceg, I., Kriechbaum, M., Strasser, V., Přibyl, J., Šegota, S. (2020). The structural integrity of the model lipid membrane during induced lipid peroxidation: The role of flavonols in the inhibition of lipid peroxidation. *Antioxidants*, 159(5), 1-28.

Safinya, C. R., Ewert, K. K., Majzoub, R. N., & Leal, C. (2014). Cationic liposome–nucleic acid complexes for gene delivery and gene silencing. *New Journal of Chemistry*, *38*(11), 5164-5172.

Sanità, G., Carrese, B., & Lamberti, A. (2020). Nanoparticle Surface Functionalization: How to Improve Biocompatibility and Cellular Internalization [Review]. *Frontiers in Molecular Biosciences*, *7*(381), 1-20. https://doi.org/10.3389/fmolb.2020.587012.

Sanwal, R., & Chaudhary, A. K. (2011). Wound healing and antimicrobial potential of Carissa spinarum Linn. in albino mice. *Journal of Ethnopharmacology*, *135*(3), 792-796. https://doi.org/10.1016/j.jep.2011.04.025.

Saranya, T. S., Rajan, V. K., Biswas, R., Jayakumar, R., & Sathianarayanan, S. (2018). Synthesis, characterisation and biomedical applications of curcumin conjugated chitosan microspheres. *International Journal of Biological Macromolecules, 110*, 227-233. https://doi.org/10.1016/j.ijbiomac.2017.12.044.

Sawant, V. J., & Kupwade, R. (2015). Functionalization of TiO2 nanoparticles and curcumin loading for enhancement of biological activity. *Der Pharmacia Lettre*, *7*, 37-44.

Scheepens, A., Tan, K., & Paxton, J. W. (2010). Improving the oral bioavailability of beneficial polyphenols through designed synergies. *Genes and Nutrition*, *5*(1), 75-87. https://doi.org/10.1007/s12263-009-0148-z.

Sebaaly, C., Trifan, A., Sieniawska, E., & Greige-Gerges, H. (2021). Chitosan-Coating Effect on the Characteristics of Liposomes: A Focus on Bioactive Compounds and Essential Oils: A Review. *Processes*, *9*(3), 1-47. https://doi.org/10.3390/pr9030445.

Sehgal, S., & Rogers, J. A. (1995). Polymer-coated liposomes: Improved liposome stability and release of cytosine arabinoside (Ara-C). *Journal of Microencapsulation*, *12*(1), 37-47. https://doi.org/10.3109/02652049509051125.

Shade, C. W. (2016). Liposomes as Advanced Delivery Systems for Nutraceuticals. *Integrative Medicine: A Clinician's Journal*, *15*(1), 33-36.

Shafaei, A., Saeed, M., Aisha, A., & Ismail, Z. (2017). Pharmacokinetics and bioavailability of Orthosiphon stamineus ethanolic extract and its nano liposomes in Sprague–Dawleyrats. *International Journal of Pharmacy and Pharmaceutical Sciences 9, 199*-206.

Shariare, M. H., Rahman, M., Lubna, S. R., Roy, R. S., Abedin, J., Marzan, A. L., Altamimi, M. A., Ahamad, S. R., Ahmad, A., Alanazi, F. K., & Alanazi, F. K. (2020). Liposomal drug delivery of Aphanamixis polystachya leaf extracts and its neurobehavioral activity in mice model. *Scientific Reports*, *10*(1), 1-16.

Shariati, A., Arshadi, M., Khosrojerdi, M.A., Abedinzadeh, M., Ganjalishahi, M., Maleki, A., Heidary, M., & Khoshnood, S. (2022). The resistance mechanisms of bacteria against ciprofloxacin and new approaches for enhancing the efficacy of this antibiotic. *Frontiers in Public Health*, 21(10), 1-28.

Sharma, N., Kumar, V., Gupta, N., Shekhar, P., & Kaur, P. S. (2023). Traditional Importance, Phytochemistry, Pharmacology, and Toxicological Attributes of the Promising Medicinal Herb Carissa spinarum L. *Separations*, *10*(3), 1-19.

Shashidhar, G., & Manohar, B. (2018). Nanocharacterization of liposomes for the encapsulation of water soluble compounds from Cordyceps sinensis CS1197 by a supercritical gas anti-solvent technique. *RSC Advances*, *8*(60), 34634-34649.

Sherin, S., Balachandran, S., & Abraham, A. (2020). Curcumin incorporated titanium dioxide nanoparticles as MRI contrasting agent for early diagnosis of atherosclerosis- rat model. *Veterinary and Animal Science*, *10*, 1-6. https://doi.org/10.1016/j.vas. 2020.100090.

Shi, N. Q., & Qi, X. R. (2017). Preparation of Drug Liposomes by Reverse-Phase Evaporation. In W. L. Lu & X. R. Qi (Eds.), *Liposome-Based Drug Delivery Systems*. Springer Berlin Heidelberg. https://doi.org/10.1007/978-3-662-49231-4_3-1.

Shome, S., Talukdar, A. D., Tewari, S., Choudhury, S., Bhattacharya, M. K., & Upadhyaya, H. (2021). Conjugation of micro/nanocurcumin particles to ZnO nanoparticles changes the surface charge and hydrodynamic size thereby enhancing its antibacterial activity against Escherichia coli and Staphylococcus aureus. *Biotechnology and Applied Biochemistry*, *68*(3), 603-615. https://doi.org/10.1002/bab. 1968.

Siddiqi, K. S., ur Rahman, A., Tajuddin, N., & Husen, A. (2018). Properties of Zinc Oxide Nanoparticles and Their Activity Against Microbes. *Nanoscale Research Letters*, *13*(1), 141. https://doi.org/10.1186/s11671-018-2532-3.

Simon, A. K., Hollander, G. A., & McMichael, A. (2015). Evolution of the immune system in humans from infancy to old age. *Proceedings of the Royal Society B: Biological Sciences*, *282*(1821), 20143085.

Sirelkhatim, A., Mahmud, S., Seeni, A., Kaus, N. H. M., Ann, L. C., Bakhori, S. K. M., Hasan, H., & Mohamad, D. (2015). Review on Zinc Oxide Nanoparticles: Antibacterial Activity and Toxicity Mechanism. *Nano-micro Letters*, *7*(3), 219-242.

Sivakumar, P., Lee, M., Kim, Y.-S., & Shim, M. S. (2018). Photo-triggered antibacterial and anticancer activities of zinc oxide nanoparticles [10.1039/C8TB00948A]. *Journal of Materials Chemistry B*, *6*(30), 4852-4871. https://doi.org/10.1039/C8TB00948A.

Siyum, Z. H., & Meresa, T. A. (2021). Physicochemical properties and nutritional values of Carissa Spinarum L. /"AGAM" FRUIT. *International Journal of Fruit Science*, *21*(1), 826-834. https://doi.org/10.1080/15538362. 2021. 1936348.

Slathia, P., Paul, N., Gupta, S., Sharma, B., Kumar, R., & Kher, S. (2017). Traditional uses of under-utilized tree species in sub tropical rainfed areas of Kathua, Jammu & Kashmir. *Indian Journal of Traditional Knowledge*, *16*, 164-169.

Slavin, Y. N., Asnis, J., Häfeli, U. O., & Bach, H. (2017). Metal nanoparticles: understanding the mechanisms behind antibacterial activity. *Journal of Nanobiotechnology*, *15*(1), 1-20. https://doi.org/10.1186/s12951-017-0308-z.

Sokoudjou, J. B., Atolani, O., Njateng, G. S. S., Khan, A., Tagousop, C. N., Bitombo, A. N., & Kodjio, N., & Gatsing, D. (2020). Isolation, characterization and in vitro anti-salmonellal activity of compounds from stem bark extract of Canarium schweinfurthii. *BMC Complementary Medicine and Therapies*, *20*(1), 1-10. https://doi.org/10.1186/s12906-020-03100-5.

Song, J. L., Zhu, K., Feng, X., & Zhao, X. (2015). Protective effect Malus pumila Mill leaf polyphenols in reserpine-induced gastric ulcer in mice. *Journal of the Korean Society for Applied Biological Chemistry*, *58*(2), 249-256. https://doi.org/10.1007/s13765-015-0021-2.

Sonohara, R., Muramatsu, N., Ohshima, H., & Kondo, T. (1995). Difference in surface properties between Escherichia coli and Staphylococcus aureus as revealed by electrophoretic mobility measurements. *Biophysical Chemistry*, *55*(3), 273-277. https://doi.org/10.1016/0301-4622(95)00004-h.

Spratt, T., Bondurant, B., & O'Brien, D. F. (2003). Rapid release of liposomal contents upon photoinitiated destabilization with UV exposure. *Biochim Biophys Acta*, *1611*(1-2), 35-43. https://doi.org/10.1016/s0005-2736(02)00602-8.

Sriwidodo, Umar, A. K., Wathoni, N., Zothantluanga, J. H., Das, S., & Luckanagul, J. A. (2022). Liposome-polymer complex for drug delivery system and vaccine stabilization. *Heliyon*, *8*(2), 1-16. https://doi.org/10.1016/j.heliyon. 2022.e08934.

Stankovic, M., Zia-Ul-Haq, M., Bojovic, B., & Topuzovic, M. (2014). Total phenolics, flavonoid content and antioxidant power of leaf, flower and fruits from cornelian cherry (Cornus mas L.). *Bulgarian Journal of Agricultural Science*, *20*(2), 358-363.

Šturm, L., & Poklar Ulrih, N. (2021). Basic Methods for Preparation of Liposomes and Studying Their Interactions with Different Compounds, with the Emphasis on Polyphenols. *Internatonal Journal of Molecular Scences*, *22*(12), 1-20. https://doi.org/10.3390/ijms22126547.

Sung, Y. K., & Kim, S. W. (2020). Recent advances in polymeric drug delivery systems. *Biomaterials Research*, *24*(1), 1-12. https://doi.org/10.1186/s40824-020-00190-7.

Swallah, M. S., Fu, H., Sun, H., Affoh, R., & Yu, H. (2020). The Impact of Polyphenol on General Nutrient Metabolism in the Monogastric Gastrointestinal Tract. *Journal of Food Quality*, *2020*, 1-12. https://doi.org/10.1155/2020/5952834.

Sych, T., Mély, Y., & Römer, W. (2018). Lipid self-assembly and lectin-induced reorganization of the plasma membrane. *Philosophical Transactions of the Royal Society B: Biological Sciences*, *373*(1747),1-9. https://doi.org/doi:10.1098/rstb.2017. 0117.

Szymańska, E., & Winnicka, K. (2015). Stability of Chitosan—A Challenge for Pharmaceutical and Biomedical Applications. *Marine Drugs*, *13*, 1819-1846. https://doi.org/10.3390/md13041819.

Ta, T., & Porter, T. M. (2013). Thermosensitive liposomes for localized delivery and triggered release of chemotherapy. *Journal of Control Release*, *169*(1-2), 112-125. https://doi.org/10.1016/j.jconrel.2013.03.036.

Tapia, M. J., Monteserín, M., Burrows, H. D., Seixas de Melo, J. S., & Estelrich, J. (2013). Effect of the Phospholipid Chain Length and Head Group on Beta-Phase Formation of Poly(9,9-dioctylfluorene) Enclosed in Liposomes. *Photochemistry and Photobiology*, *89*(6), 1471-1478. https://doi.org/10.1111/php.12143.

Taylor, E., & Webster, T. J. (2011). Reducing infections through nanotechnology and nanoparticles. *International Journal of Nanomedicine*, *6*, 1463-1473.

Thai, T., Salisbury, B. H., & Zito, P. M. (2023). *Ciprofloxacin.* In *StatPearls*. StatPearls Publishing. WEKA LINLK

Tiruneh, T. A., Tiruneh, G. A., Abebe, E. C., & Ayele, T. M. (2022). Phytochemical Investigation and Determination of Antibacterial Activity of Solvent Leave Extracts of Carissa spinarum. *Infection and Drug Resistance*, *15*, 1-13.

Tito, A., Colantuono, A., Pirone, L., Pedone, E., Intartaglia, D., Giamundo, G., Conte, I., Vitaglione, P., & Apone, F. (2021). Pomegranate Peel Extract as an Inhibitor of SARS-CoV-2 Spike Binding to Human ACE2 Receptor (in vitro): A Promising Source of Novel Antiviral Drugs [Original Research]. *Frontiers in Chemistry*, *9*(231), 1-11. https://doi.org/10.3389/fchem.2021.638187.

TM, M. W., Lau, W. M., & Khutoryanskiy, V. V. (2018). Chitosan and Its Derivatives for Application in Mucoadhesive Drug Delivery Systems. *Polymers (Basel)*, *10*(3), 1-37. https://doi.org/10.3390/polym10030267.

Toh, M.-R., & Chiu, G. N. (2013). Liposomes as sterile preparations and limitations of sterilisation techniques in liposomal manufacturing. *Asian Journal of Pharmaceutical Sciences*, *8*(2), 88-95.

Toro-Uribe, S., Ibáñez, E., Decker, E. A., & McClements, D. J. (2018). Design, Fabrication, Characterization, and In Vitro Digestion of Alkaloid-, Catechin-, and Cocoa Extract-Loaded Liposomes. *66*(45), 12051-12065. https://doi.org/10.1021/acs.jafc.8b04735.

Tsao, R. (2010). Chemistry and biochemistry of dietary polyphenols. *Nutrients*, *2*(12), 1231-1246. https://doi.org/10.3390/nu2121231.

Uddin,T.M., Chakraborty, A.J., Khusro, A., Zidan, B.R., Mitra, S., Emran, T.B., Dhama, K., Ripon, M.K., Gajdács, M., Sahibzada, M.U.(2021) Hossain MJ. Antibiotic resistance in microbes: History, mechanisms, therapeutic strategies and future prospects. *Journal of Infection and Public Health*, 14(12),1750-1766.

Upputuri, R. T. P., & Mandal, A. K. A. (2017). Sustained release of green tea polyphenols from liposomal nanoparticles; release kinetics and mathematical modelling. *Iranian Journal of Biotechnology*, *15*(4), 277-283.

van Hoogevest, P., & Fahr, A. (2019). *Phospholipids in cosmetic carriers. In Nanocosmetics* Springer. https://link.springer.com/chapter/10.1007/978-3-030-16573-4_6.

Varaprasad, K., Yallapu, M. M., Núñez, D., Oyarzún, P., López, M., Jayaramudu, T., & Karthikeyan, C. (2019). Generation of engineered core–shell antibiotic nanoparticles. *RSC Advances*, *9*(15), 8326-8332.

Varona, S., Martin, A., & Cocero, M. A. J. (2011). Liposomal incorporation of lavandin essential oil by a thin-film hydration method and by particles from gas-saturated solutions. *Industrial & Engineering Chemistry Research*, *50*(4), 2088-2097.

Vassallo, A., Silletti, M. F., Faraone, I., & Milella, L. (2020). Nanoparticulate Antibiotic Systems as Antibacterial Agents and Antibiotic Delivery Platforms to Fight Infections. *Journal of Nanomaterials*, *2020*, 6905631. https://doi.org/10.1155/2020/6905631.

Venkataraju, J. L., Sharath, R., Chandraprabha, M., Neelufar, E., Hazra, A., & Patra, M. (2014). Synthesis, characterization and evaluation of antimicrobial activity of zinc oxide nanoparticles. *Journal of Biochemical Technology*, *3*(5), 151-154.

Vila-Corcoles, A., Ochoa-Gondar, O., Rodriguez-Blanco, T., Raga-Luria, X., Gomez-Bertomeu, F., & Group, E. S. (2009). Epidemiology of community-acquired pneumonia in older adults: a population-based study. *Respiratory Medicine*, *103*(2), 309-316.

Viter, R., Tereshchenko, A., Smyntyna, V., Ogorodniichuk, J., Starodub, N., Yakimova, R., Khranovskyy, V., & Ramanavicius, A. (2017). Toward development of optical biosensors based on photoluminescence of TiO2 nanoparticles for the detection of Salmonella. *Sensors and Actuators B: Chemical*, *252*, 95-102. https://doi.org/10.1016/j.snb.2017.05.139.

Wang, D. Y., van der Mei, H. C., Ren, Y., Busscher, H. J., & Shi, L. (2020). Lipid-Based Antimicrobial Delivery-Systems for the Treatment of Bacterial Infections [Review]. *Frontiers in Chemistry*, *7*, 1-15. https://www.frontiersin.org/article/10.3389/fchem.2019.00872.

Wang, L., Hu, C., & Shao, L. (2017a). The antimicrobial activity of nanoparticles: Present situation and prospects for the future. *International Journal of Nanomedicine*, *12*, 1227–1249.

Wang, M., Firrman, J., Liu, L., & Yam, K. (2019). A Review on Flavonoid Apigenin: Dietary Intake, ADME, Antimicrobial Effects, and Interactions with Human Gut Microbiota. *BioMed Research International*, *2019*, 1-19. https://doi.org/10.1155/2019/7010467.

Wang, Q., Chen, X., Liu, N., Wang, S., Liu, C., Meng, X., & Liu, C.-G. (2006). Protonation constants of chitosan with different molecular weight and degree of deacetylation. *Carbohydrate Polymers*, *65*, 194-201. https://doi.org/10.1016/j.carbpol.2006.01.001.

Wang, S., Zhu, B. B., Li, D. Z., Fu, X. Z., & Shi, L. (2012). Preparation and characterization of TIO2/SPI composite film. *Materials Letters*, *83*, 42–45. https://doi.org/10.1016/j.matlet.2012.05.104.

Wang, W., Meng, Q., Li, Q., Liu, J., Zhou, M., Jin, Z., & Zhao, K. (2020). Chitosan Derivatives and Their Application in Biomedicine. *International Journal of Molecular Sciences, 21*(2), 1-26. https://doi.org/10.3390/ijms21020487.

Wang, X., Du, Y., Fan, L., Liu, H., & Hu, Y. (2005). Chitosan- metal complexes as antimicrobial agent: Synthesis, characterization and Structure-activity study. *Polymer Bulletin*, *55*, 105-113. https://doi.org/10.1007/s00289-005-0414-1.

Wang, Z., Ma, Y., Khalil, H., Wang, R., Lu, T., Zhao, W., Zhang, Y., Chen, J., & Chen, T. (2016). Fusion between fluid liposomes and intact bacteria: study of driving parameters and in vitro bactericidal efficacy. *International Journal of Nanomedicine*, *11*, 4025-4036. https://doi.org/ 10.2147/IJN.S55807.

Watwe, R. M., & Bellare, J. R. (1995). Manufacture of liposomes: A review. *Current Science*, 715-724.

Weerasuriya, D.R.K., Bhakta, S., Hiniduma, K., Dixit, C.K., Shen, M., Tobin, Z., He, J., Suib, S.L., & Rusling, J.F. (2021). Magnetic Nanoparticles with Surface Nanopockets for Highly Selective Antibody Isolation. *ACS Applied Bio Materials*, *4*(8), 6157-6166.

Wei, M., Guo, X., Tu, L., Zou, Q., Li, Q., Tang, C., Chen, B., Xu, Y, & Wu, C., (2015). Lactoferrin-modified PEGylated liposomes loaded with doxorubicin for targeting delivery to hepatocellular carcinoma. *International Journal of Nanomedicine*, *10*, 5123-5137.

Weingart, J., Vabbilisetty, P., & Sun, X. L. (2013). Membrane mimetic surface functionalization of nanoparticles: methods and applications. *Advances in Colloid and Interface Science*, *197*, 68-84.

Wen, Z., You, X., Liu, B., Zheng, Z., Pu, Y., Jiang, L., & Li, Q. (2011). Formation of atractylone liposomes by rapid expansion from supercritical to surfactant solution. *Asia-Pacific Journal of Chemical Engineering*, *6*(4), 624-630.

Wieszczycka, K., Staszak, K., Woźniak-Budych, M. J., Litowczenko, J., Maciejewska, B. M., & Jurga, S. (2021). Surface functionalization – The way for advanced applications of smart materials. *Coordination Chemistry Reviews*, *436*, 213846. /https://doi.org/10. 1016/j.ccr.2021.213846 .

Wintola, O. A., & Afolayan, A. J. (2015). The antibacterial, phytochemicals and antioxidants evaluation of the root extracts of Hydnora africanaThunb. used as antidysenteric in Eastern Cape Province, South Africa. *BMC Complementary Alternatve Medicine*, *15*, (307), 1-12. https://doi.org/10.1186/s12906-015-0835-9.

Xu, Q., Zhao, Y., Xu, J., & Zhu, J. J. (2006). Preparation of functionalized copper nanoparticles and fabrication of a glucose sensor. *Sensors and Actuators B: Chemical*, *114*, 379-386. https://doi.org/10.1016/j.snb.2005.06.005.

Yadav, D., Sandeep, K., Pandey, D., & Dutta, R. K. (2017). Liposomes for drug delivery. *Journal of Biotechnology and Biomaterials, 7*(4), 1-8.

Yan, D., Li, Y., Liu, Y., Li, N., Zhang, X., & Yan, C. (2021). Antimicrobial Properties of Chitosan and Chitosan Derivatives in the Treatment of Enteric Infections. *Molecules*, *26*(23), 1-27.

Yang, S., Liu, L., Han, J., & Tang, Y. (2020). Encapsulating plant ingredients for dermocosmetic application: An updated review of delivery systems and characterization techniques. *International Journal of Cosmetic Science*, *42*(1), 16-28.

Yazdani, M. R., Virolainen, E., Conley, K., & Vahala, R. (2018). Chitosan–Zinc(II) Complexes as a Bio-Sorbent for the Adsorptive Abatement of Phosphate: Mechanism of Complexation and Assessment of Adsorption Performance. *Polymers (Basel)*, *10*(1), 1-19.

Ydjedd, S., Bouriche, S., López-Nicolás, R., Sánchez-Moya, T., Frontela-Saseta, C., Ros-Berruezo, G., Rezgui, F., Louaileche, H., & Kati, D.E.(2017). Effect of in Vitro Gastrointestinal Digestion on Encapsulated and Nonencapsulated Phenolic Compounds of Carob (C*eratonia siliqua* L.) Pulp Extracts and Their Antioxidant Capacity. *Journal of Agricultural and Food Chemistry*, *65*(4),827-835. https://doi.org/10.1021/acs.jafc.6b05103.

Yeshi, K., Crayn, D., Ritmejerytė, E., & Wangchuk, P. (2022). Plant Secondary Metabolites Produced in Response to Abiotic Stresses Has Potential Application in Pharmaceutical Product Development. *Molecules*, *27*(1), 1-31 https://doi.org/10.3390/molecules 27010313.

Yetisgin, A. A., Cetinel, S., Zuvin, M., Kosar, A., & Kutlu, O. (2020). Therapeutic Nanoparticles and Their Targeted Delivery Applications. *Molecules*, *25*(9). https://doi.org/10.3390/molecules25092193.

Yilmaz Atay, H. (2020). Antibacterial Activity of Chitosan-Based Systems. *Functional Chitosan: Drug Delivery and Biomedical Applications*, *2020,* 457-489.

Yin, S., Liu, J., Kang, Y., Lin, Y., Li, D., & Shao, L. (2019). Interactions of nanomaterials with ion channels and related mechanisms. *British Journal of Pharmacology*, *176*(19), 3754-3774.

Yu, M., Song, W., Tian, F., Dai, Z., Zhu, Q., Ahmad, E., Guo, S., Zhu, C., Zhong, H., Yuan, Y., & Zhang, T. (2019). Temperature-and rigidity-mediated rapid transport of lipid nanovesicles in hydrogels. *Proceedings of the National Academy of Sciences,116*(12),5362-5369.

Zamani-Ghaleshahi, A., Rajabzadeh, G., Ezzatpanah, H., & Ghavami, M. (2020). Biopolymer Coated Nanoliposome as Enhanced Carrier System of Perilla Oil. *Food Biophysics*, *15*(3), 273-287. https://doi.org/10.1007/s11483-019-09621-y.

Zhang, H. (2017). *Thin-film hydration followed by extrusion method for liposome preparation. In Liposomes*. Springer. http://www.springer.com/series/7651.

Zhang, J., Sun, J., Li, C., Qiao, H., & Hussain, Z. (2023). Functionalization of curcumin nanomedicines: A recent promising adaptation to maximize pharmacokinetic profile, specific cell internalization and anticancer efficacy against breast cancer. *Journal of Nanobiotechnology*, *21*(1), 1-38. https://doi.org/10.1186/s12951-023-01854-x.

Zhang, Q., Bastard, P., Cobat, A., & Casanova, J. L. (2022). Human genetic and immunological determinants of critical COVID-19 pneumonia. *Nature*, *603*(7902), 587-598.

Zhang, Y., R Nayak, T., Hong, H., & Cai, W. (2013). Biomedical applications of zinc oxide nanomaterials. *Current Molecular Medicine*, *13*(10), 1633-1645.

Zhao, D., Yu, S., Sun, B., Gao, S., Guo, S., & Zhao, K. (2018). Biomedical Applications of Chitosan and Its Derivative Nanoparticles. *Polymers (Basel)*, *10*(4). https://doi.org/10.3390/polym10040462.

Zheng, C., Wang, Y., Phua, S. Z. F., Lim, W. Q., & Zhao, Y. (2017). ZnO–DOX@ ZIF-8 core–shell nanoparticles for pH-responsive drug delivery. *ACS Biomaterials Science and Engineering*, *3*(10), 2223-2229.

Zheng, P., Zhang, B., Jin, B., Guan, W., Bai, B., & Dai, S. (2018). Synergistic enhancement in antibacterial activity of core/shell/shell SiO2/ZnO/Ag3PO4 nanoparticles. *ChemNanoMat*, *4*(9), 972-981.

Zhou, W., Cheng ,C., Ma, L., Zou, L., Liu, W., Li, R., Cao, Y., Liu, Y., Ruan, R., Li, J.(2021). The formation of chitosan-coated rhamnolipid liposomes containing curcumin: stability and in vitro digestion. *Molecules*, 26(3), 1-13.

Zook, J. M., & Vreeland, W. N. (2010). Effects of temperature, acyl chain length, and flow-rate ratio on liposome formation and size in a microfluidic hydrodynamic focusing device [10.1039/B923299K]. *Soft Matter*, *6*(6), 1352-1360. https://doi.org/10. 1039/B923299K.

RESEARCH OUTPUTS

Published papers

Rubaka, C., Gathirwa, J. W., Malebo, H. M., Swai, H., & Hilonga, A. (2022). Inorganic Nanocarriers: Surface Functionalization, Delivery Utility for Natural Therapeutics. A review. *Journal of Biomimetics, Biomaterials and Biomedical Engineering, 19*(58) 81- 96. https://doi.org/10.4028/p-96l963.

Rubaka, C., Gathirwa, J. W., Malebo, H. M., Swai H., Sibuyi, N. R., Hilonga, A., & Dube, A. (2023). Chitosan-coated liposomes of *Carissa spinarum* extract: synthesis, analysis and antipneumococcal potency. *Bioinspired, Biomimetic and Nanobiomaterials,12*(1),12- 23. https://doi.org/10.1680/jbibn.22.00046.

Rubaka, C., Gathirwa, J. W., Malebo, H. M., Swai, H., & Hilonga, A. (2023). Development and Characterization of Nanovesicles Containing Phenolic Compounds of *Carissa spinarum*: Encapsulation, Release Kinetics, Antimicrobial Activity and Mathematical Modeling. *Journal of Biomimetics, Biomaterials and Biomedical Engineering*, *60*, 43-52. https://doi.org/10.4028/p-8mzn1a.

Poster presentation

Nanotheranostic formulation: TB therapy and monitoring